UNIVERSITY OF KWAZULU-NATAL
INYUVESI YAKWAZULU-NATALI

PERFORMANCE AND COST BENEFIT ANALYSES OF UNIVERSITY CAMPUS MICROGRIDS

by

KAYODE TIMOTHY AKINDEJI

A thesis submitted in fulfilment of the academic requirements for the degree of Doctor of Philosophy in Electrical Engineering at the School of Engineering, University of KwaZulu-Natal

Supervisor: Dr Remy Tiako

Co-Supervisor: Prof Innocent Davidson

October 2021

COLLEGE OF AGRICULTURE, ENGINEERING AND SCIENCE

DECLARATION 1- PLAGIARISM

I, **Kayode Timothy Akindeji**, declare that:

The research presented in this thesis, except where otherwise indicated, and is my original work.

(i) This thesis has not been submitted for any degree or examination at any other university.

(ii) This thesis does not contain other persons' data, pictures, graphs or other information, unless specifically acknowledged as being sourced from other persons.

(iii) This thesis does not contain other persons' writing, unless specifically acknowledged as being sourced from other researchers. Where other written sources have been quoted, then: a) their words have been re-written but the general information attributed to them has been referenced; b) where their exact words have been used, their writing has been placed inside quotation marks, and referenced.

(iv) Where I have reproduced a publication of which I am an author, co-author or editor, I have indicated in detail which part of the publication was actually written by myself alone and have fully referenced such publications.

(v) This thesis does not contain text, graphics or tables copied and pasted from the internet, unless specifically acknowledged, and the source being detailed in the thesis and in the References sections.

Kayode Timothy Akindeji Date

01 February 2022

As the candidate's supervisor I agree/do not agree to the submission of this thesis.

Dr Remy Tiako Date

……

Prof Innocent Davidson Date

……

COLLEGE OF AGRICULTURE, ENGINEERING AND SCIENCE

DECLARATION 2 – PUBLICATIONS

Details of the contribution to publications that form part/or include research presented in this thesis (include publications in preparation, submitted, in press and published and give details of the contributions of each author to the experimental work and writing of each publication).

Publication 1: **K. T Akindeji,** "A review on protection and control of Microgrid with distributed energy resources integration". Paper Presented at Protection, Automation and Control (PAC) World Conference, University of Strathclyde, Glasgow, Scotland, 29 June -2 July 2015.

Publication 2: **K.T. Akindeji,** and I. E. Davidson**,** "Microgrid and Active Management of Distribution Networks with Renewable Energy Sources". In Proceedings of the 24th South African Universities Power Engineering Conference (SAUPEC), Vanderbijlpark, South Africa, 26-28 January 2016, pp.171-175.

Publication 3: **K.T. Akindeji**, R. Tiako and I. E. Davidson, "Use of Renewable Energy Sources in University Campus Microgrid – A Review". In Proceedings of the 27th Domestic Use of Energy (DUE) Conference, Wellington, South Africa, 25-27 March 2019, pp. 87 – 94. ISBN 978-0-6399647-3-7

Publication 4: K.T. Akindeji, R. Tiako and I. E. Davidson, "Optimization of University Campus Microgrid for Cost Reductions: A Case Study". *Advanced Engineering Forum* (accepted for publication).

Dedication

To the Only Wise God, the Alpha and the Omega**.**

Acknowledgments

I give all the glory to God Almighty for being the Alpha and Omega of this work.

I am very grateful to my supervisors, Dr. Remy Tiako and Prof Innocent Davidson for their painstaking guidance and unalloyed supports throughout the course of this work.

My sincere gratitude goes to my lovely wife, Bolanle and our precious daughters, Queen-Esther, Princess-Joyce and Prince-Rejoice for their love, support, prayers and understanding always.

I will not forget to acknowledge the fundamental role played by my parents, Chief Moses Obafemi Akindeji and Mrs Gbemisola Julianah Akindeji, they gave me the best education per time.

My appreciation also goes to Dr Temitope Adefarati, Dr Arman Goudarzi, Dr Elutunji Buraimoh, Dr Anuoluwapo Aluko, Dr Samuel Williamson (University of Bristol), Prof David Dorrel and my colleagues at the department of Electrical Power Engineering, Durban University of Technology. I am indebted to Mr Trevor for granting me access to the energy management site of the five campuses of the university.

I will not fail to acknowledge and appreciate the financial support received from my employer, Durban University of Technology through the Staff Higher Education Subsidy (SHES) fund. In the same vein, I am greatly thankful to the management of University of KwaZulu-Natal (UKZN) for the opportunity given to me to study at the university and the support received from the staff of the college of Agriculture, Engineering and Science.

Finally, my profound gratitude goes to my Pastors and all the members of the Winners' Chapel International in Durban for their spiritual guidance and prayers, may the Lord bless you all. Amen.

ABSTRACT

Affordable and clean energy is one of the sustainable development goals (SDGs) to be achieved by the year 2030. Renewable energy sources such as wind, hydro, solar are free and inexhaustible globally to produce clean, reliable and cost effective power. However, most renewable energy sources are intermittent, to overcome this barrier, the concept of microgrid has been deployed in many applications to aggregate renewable energy resources, energy storage system and energy management system for sustainable, reliable, economical and environmental - friendly power system. Furthermore, considering the continuous increase in the cost of electricity and recent load shedding in South Africa, universities can reduce cost of energy demand, avoid interruption of academic activities due to load shedding and develop a test-bed or laboratory in which students and faculty staff can conduct research to advance modern power system through a self-sustaining microgrid. The university is like a separate entity and can operate as an island with sufficient resources to meet her energy demands.

This thesis analyses the performance of a university campus microgrid using the five campuses of the University of Kwa-Zulu Natal as case studies considering economical and environmental benefits. Three different studies are carried out to achieve the aim and objectives of this work. The first study considers a grid connected microgrid using the real time data from the university energy management system, the modelling and simulations are implemented in HOMER Grid®. The main objective is to determine the optimal generation mix and size of a hybrid system consisting of the utility (eThekwini Electricity), solar PV, wind turbine, diesel generator and battery system taking into consideration the cost of energy (COE), net present cost (NPC), return on investment (ROI), payback period (PBP), utility cost saving and CO_2 emission reduction. The second study aims to optimize the operational cost of a hybrid power system (PV-Wind-Diesel Generator-Battery) using two campuses as case studies. The objective function is formulated as a non-linear cost function and solved using a MATLAB function, 'quadprog' considering daily demands during summer and winter study and vacation periods with the aim of comparing the fuel costs and assess the effectiveness of the hybrid system. The third study proposes a novel optimization algorithm, the Quantum-behaved bat algorithm (QBA) to solve combined economic and emission dispatch (CEED) problem in an off-grid microgrid with onsite thermal generators and renewable energy sources (PV and Wind).

The results obtained from these studies show and validate the fact that renewable energy source (RES) can be used to meet university energy demands in an economical way and reduce carbon footprint on campuses. It is observed from the result that the annual utility bill savings range from R3.97 million to R17.42 million and directly proportional to the peak load. The average emission reduction for all campuses is 49.6% except

Pietermaritzburg where it is 33.7 %. In addition, the results will help university management as well as city management to invest wisely in renewables for energy sustainability and reliability.

TABLE OF CONTENTS

LIST OF FIGURES

LIST OF TABLES

ACRONYMS AND ABBREVIATIONS

AC	alternating current
ACS	annualized cost of the system
BA	bat algorithm
BESS	Battery Energy Storage Systems
CEED	combined economic emission dispatch
CG	conventional generator
CO_2	Carbon dioxide
COE	Cost of energy
CRF	capital recovery factor
DC	direct current
DER	distributed energy resources
DoD	depth of discharge
EMS	energy management system
EPS	Electrical Protection System
ESS	Energy storage system
EV	electric vehicle
FC	Fuel Cell
GHG	Greenhouse Gas
GW	Giga Watts
HOMER	Hybrid Optimization of Multiple Energy Resources
HRES	hybrid renewable energy system
ICT	information and communication technology
IEEE	Institute of Electrical and Electronic Engineers
IRR	Internal rate of return
LCOE	Levelized Cost of energy
MAS	multi-agent system
MPPT	Maximum power point tracking
MW	Mega Watts
NPC	net present cost

PBP	Payback period
PCC	point of common coupling
PEV	plug-in electric vehicles
PMB	Pietermaritzburg
PV	Photovoltaic
QBA	quantum-behaved bat algorithm
RES	renewable energy source
RG	renewable generator
SCADA	supervisory control and data acquisition
SDG	Sustainable Development Goal
SoC	state of charge
UCM	University Campus Microgrid
UKZN	University of Kwa-Zulu Natal
WECS	wind energy conversion system
WT	Wind Turbine

List of Symbols

A	area of wind turbine blade
A_i	loudness of the i^{th} bat
a_i, b_i, c_i , d_i.	fuel coefficients of generator
B_{ij}, B_{oi}, B_{oo}	loss coefficient of the generators
B_{soc}	battery state of charge
C_{AT}	total annualized cost
C_{NPC}	total system cost (NPC)
C_p	performance coefficient of wind turbine
C_{PV}	rated capacity of the PV panel or array (kW)
d_i	direct cost of the i^{th} renewable generator
D_{PV}	derating factor (in %) of the PV array
e_i, f_i, g_i , h_i	emission coefficient of generator
F_c	fuel cost
F_e	emission value in (kg/h)
f_i	frequency of the i^{th} bat
f_{max}	maximum tolerable frequency
f_{min}	minimum tolerable frequency
F_T	total system cost
h_{new}	desired hub height
h_{ref}	reference hub height
I_{MPPT}	current of the maximum power point of the PV module
I_{PV}	current of the PV module
i_r	real interest rate
I_{SC}	short-circuit current of the PV module
I_T	solar radiation incident on the PV array (kW/m^2)
$I_{T,\,STC}$	incident solar radiation under standard test conditions ($1kW/m^2$)
k_i	price penalty factor in $/h
K_i	current temperature coefficient
$k_{p,i}$	penalty cost coefficient of the i^{th} renewable generator

$k_{r,i}$	reserve cost coefficient of the ith renewable generator
K_v	voltage temperature coefficient
N_{RG}	total number of renewable generator
P_{bc}	power received by the battery
P_{bd}	power emitted by the battery
P_D	total load demand (MW)
P_{dg}	power output of diesel generator
$P_{dg,rated}$	diesel generator rated capacity
P_{gi}	real power output of generator
P_L	transmission loss in (MW)
P_{PV}	Power output of PV module
P_{rated}	rated power of the wind turbine
$P_{RG,i}$	power generation of the ith renewable generator
P_w	power available to the turbine
$P_{WT,STP}$	output of the wind turbine at the normal temperature and pressure in kW
R_i	rate of pulse emission
T_C	PV cell temperature (°C)
$T_{C,STC}$	temperature of the PV cells in normal test conditions (25 ° C)
T_{PV}	cell temperature in °C
V	wind velocity/speed
V_{in}	cut-in wind speed of the wind turbine
V_{MPPT}	voltage of the maximum power point of the PV module
V_{new}	wind speed at the desired hub height
V_{OC}	open-circuit voltage of the PV module
V_{out}	cut-out wind speed of the wind turbine
V_{PV}	voltage of the PV module
V_{rated}	rated speed of the wind turbine
V_{ref}	wind speed at the reference height
α_P	temperature coefficient of power (%/°C)
β	pitch angle

η_c	battery charging efficiency
η_d	battery discharging efficiency
λ	turbine blade tip speed ratio
ρ	density of air

CHAPTER ONE

INTRODUCTION

1.1 Background

The importance of the Sustainable Development Goals (SDGs), specifically SDG 7(the Affordable and Clean Energy), cannot be overemphasized with respect to Africa's fastest-growing population, leading to increased energy demand for cooling, industrial production, and mobility. Presently, about 600 million people in the African continent are without access to electricity, and 900 million lack access to clean energy for cooking in the same region [1]. Moreover, despite having the richest solar resources globally, Africa has only 5 GW of solar PV installed, less than 1% of the world's total. SDG 7 aims to ensure access to sustainable, reliable, modern, and affordable energy for all by 2030 [2, 3]. Table 1.1 shows the targets and indicators for SDG 7.

1.2 Problem Statement

The reliability of the electrical power supply is vital for the successful operation of the university as significant activities in the university such as teaching, learning, and research are energy-consuming. For example, research outputs are not determined only by adequate human resources but also the availability of well-equipped laboratories and facilities that need electrical power to function. The frequent load shedding in South Africa is a major concern for universities; hence, there is a need to find alternative sources in form of renewable energy sources (RES). Outages on campuses could lead to loss of revenues; which may include the cost of replacing damaged equipment, cost of sustaining teaching, learning, and research. The question is, what combination of available RES will be technically, economically, and environmentally viable for a university campus microgrid? Microgrid technology has evolved as a technical tool to solve both present and future challenges of the traditional power system. Microgrids produce energy locally thereby reducing energy cost and gas emission by using distributed energy resourses (DER). Microgrids offer technical,economics and environmental benefits because they utilise low carbon energy sources such as solar, biomass and wind; the fact that they are localised also implies reduction in transmission infrastructure cost. Hence, the project seeks to deploy microgrid technology on the UKZN campuses. The engineering optimization technique will be utilized to determine the optimum generation mix for a hybrid renewable energy system, and viable options will be determined based on several economic indices. The results are expected to inform University and municipality management on investment decisions in renewable energy sources for energy sustainability and reliability.

Table 1. 1: SDG 7 targets and indicators [2]

S/N	Targets	Indicators
7.1	Ensure that everyone has access to cheap, dependable, and advanced energy services by 2030.	• The percentage of the population who has access to electricity • The proportion of the population that rely on clean fuels and technologies as their major source of energy
7.2	Increase the contribution of renewable energy in the global energy mix by a significant amount by 2030.	The proportion of renewable energy in total final energy consumption
7.3	Double the global rate of energy efficiency improvement by 2030.	In terms of primary energy and GDP, energy intensity is assessed.
7a	Enhance international collaboration by 2030 to make clean energy research and technology, such as renewable energy, energy efficiency, and advanced and cleaner fossil-fuel technology, more accessible, and to encourage investment in energy infrastructure and clean energy technology.	Starting in 2020, a certain amount of US funds will be mobilized each year to contribute to the $ 100 billion pledge.
7b	Expand infrastructure and technology to provide modern and sustainable energy services to all developing nations, particularly least developed countries, small island developing states, and landlocked developing countries, by 2030, in accordance with their specific assistance programs.	The amount of foreign direct investment in financial transfer for infrastructure and technology to sustainable development services as a percentage of GDP and the amount of energy efficiency investments as a percentage of GDP

1.3 Objectives and Methodology

This research investigates the feasibility and viability of using RESs as part of the energy sources on the university campus to provide reliable, cheaper, secure, and better quality power supply to meet all the load demands on campus. Therefore, this thesis aims to analyze the performance of a university campus-based microgrid considering its technical performance, economic implications, and environmental impact. Based on the aim, the objectives of the thesis are;

i) To develop a hybrid generation system based on a bi-objective optimization method that maximizes energy savings and minimizes greenhouse gas emission for university campus-based microgrid.

ii) To establish the generation mix for the university campus minimize environmental impacts and fuel costs, polynomial based multi-objective optimization problem is formulated that prioritizes renewable generation and minimizes fuel costs.

iii) To propose a hybrid off-grid microgrid that is useful for pre-evaluation and feasibility studies for critical facilities.

iv) To determine the optimal contribution of each component of a hybrid renewable energy system to a university campus-based microgrid.

v) To, via simulation studies, optimize the university campus microgrid (UCM) system to minimize energy consumption and costs.

vi) To estimate the consequent reduction of CO_2 and other greenhouse gas emissions that will result from the optimized configuration of a hybrid renewable energy system.

vii) To propose a new algorithm to solve the combined economic emission dispatch problem for power systems considering renewable energy integration.

The methodology used in this work is to optimize hybrid renewable energy systems for utility cost saving and reduction of emission on university campus. HOMER software was used in the scenario to size, model and simulate a grid connected microgrid for the five campuses. In the second scenario, the MATLAB function “quadprog” was used to optimize an off grid microgrid for two campuses during summer study, summer vacation, winter study and winter vacation periods. The third scenario employed the quantum-behaved bat algorithm with cubic criterion function to investigate the combined economic and emission dispatch of two campuses.

1.4 Contribution

The contributions reported in this thesis can be highlighted as follows:

- Proposes multi-objective constrained optimization formulations that help to determine optimal generation mix for the micro-grids of the two university campuses, in which economic, environmental and technical aspects were considered.
- Development of optimal dispatch models that reduce operational cost and maximize the use of renewable energy sources for two university campuses considering the availability of renewable energy sources for different climatic conditions and academic calendars. The optimization problem

is formulated as a non-linear quadratic objective function that minimizes the fuel cost by prioritizing the renewable energy sources and energy storage system over the conventional generating plants.

- Proposing a new metaheuristic optimization algorithm to solve the combined economic emission dispatch (CEED) problem using two university campuses as study cases. The proposed algorithm is the quantum-behaved bat algorithm (QBA), which improves the conventional bat algorithm. QBA has better convergence, easy of implementation, higher computational efficiency compared to other algorithms considered. The results show that the CEED objective function is superior at minimizing fuel cost as well as emission cost than the economic and emission dispatch objective functions. It is also shown that the proposed algorithm performs better with reduced total cost and emission levels when compared with the artificial bee colony algorithm. To the best of the author's knowledge, no other study of this nature has been published.
- In this work, the proposed microgrid architectures give a clear understanding of university campus energy demand, show the economic benefits of the integration of RES in off-grid microgrid application and establish the reduction of CO_2 emission. Furthermore, other government institutions, industries, businesses and private entities can adopt the proposed models with a view to enhance the reliability and security of energy supply.

1.5 Scope of study

The study presents the performances of campus microgrids considering the technical, economic and environmental benefits. The microgrids considered all through this study are AC microgrids due to the fact that the university campuses are connected to AC grid and all electrical networks operate in AC. This study investigates the impacts of hybrid renewable energy systems in microgrids operating both in grid connected and off-grid modes. The study was conducted by modelling and simulation using HOMER software and MATLAB. The five campuses of UKZN were used as case studies, four in the city of Durban and one in the city of Pietermaritzburg, South Africa.

1.6 Thesis outline

The remainder of this thesis is organized as follows:

- Chapter Two provides a state-of-the-art literature survey on off-grid microgrids. First, it covers the framework of a microgrid, including its control and protection systems. Next, a review of several microgrid components and sources is presented. Finally, the application of off-grid microgrids for university campuses is reviewed, and the environmental, economic, and technical benefits are presented.

- Chapter Three presents the economic and environmental analysis of a hybrid renewable energy microgrid for five university campus microgrids. The economic analysis entails the cost of energy, net present cost, payback period, and internal rate of return, while the environmental analysis is based on the CO_2 emission and annual fuel consumption level.
- Chapter Four presents the optimization of hybrid renewable energy systems for off-grid applications. Two university campuses with different weather conditions (different locations) are used for this study. Four case studies – summer study period, summer vacation period, winter study period, and winter vacation – are used as scenarios to determine the optimal sizing of the hybrid generation system considering the least fuel consumption index.
- Chapter Five present a new optimization algorithm for the CEED problem for power systems integrating renewable energy systems. The formulation of the proposed algorithm is based on the bat algorithm to form the new quantum-behaved bat algorithm. The system models and parameters used are similar to those used in Chapter 4. Two seasons are considered – summer and winter, with the base case involving only conventional generators and the study case involving the integration of renewable generators to the power mix. The objective of the CEED is to simultaneously minimize fuel cost and emission cost while keeping the conventional generators within the operating constraints.
- Chapter Six provides the conclusion of this thesis, and future work is presented.

CHAPTER TWO

LITERATURE REVIEW

2.1 Introduction

This chapter gives a comprehensive review of previous work reported in the literature on microgrids and, by extension, university campus microgrids. The technical, economic, environmental benefits of a microgrid are also highlighted.

2.2 Overview of microgrid

The electrical power system is experiencing a continuous paradigm shift as a result of continuous load growth and the infiltration of distributed energy resources into the distribution network. Therefore, the structure and landscape of the power system must evolve continuously to accommodate new technologies to increase the reliability, security, and efficiency of the entire system. With the advent of information and communication technology (ICT), new control methods, and advanced power electronics devices into power networks, the traditional or conventional power system must give way to a smartgrid. Smartgrid is a power grid that metamorphoses the present grid into a more reliable, sustainable, efficient, and consumer-oriented grid using advanced metering, communication technologies, protection, and distributed intelligence [4-6]. Among the major drivers for smartgrid implementation are (i) integration of renewable energy resources, (ii) reduction in losses, (iii) management of peak demands, (iv) short- falls in electricity supply, and many more [7]. Some parts of the building blocks of the future smartgrid include microgrid, virtual power plant (VPP), and active distribution network (ADN); among these, microgrid has become a vital and inevitable component for the evolution of smartgrid [8, 9]. Microgrid, even though a smaller version of the traditional grid, is distinct in its composition. A microgrid is made up of distributed generations (both conventional and renewable), energy storage, and controllable loads located in close proximity to the consumer [10]. Various definitions of microgrid abound in literature; some are quoted below;

"A microgrid is an electrical entity that facilitates high depth of DER units and relies on ICTs and advanced control/protection strategies" [4]

"Microgrids are localised grids that can connect from the traditional main grid to operate autonomously and help mitigate good distribution to strengthen grid resilience and can play an important role in transforming the national electric grid" [11].

"Microgrids comprise LV distribution systems with distributed energy resources (DER) (microturbines, fuel cells, PV, etc.) together with storage devices (flywheels, energy capacitors, and batteries) and flexible loads. Such systems can be operated in a non-autonomous way if interconnected to the grid, or in an

autonomous way if disconnected from the main grid. The operation of microsources in the network can provide distinct benefits to the overall system performance if managed and coordinated efficiently" [12].

"A Microgrid is any small or local electric power system that is independent of the bulk electric power network. For example, it can be a combined heat and power system based on a natural gas combustion engine (which cogenerates electricity and hot water or steam from water used to cool the natural gas turbine), or diesel generators, renewable energy, or fuel cells. A Microgrid can be used to serve the electricity needs of data centers, colleges, hospitals, factories, military bases, or entire communities (i.e., "village power")" [8].

" Microgrid is a group of interconnected loads and distributed energy resources within clearly defined electrical boundaries that acts as a single controllable entity with respect to the grid. A microgrid can connect and disconnect from the grid to enable it to operate in both grid-connected or island-mode."[13].

"Microgrid is a group of interconnected loads and distributed energy resources with defined electrical boundaries forming a local electric power system at distribution voltage levels, that acts as a single controllable entity and is able to operate in either grid-connected or island mode."[14].

Recently, a lot of factors such as technical, cost, and social have fuelled the drive for the implementation of the microgrid concept. Likewise, climate change continues to motivate the global interest in RES to increase the energy and electricity supply capacity worldwide. As at the end of 2018, South Africa had a net generating capacity of 6,065 MW from RES. Table 2.1 shows the overall generating capacity of power plants and other facilities that employ renewable energy sources to generate electricity. The data displays the capacity deployed and connected at the end of the calendar year for the majority of nations and technologies. Total capacity includes pumped storage, although total generation does not. The capacity and generating data are shown in megawatts (MW) and gigawatt-hours (GWh), respectively [1, 15]. One of the challenge with RES is the intermittent nature of their energy sources (wind, sun); the power generated is also intermittent or not of required power quality. As a result, there are stability, reliability, and power quality problems when they are connected to the main grid without a technical platform.

Microgrid technology provides a viable solution for the integration of distributed energy resources (DERs) into the electrical distribution networks at low-voltage and medium-voltage. As the share of renewable energy in the generating mix climbs, microgrid technologies are growing at a rapid pace. Micro-grids can assist to lessen the need for new utility production, transmission, and distribution by providing clean electricity and reducing grid congestion during peak hours. Furthermore, the cost of generating such electricity is reasonable [16]. Even though microgrids can provide several benefits to end-users, their

integration into present distribution networks is still hampered by several challenges, most notably their operation, protection, and control [17].

Table 2. 1: Capacity and production of electrical power from RES [1]

Capacity (MW)					
Year	2014	2015	2016	2017	2018
Total Renewable Energy					
World	1 692	1 845 621	2 007 256	2 181 577	2 356 346
Africa	33 032	35 297	37 930	42 702	46 251
South Africa	2 710	3 429	4 650	5 587	6 065
Wind					
World	349 202	416 211	466 957	514 747	563 659
Africa	2 398	3 318	3 830	4 576	5 465
South Africa	569	1 079	1 473	2 094	2 094
Solar PV					
World	171 597	217 373	290 975	383 316	480 619
Africa	1 559	1 926	2 968	3 778	5 122
South Africa	1 063	1 252	1 974	2 186	2 559
Production (GWh)					
	2013	2014	2015	2016	2017
Total Renewable Energy					
World	5 041 315	5 330 716	5 526 664	5 897 647	6 190 948
Africa	128 408	137 052	141 196	142 833	152 721
South Africa	1 566	3 413	5 948	8 011	10 453
Wind					
World	635 110	712 027	828 251	954 658	1 134 451
Africa	3 522	5 521	7 696	10 355	11 722
South Africa	37	1 057	2 484	3 698	4 924
Solar PV					
World	131 701	183 943	242 372	314 060	425 810
Africa	637	1 794	3 022	4 206	6 140
South Africa	54	1 075	2 136	2 842	3 725

Non-linearity in microgrid operation, changes in load demand, and uncertainty in renewable energy output all provide substantial obstacles in determining the best microgrid operation planning [18]. From unit commitment to economic dispatch to efficient power flow, the microgrid operating challenge is hierarchical. Focusing on the first two, the task at hand is to commit and deploy dispersed devices in a grid-connected mode to reduce energy and CO_2 emissions while fulfilling hourly power and heat demands [19].

2.2.1 Architecture and design

Microgrids operate in two modes; these are grid-connected and islanding modes. The transition from grid-connected mode to island mode can be triggered by poor power quality at the main grid, such as voltage or frequency deviations and unscheduled events, i.e., major faults at the main grid. Two IEEE standards, IEEE 2030.7(IEEE standard for the specification of microgrid controllers) and IEEE 2030.8 (IEEE standard for the testing of microgrid) address the control functions of a microgrid in connecting to and disconnecting from the main grid [20]. Islanding detection of distributed generators is one of the most important aspects of interconnecting them to the distribution system. Remote approaches linked with islanding detection in utility sides and local methods are two types of islanding detection techniques (including passive, active, and hybrid techniques) associated with islanding detection on the microgrid side [21]. As a result, accurate islanding detection and prompt distribution generator disconnection are required to minimize safety issues and equipment damage caused by microgrid islanding operations. The most prevalent islanding protection solution is based on passive technology, which does not disrupt the system but has huge non-detect zones.. Khamis [22] proposed a simple and effective passive islanding detection method using the phase space technique and probabilistic neural network. The method was able to sense the difference between the islanding condition and other system disturbances. The voltage magnitude and angle were monitored on both sides of the circuit breaker for resynchronization. The voltage angle was measured using a phase-locked loop (PLL). Whenever the voltage angles and magnitudes on both sides were the same, the circuit breaker closee. Resynchronization could be sluggish and take anything from a few milliseconds to several minutes, depending on the network traffic and settings. As a result, a broad resynchronization, self-healing, and autonomous supply restoration method was required. The following technical requirements must be met for resynchronization to the main grid [6, 20];

i. Frequency deviation at the point of common coupling (PCC) < 0.1 Hz

ii. Voltage angle difference at the PCC < 1º

iii. Voltage magnitude difference at the PCC < 5%

Maintaining system stability during and after the transition between grid-connected and islanded operating modes involves significant technological hurdles. The most important and comprehensive international

standard for connecting islanded power systems with the public grid is IEEE 1547.4. In terms of the grid, the standard provides two operating modes (grid-connected and island) and two transitional modes (transition to island and reconnection) for the microgrid. There are different criteria in terms of voltage and frequency operating limitations for each operation mode. The IEEE 1547 codes have been designed for the interconnection to ensure that the island occurrence has to be detected within a specified time interval of 2 s [23, 24].

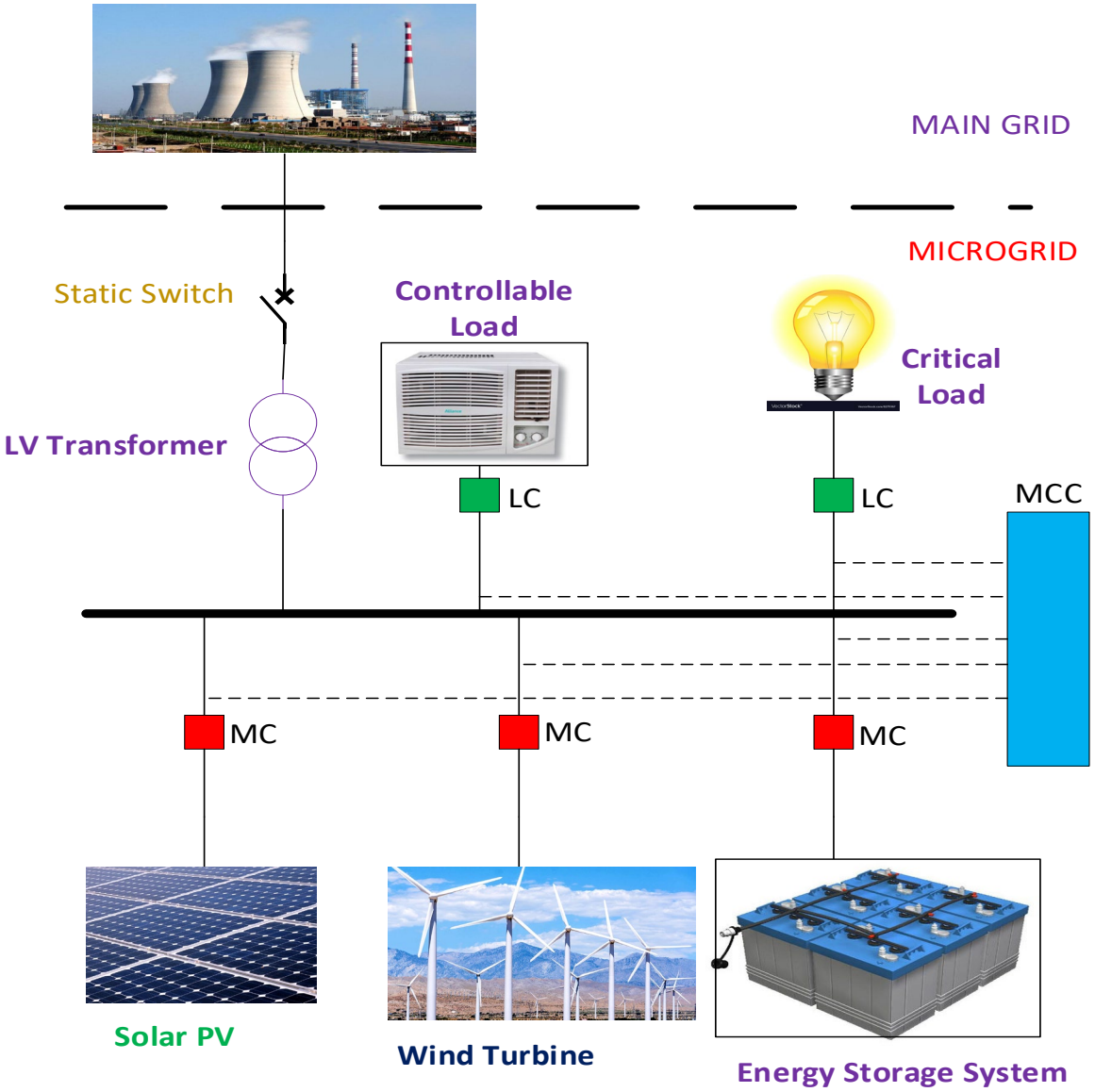

Figure 2. 1: A typical microgrid overview

LC-Load Controllers, MC-Microsource Controller and MCC-Microgrid Central Controller)

2.2.2 Control and Protection

To operate in parallel with the grid, island, or transition modes, a microgrid must be capable of managing load voltage and frequency while also protecting the microgrid's network and equipment. Therefore, for the reliable operation of a microgrid, the control, and protection system must be well designed. Given the above, advanced communication technologies or devices would be the backbone of a Microgrid, especially in terms of power control and protection. The available communication system includes a power-line carrier, radio communication, leased telephone lines, and global mobile (GSM) communication systems. The major challenges relating to Microgrid protection and control as identified in the literature include [9]:

- Bidirectional power flow
- Stability issues
- Low inertia of DER
- Uncertainty (intermittent nature of RES)
- Correct protection operation in grid and islanding modes, considering the vast differences between the fault current levels of islanding and grid modes.

2.2.2.1 Control of microgrid

The control of microgrid is a function of many factors such as configuration, type, existing distribution network, hence, there is no specific control architecture. However, there are primary control functionalities required in a microgrid as summarised in figure 2.2. The major control variables in microgrids are frequency, voltage, real power and reactive power [12, 25].

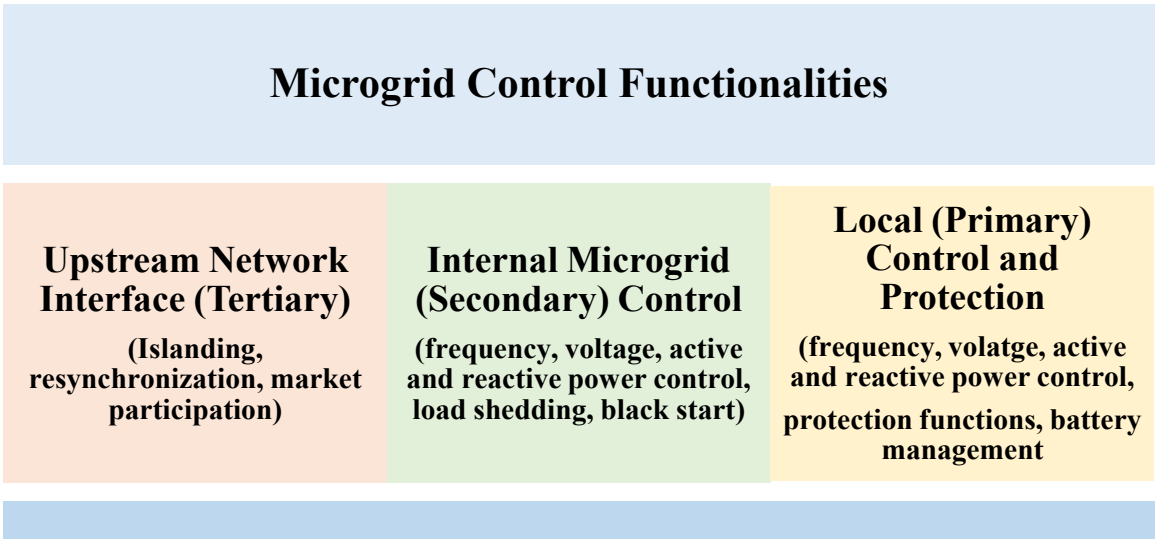

Figure 2. 2: Overall microgrid control system functionalities [12].

The major difference between a microgrid and a distribution network with DERs is that the main grid sees a microgrid as a coordinated and controllable entity. The control and management of microgrid operations involve many tasks with multiple objectives that include regulating power flow, controlling power electronic devices, managing different energy resources, and power quality [26]. The control architectures are typically designed in hierarchical layers, lower and upper. The lower layers carry out the upper layer decisions and balance the system in real-time, relying on the local controller of each component, while the upper layers handle the medium-term microgrid management [27]. The three-level hierarchical control system is needed in the case whereby multiple microgrids are interconnected within a network; hence control methods applied in the microgrid are classified as primary, secondary, and tertiary controls. The primary control represents the fundamental control responsible for balancing the frequency and voltage distributed between the grid and the microgrid load. The secondary control takes care of errors that are not removed by the primary control, while the tertiary control manages energy exchange between the grid and microgrid and peak shaving[6] [28, 29]. The hierarchical control can also define the level of operation in the microgrid's energy management system (EMS). According to [30], the primary level ensures a balance between generation and load in case of unintentional islanding or sudden load increase; the secondary control reduces the deviations due to the tertiary control taking into consideration forecasts and real measurement while the tertiary limits microgrid operating cost by considering loads, weather and mobility profile forecasts. In [3], a primary control for DER converters used in autonomous microgrids was developed to operate in voltage-controlled mode following a droop control algorithm for proper system load sharing among the DERs.

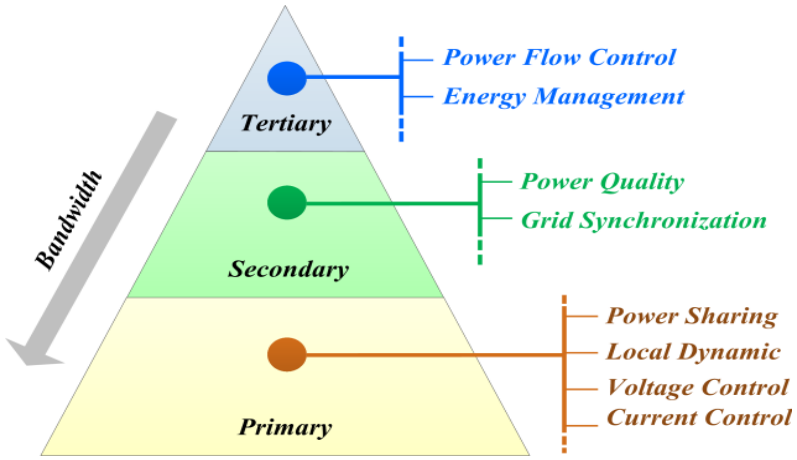

Figure 2. 3: A typical hierarchical control system [26].

Other control architectures for microgrids include centralised and decentralised controls.

- ***Centralised***: Microgrids can be controlled centrally by expanding and adapting the service of present EMS properly. The principal attribute of centralised control is that the microgrid operator is responsible for the operation of the DER [12]. Some of the disadvantages of centralised control are listed below [31]:
    i. Huge investment in data and communication process
    ii. Maintenance requires that the entire system to shut down
    iii. The entire system may crash if the central controller fails

Centralized control is generally employed in various supervisory control and data acquisition (SCADA) systems. As a result, the system operator has direct control over the whole power system in a single control environment, allowing optimal system-wide optimization. A microgrid, on the other hand, is a complex and diverging system with several controlling components. A dependable, high-speed communication network between the central controller and local regulators is required for a centralized microgrid EMS [32].

- ***Decentralised***: The design and development of the decentralised control system are founded on multi-agent system (MAS) theory, i.e., a system having two or more coordinated agents. The fundamental concept of MAS is that an independent control process is presumed by each controllable unit, namely power converters, loads, or distributed generators. The MAS concept illustrates the coordination algorithm, the communication (information exchange) between the agents, and the entire system's arrangement, making the system more resilient to faults [12, 27]. For example, decentralised control can be used to control bus voltage where measurement and communication methods are not feasible. One advantage of this control method is improving the power system operation without huge investments in communication systems, thereby saving costs [33]. A decentralised control was used in [34] to improve the system stability of a grid with multiple microgrids in which back-to-back (B2B) converters were used to provide reliable interface and isolation between the grid and microgrids. Decentralised control is a potential panacea to microgrid control and energy management problems. For example, the need of a central controller is not crucial; the remaining part of the system will still work if the central controller fails. However, due to innate security issues, decentralised control makes microgrids vulnerable to physical and cyber-attacks; hence, the successful operation depends largely on efficient communications between local agents and their neighbours [32]. As stated in [35], both hierarchical and decentralised control schemes can be employed to aggregate independent microgrids to offer their excess capacity to the utility and aggregate individual distributed generators to tender their capacity to the consumers in the microgrid. In this control, decision-making follows a hierarchical structure.

A vital aspect of microgrid control is energy management (EM) to maximize the benefits of microgrid and ensure a stable and reliable operation. Microgrid EM is application software that can distribute most appropriately the power output among the distributed generators, supply the load at a low-cost, and facilitate automatic system reconnection in response to transition between grid-connected and autonomous modes. Therefore, the primary objective of EM is to make the microgrid economically feasible by making decisions for the generation and dispatch of electric power using present and estimated weather, load, cost of fuel, price of electricity, environmental and government policies [25, 32, 36, 37].

2.2.2.2 Microgrid protection

An Electrical Protection System (EPS) must be installed on all electric power systems to safeguard them from electrical breakdowns. The EPS should prevent an electrical failure from spreading across the electrical network and disrupting the remainder of the power system. In addition, the EPS must protect persons, assets, and infrastructure in the impacted region, lowering the risk of harm at the very least. The essential needs for EPSs are as follows:

(i) Reliability: It is the characteristic that ensures that the protection will work in any situation;
(ii) Selectivity or discrimination: This implies that the EPS should only disconnect and isolate the network segment that is damaged; this characteristic is directly connected to the coordination of protection;
(iii) Sensitivity: It refers to the capacity to identify faults accurately, as well as the coordination of protection;
(iv) Response time: It refers to the capacity to isolate an issue in a short amount of time. ; and finally
(v) Stability: This means that the system must stay stable even if an unforeseen incident occurs in a protected zone. [38].

Microgrid protection is a major operational problem, especially with integrating DERs that may lead to different fault current levels, particularly when operating in islanded mode. This can interfere with the operation of the protection relays; consequently, faults can be misclassified or not detected. The concept of Optimal Wavelet Functions Matching Pursuit (OWFMP) was introduced in [39] derived from particle swarm optimization (PSO) technique that selects the optimal wavelet function combination capable of extracting hidden features in transient signals for reliable fault detection and classification in MG operations. Another significant difficulty that must be addressed when establishing a microgrid is designing an acceptable protection strategy. In fact, unlike standard distribution networks, fault currents in microgrids can vary unpredictably and iregularly depending on where the fault is located. This is primarily due to the availability of inverter-based DER and the ability of microgrids to modify their architecture and operating mode dynamically. As used in traditional distribution system protection schemes, fixed relay settings appear

to be ineffective for microgrid protection, particularly for microgrids that may operate in both grid-connected and islanded modes [17]. In [40], the authors suggested a method for monitoring essential components of a campus MG in order to perform preventative maintenance and protection. They deployed a smart sensor network that gathered status information from intelligent devices and offered input to protective switchgears using wired and wireless connections and industry-standard protocol. The findings suggested that smart monitoring and distributed control may save energy and generate maintenance warnings. Fault disruptions must be detected as soon as possible to improve microgrid performance. Panigrahi presented a new approach for detecting and classifying distinct faults in microgrids (comprising Wind Turbines (WT), diesel generators, Solid Oxide Fuel Cells (SOFC), and micro-turbines) [39]. Using a multi-resolution method, the Wavelet transform and Wavelet Packet Transform (WPT) were employed for detection and feature extraction to describe the various faulty signals [41]. Another concern regarding microgrid protection is the gradual increase in the penetration levels of intermittent RESs, leading to power quality problems and voltage instability. Thus, the need for the development of effective signal processing methods (SPTs) for the quick and accurate identification and categorization of disturbances in order to ensure the microgrid's dependable functioning. For handling islanding and power quality problems in microgrid environments, SPTs such as the Fourier transform (FT), short-time FT, Hilbert transform (HT), Hilbert–Huang transform (HHT), parallel computing, wavelet transform, wavelet packet transform (WPT), Gabor transforms, S-transform and others are commonly used [16]. In another perspective, the security mechanism is harmed by the dynamic behavior of micro-grids, such as mode of operation (grid-connected and islanded) and non-linear behavioural features of system components. Due to the following operational concerns, traditional overcurrent (OC) relays may have major relaying problems: In islanded mode, the contribution of fault current is much lower than in grid-connected mode, and (ii) the contribution of fault current is largely dependent on the kind of DERs employed (synchronous or inverter-based) . External devices such as fault current limiters (FCLs) and fault current sources (FCSs) can be added to microgrids to assist protection measures and maintain constant performance regardless of the mode of operation. [42].

2.2.3 Classification of microgrid

Microgrids are classified based on different factors as listed below;

- ✓ Mode of operation: Islanded(off grid) and Grid connected
- ✓ Type: AC, DC and Hybrid
- ✓ Source: Renewables, Diesel and Hybrid
- ✓ Application/Scenario: Residential, Industrial, Commercial, Campus, Military, Community

Some of the existing types of microgrids are discussed below.

2.2.3.1 Off-grid/Islanded

Most dwellers in remote or rural areas of developing countries have no or limited access to electricity as a result of the distance to the grid, high operational costs. Most of these rural villages rely on a sort of microgrid known as off-grid microgrids for power delivery. An off-grid microgrid is a variation of a microgrid that operates in islanded conditions. According to African Development Bank (AfDB) [43], a new proposal to deliver power to 205 million people in Africa will boost the continent's overall economic development. This new strategy asks for the construction of several on-grid and off-grid microgrids that rely on renewable energy sources. The African Development Bank's suggestion for off-grid microgrids is significant support for decentralized power generating systems. Quality and dependable energy sources will aid Africa's industrialisation and supply people with clean energy for cooking and other uses. As reported in [44], in an off-grid hamlet, a Canadian utility evaluated the use of utility-scale photovoltaic (PV) power and Battery Energy Storage Systems (BESS) to augment existing diesel generators. Islanded microgrids, in particular, can provide a dependable energy supply in tiny distant locations where power grid growth or extension is technically and/or economically impossible. Because the main grid does not support these systems, they serve as a helpful test bed for developing adequate control functions that can assure a consistent supply of power [17]. Microgrids have the potential to improve the resilience and dependability of bulk transmission lines, in addition to promoting energy independence in rural areas. Resilience is defined as “the ability of power system to withstand large-scale, low-frequency events like hurricanes, avalanches, wildfires, earthquakes etc.” In contrast, reliability of a power system is defined as “its ability to provide uninterrupted power to its consumers even when the network is impacted by sudden perturbation”. Microgrids, on the other hand, are not often subjected to the same dependability requirements as transmission grids, putting isolated populations at danger of prolonged blackouts [43]. Therefore, optimized hybrid renewable energy system (HRES) has become a more viable alternative to power rural communities, a system that is economical with high level of sustainability. Prominent among the DERs used in HRES are solar PV, fuel cell, wind turbine, biomass, diesel generator and energy storage devices. Some of these HRES designed for rural electrification are reported in [43, 45-50].

2.2.3.2 Community

A community microgrid is a collection of interconnected loads and distributed energy resources that operate as a single controlled entity in relation to the grid and are contained within well defined electrical limits. In other words, when members of a community decide to pool their resources (generation, load, and/or storage devices) in order to cut expenses, enhance profits, and make better use of their assets, they form a community microgrid. As a result, a community microgrid is a collection of organizations that trade energy and services according to the community's norms. A community microgrid may connect to the grid or

disengage from it, allowing it to function in grid-connected or island-mode. Furthermore, a community microgrid is physically connected to its community and might be owned by the community or another entity [51]. In the developing world, community microgrids can be used to achieve electrification for the first time and to help communities achieve renewable energy targets [52]. Microgrids are used to serve a single consumer or energy user, such as a university or hospital. The growing community microgrid, on the other hand, frequently serves numerous clients. A community microgrid's primary goal is to ensure that citizens access key services during a grid outage. Police and fire stations, hospitals, waste water treatment plants, schools, emergency shelters, grocery stores, gas stations, communications centers, and other facilities may all be part of a community microgrid [53]. Microgrids in communities must be managed and operated in a lean and flexible way that is tailored to the needs and capacities of the main stakeholders. They will be unsustainable in particular if they are significantly burdened by poor governance, complicated legal requirements, and expensive transaction costs. Some towns' environmental endeavors have resulted in the creation of community microgrids that use a large percentage of renewable energy, if not all of it. Furthermore, one of the most common social goals of community microgrids is to offer inexpensive power to the whole local community, and they may be forced to give service to disadvantaged consumers at a non-economic price. The socio-economic and socio-technical nature of community microgrids necessitates novel approaches to bring together the goals and interests of all stakeholders, especially the community, the investor, and the service provider, while fostering community participation and equity, and encouraging long-term investments, all while balancing social and economic objectives to achieve better outcomes for the co-op [54]. In [55], in a community microgrid, the author explored the best scale of renewable energy generating resources. The cost of renewables and community welfare were optimized, while air conditioning systems were used to maintain the comfort zone of indoor temperature in all households. With varying time-of-use energy rates, community welfare was assured by limiting purchased power from and maximizing sold power to the utility system.

2.2.3.3 Hybrid

In this context, a hybrid microgrid (HM) is made up of multi-bidirectional power electronic converters that connect DC and AC networks. Because it incorporates the benefits of both ac and dc systems, hybrid ac–dc microgrid design is gaining a lot of interest. However, as additional dc loads (such as data and communication centers, LED lights, and computers) and dc DERs (such as solar PV, fuel cells, and distributed energy storage (DES) become available, hybrid ac/dc microgrids will become increasingly appealing. Hybrid microgrids allow you to combine the advantages of both ac and dc microgrids [56]. One or more "interlinking converters" connect the separate ac and dc subgrids (IC). The ac and dc components (sources, loads, and storages) are separated and linked to their own subgrids to decrease the number of

power conversion stages and therefore improve overall efficiency. As a result, the hybrid ac-dc power design increases the entire system's dependability and power quality. Ac generators such as induction generator interfaced wind turbines, synchronous generators fueled by diesel, small-hydro, and other ac generators, as well as ac loads like pumps and fans, make up the HM's ac subgrid. Photovoltaic (PV) modules, fuel cells, other dc power sources, and dc loads like LEDs and digital computers make up the dc subgrid. Appropriate ac/dc storage is interfaced either on ac/dc buses or inside the IC [57]. Ac loads and DERs may be connected to ac buses, whereas dc loads and DERs could be connected to dc buses in hybrid microgrids. As a result, the number of needed converters and the related conversion power losses would be reduced, lowering the planning cost and enhancing energy efficiency [56]. However, compared to the pure ac or dc microgrids, the power management for the HM is more complex because of the coexistence and interaction of ac and dc subgrids. Without a proper power management strategy, the stable and reliable operation of the HM will be degraded [58]. Although the integration of AC microgrids into distribution networks is relatively simple and inexpensive due to the fact that it only requires a partial expansion or upgrade of existing electricity infrastructure, the extensive use of AC/DC converters poses a number of challenges in terms of microgrid protection, communication, and operation. As a result, DC microgrids have lately emerged as a viable option for connecting a small number of isolated DC devices into brand-new networks [17]. Due to the advent of new semiconductor technology and sustainable dc power sources such as solar energy, DC grids are making a comeback. There has also been a surge in dc loads linked to the grid to conserve energy and reduce greenhouse gas emissions, such as plug-in electric vehicles (PEVs) and light-emitting diodes. Environmental concerns raised by traditional fossil-fuelled power plants have fueled this rise [59]. On the other hand, HM has a role in applications where power quality and dependability are critical, such as data centers and telecom towers. In addition to these systems, the HMG's dc subsystem may be utilized to increase the power ride-through capabilities and the voltage profile of the ac distribution network. HM can also enhance power quality by acting as a "virtual" active power filter or compensating for reactive power. The dc subgrid can also be used as an electric car charging station. By allocating suitable DERs to distinct customer nodes, HM may also guarantee a set level of dependability (type, site and size) [57]. A small HM was modelled and simulated using Matlab/Simulink in [60] to reduce multiple conversions of AC-DC-AC or DC-AC-DC as obtained in single AC or DC microgrid. The results showed that the system could maintain stability using coordinated control during the transition from grid mode to autonomous mode. Also, Liu [61] proposed a HM comprising of the wind turbine, diesel generators, solar PV, fuel cells, conventional AC loads, and DC loads. The simulation results showed that the system was stable under different microgrid configurations with higher efficiency than individual AC or DC microgrids. An HM architecture was proposed in [62] for smart buildings to enhance the integration of DER and remove

any interference from the grid. This architecture offered, among other benefits, peak shaving capacity of ESS.

2.2.3.4 Campus

Campus microgrid refers to university campuses, corporate campuses, and military bases. Most campuses are located in remote areas, especially military bases, where transportation of diesel fuel might be a challenge hence the need to integrate RES such as solar PV and energy storage into the energy system [52]. Military microgrids in the United States exhibit some of the most complex and inventive uses of distributed energy, with a focus on national security . Four outstanding military microgrids were highlighted in [63], these include;

i. San Diego's Miramar microgrid: This includes 1.3 MW solar PV, a 6.45 MW diesel and natural gas plant, a 3.2 MW landfill gas, energy storage system (Lithium-ion, flow batteries, and V2G), EV charging station, SCADA system, etc. In addition to meeting the base load, the microgrid was intended to help the base go green, improve cybersecurity, minimize demand charges, control overall energy load, participate in demand response, and offer grid services, among other things.
ii. Otis microgrid (Cape Cod, Mass): While islanded, the microgrid can meet all of the military facility's power demands. All included Raytheon's microgrid controller, a 1.5 MW wind turbine, a 1.6 MW diesel backup generator, and a 1.6 MW/1.2 MWh lead-acid battery energy storage and management system.
iii. Parris Island microgrid: At the US Marine Corps Recruit Depot (MCRD) Parris Island, South Carolina, a 10-MW microgrid was built to resist hurricanes and earthquakes. The military expected to save $6.9 million per year in utility and operating expenditures and reduce utility energy demand by 75% and water use by 25%.

In [64], an EMS was proposed to optimise the operation of a remote military microgrid to ensure continuous supply to critical loads. Garcia [65] used two mixed-integer linear programming to minimize the total cost of electricity and fuel consumption of diesel generators for a US Army base camp. The results showed that using different generator sizes produced fuel-saving, adding battery storage system increased the fuel savings and the addition of solar PV produced significant fuel savings. Universities are gradually establishing campus microgrids across the world, as they play an important role in reacting to climate change by developing knowledge and incorporating climate concerns into educational and research programs, as well as direct and indirect operational operations. Universities have a critical role to play in combating climate change. Many university campuses have implemented energy efficiency initiatives and

installed renewable energy sources to reduce the environmental consequences and expenses connected with power use.

2.3 University campus microgrid and renewable energy sources

The potentiality for the use of RES on universities campuses is valuable and constitutes a promising way to meet the institution's energy needs and at the same time reduce the emission of greenhouse gas (GHG) [66]. The university campus is an ideal environment to encourage the development of energy sustainability and utilization of RE. Institutional or university campuses can be easily transformed into microgrids having many buildings that are closely located. These buildings are connected electrically within the same network that is usually connected to the main grid through a single PCC, allowing a seamless transition between islanding and grid-connected modes. In other words, due to the small distance between DERs, and loads in university campuses, the development of a microgrid comes handy. A typical campus microgrid could consist of (i) the energy generation (both controllable and RES), (ii) the energy storage system, (iii) the load (critical and non-critical), and (iv) controllers for interconnection with the main grid [20]. In the USA at the McNeese State University, Lake Charles, Louisiana, a functional microgrid was implemented comprising 15 kW of solar PV (Chroma Inc), two 65 kW of CHP units (Capston Inc), battery storage, a smart inverter (ABB Inc) and many rotating and resistive loads. The campus microgrid control was decentralized using an 800-XA system from ABB Inc [40]. Another campus microgrid was developed at the University of Genoa, Savona campus; the Smart Poly-generation Microgrid (SPM) consists of two wind mills, a micro-cogeneration gas turbine, two CSP systems, a solar PV farm, electrical storage (Sodium-Nickel batteries), smart meters, two absorption chillers and two charging stations for electric vehicle [67].

2.3.1 Solar photovoltaic (PV)

Solar energy, without a doubt, continue to grow as the predominant source of renewable energy for the future. The sun, the primary source of most renewable energy, has inexhaustible potential to meet the increasing world demand for energy. The deployment of technologies that employ solar PV to produce electricity or heat devoid of pollutants will definitely reduce GHG emissions in the environment. PV cells are conceivably one of the notable solar technologies. They convert light radiation into electrical energy. For the purpose of installations, individual PV cells are arranged in modules; the modules are combined in panels while the panels are assembled to form arrays. The arrangement of the arrays (series or parallel) determines the overall current, voltage, and consequently power output of the arrays. PV technology is categorized into three cohorts of (i) thin-film PV technology, (ii) wafer-based crystalline silicon technology, and (iii) depending on the basic material utilized and the level of commercial development, CPV / organic PV (OPV) technology can be employed. Also, the type of semiconductor materials employed in PV energy generation dictates its power output to some extent; popular types of PV cells are listed below[68, 69]:

• Single-crystal silicon or monocrystalline cells

• Polycrystalline or multicrystalline cells

• Ribbon silicon cells

• Thin-film cells

The parameters of typical monocrystalline and poly-crystalline solar panels are given in Table 2.2 [70, 71] while a 5kWp array of poly-crystalline installed on the roof top at Durban University of Technology is shown in figure 2.4. The power generated from solar PV array or farm depends on solar irradiance and ambient temperature of the geographical location as well as the seasons of the year. Equations 2.1 – 2.4 describe the voltage-current relationship of a solar PV panel under given temperature and solar radiation.

$$FF = \frac{V_{MPPT} \times I_{MPPT}}{V_{OC} \times I_{SC}} \quad (2.1)$$

$$T_{PV} = T_A - s\left(\frac{N_{OT}-20}{0.8}\right) \quad (2.2)$$

$$V_{PV} = V_{OC} - K_v \times T_{PV} \quad (2.3)$$

$$I_{PV} = s[I_{SC} + K_i(T_{PV} - T_{AB})] \quad (2.4)$$

Where *FF* represents the fill factor of the solar PV module; I_{PV} and V_{PV} are the current and voltage of the PV module respectively, I_{MPPT} and V_{MPPT} are the current and voltage of the maximum power point of the PV module; I_{SC} denotes the short-circuit current and V_{OC} is the open-circuit voltage of the PV module. K_v and K_i are the voltage, and current temperature coefficients, respectively, T_{AB} and T_{PV} are the ambient and cell temperature in °C respectively. The power generated in watt from a PV array can be calculated by equation 2.5.

$$P_g = N \times FF \times V_{PV} \times I_{PV} \quad (2.5)$$

Where Pg is the total power output of the PV array and N is the number of PV modules in the array.

Table 2. 2: Parameters of a Mono-crystalline and Poly-crystalline PV Panel [72]

Parameters	Value		Unit
	Mono-Crystalline	Poly-crystalline	
Nominal capacity	220	220	W
Optimal Operating Voltage	28.36	38.95	V
Optimal Operating Current	7.76	5.65	A
Open circuit voltage	36.96	45.75	V
Short circuit current	8.36	6	A
Operating temperature	43	44	°C
Current temperature coefficient	0.00545	0.03%	A/°C
Voltage temperature coefficient	0.1278	-0.32%	V/°C

Figure 2. 4: A roof-mounted solar PV array at DUT

2.3.2 Wind Turbine

The wind is another free, inexhaustible, and clean source of energy that originates from the uneven heating of the atmosphere by the sun, roughness of the earth's surface and rotation of the earth. The geographical topography, ambient factors, and structures all influence wind flow patterns. This wind movement, or motion energy, may be captured by contemporary wind turbines and used to create power. The words wind energy and wind generation refer to the wind's ability to generate mechanical or electrical power. The kinetic energy inside wind turbines is converted into mechanical power by wind turbines [73]. A wind farm is a grouping of wind energy conversion systems (WECS) ranging in size from tens to hundreds that are coupled to provide a single output. A WECS comprises of a turbine (blades and rotor), a gearbox, a generator, and power electronic converters and transformers, which may or may not be present. The turbine

can be a fixed-speed wind turbine (FSWT) or a variable-speed wind turbine (VSWT); it can be coupled to the generator through the gearbox or not, and the generator can be a squirrel cage induction generator (SCIG), doubly fed induction generator (DFIG), or permanent magnet synchronous generator (PMSG). The generator of the WECS differs from those used in conventional power plants; they are majorly induction generators having different characteristics from the synchronous generators used in conventional power plants; however, permanent magnet synchronous generators have gained attention in the wind energy industry [74, 75]. The kinetic energy in the wind with density ρ and velocity V hitting a surface with area A of the turbine blades contains the power given by

$$P_k = {}^1\!/_2\, \rho A V^3 \tag{2.6}$$

However, only a fraction of P_k can be extracted by the wind turbine, which is given by

$$P_w = {}^1\!/_2\, \rho A V^3 C_p \tag{2.7}$$

Where P_w is the power available to the turbine and C_p, is a dimensionless quantity known as power coefficient or performance coefficient of the turbine, which is a function of the turbine blade tip speed ratio λ and pitch angle β, the blade tip speed ratio defined by

$$\lambda = \frac{R\Omega_m}{V} \tag{2.8}$$

Where R is the length of the turbine blade (radius of turbine rotor) and Ω_m is the angular speed of the rotor. Equation (2.7) can be rewritten as

$$P_w = {}^1\!/_2\, \rho \pi R^2 V^3 C_p(\lambda, \beta) \tag{2.9}$$

Theoretically, the numerical approximation of C_p cannot exceed 0.59 which is known as Betz limit, which implies that without power losses, only 59% of power can be extracted from the wind by the wind turbine for conversion into electrical power by the generator.

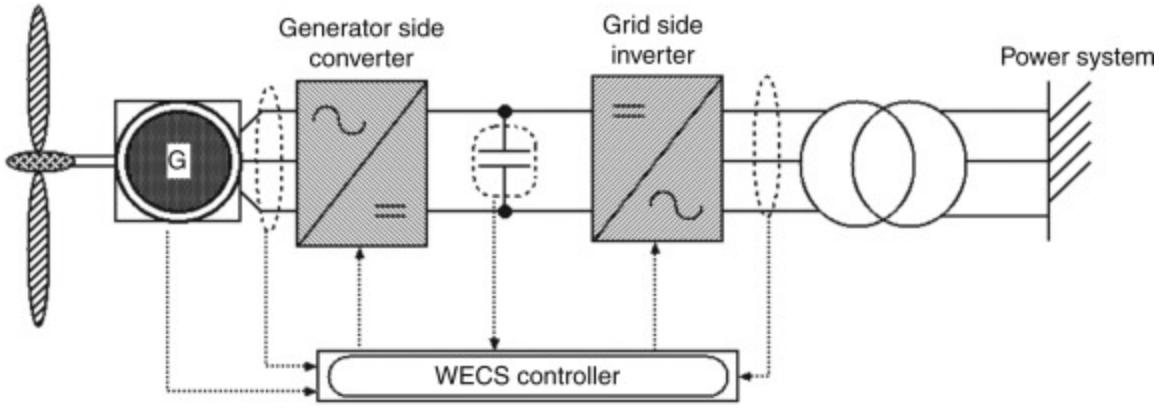

Figure 2. 5: Schematic diagram of a WECS [72].

2.3.3 Fuel Cell

During the last decade, fuel cells have grown in popularity in microgrids. Fuel cells are energy conversion devices that transform chemical energy from a fuel, often hydrogen, into electricity via a chemical reaction with only water and heat as by-products. Fuel cell stacks, dc-dc converters, dc-ac converters, ripple filter, step-up transformer, and grid are the major components in grid integration of fuel cells. Anode, cathode, electrolyte, and external circuit are well-known components of a fuel cell (load). A fuel cell's functioning concept is simple, despite its sophisticated architecture. The anode electrode of a fuel cell is continually provided with hydrogen fuel, while the cathode electrode is fed with the oxidant in the air, as illustrated in figure 2.6. Positive and negative ions are separated from the hydrogen fuel in the anode.

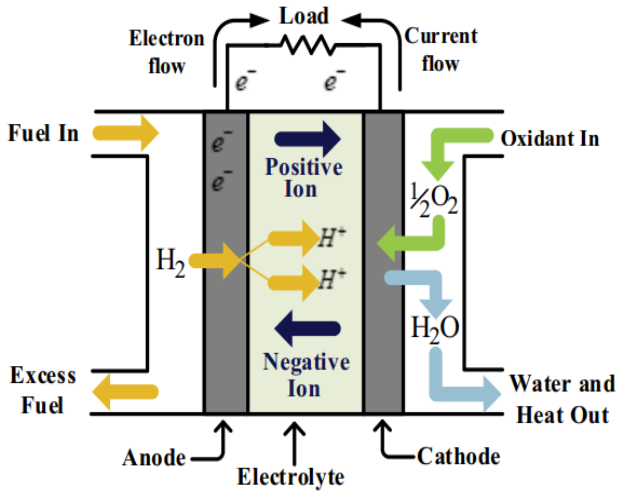

Figure 2. 6:Basic structure of a typical fuel cell[76].

To maintain stability, these electrons desire to join with the opposite side of the electrolyte layer, and the free electrons flow through a separate circuit on the cathode side (load). During this transition, these electrons transport electricity to the stage. Positive and negative ions and oxidant recombination generate

the exhausted oxidant or pure water in the cathode. Between the two electrodes lies the electrolyte membrane. At the anode, hydrogen gas is oxidized, while air (oxygen) is reduced at the cathode. The following equations describe the reactions at both electrodes and the entire chemical processes that occur in a fuel cell [76, 77]**.**

Anode equation: $2H_2 = 4H^+ + 4e^-$ (2.10)

Cathode equation: $O_2 + 4e^- + 4H^- = 2H_2O$ (2.11)

Total reaction: $O_2 + 2H_2 = 2H_2O + Heat + Electricity$ (2.12)

Based on concept and components, to generate electricity, six distinct types of fuel cells are used. :

a. Proton exchange membrane fuel cell (PEMFC)
b. Solid-oxide fuel cell (SOFC)
c. Alkaline fuel cell (AFC)
d. Direct methanol fuel cell (DMFC)
e. Phosphoric acid fuel cell (PAFC)
f. Molten carbonate fuel cell (MCFC)

Due to the availability of a wide range of hydrocarbon-based fuels, greater operating temperature, and better power conversion efficiency, SOFC is a feasible technological solution for power output ranging from a few kW to hundreds of kW. Among many, Proton Exchange Membrane (PEM) fuel cell is considered to be appropriate due to factors such as long stack life, fast startup, high energy efficiency, low temperature, and high modularity [78, 79]**.**

FCs in microgrids have been shown to be a potential option since they can supply stable, efficient, clean, quiet, flexible, scalable, and community-friendly energy [80]. As a result, higher efficiency, low emissions, low noise, and high modularity are some of the fuel cell's most appealing features. In the near future, fuel cell (FC)-based power generation systems will see increased scalability due to benefits such as reliability, portability, and low environmental impact [81]. With the output current fluctuating in direct proportion to the fuel flow rate, the electrical output appears as a comparatively low and somewhat constant voltage. This output is usually conditioned for a microgrid using a two-stage conversion system: first, a dc-dc boost converter raises the cell output voltage to provide an intermediate dc link, and then a traditional dc-ac inverter injects the fuel cell power into the ac microgrid. In most cases, the boost converter adjusts both the fuel-cell output current and the dc-link voltage in response to load changes [78]. Fuel cells have gained popularity in recent years; however, they are better suited to metropolitan regions and grid-connected microgrids. In [82], The practicality and economics of employing fuel cell backup power systems in cell

towers to offer grid services (e.g., ancillary services, demand response) were discussed. The primary goal of the research was to determine how fuel cells may become an essential element of telecom backup power in order to minimize system costs, environmental effects, and reliance on fossil fuels while assuring the availability of critical mobile services. Internal generation in Reference [45] was improved by using a SOFC generator mixed with artificial intelligence (fuzzy logic) to increase system/service resilience in a prototype microgrid.

2.3.4 Biomass

Rice husk, agricultural residue, jute stick, wood, animal waste, municipal trash, and other biomass materials are commonly utilized as replacement energy sources in low-income nations for cooking, heating, and other critical household activities. Biomass now provides for 8.5 percent of total global energy consumption, making it the world's fourth-largest energy source [83]. Agricultural wastes are widely available in rural areas and can be used as an alternative to diesel generators for off-grid power. Biomass usage for rural development is seen from a variety of angles. Biomass is commonly used for cooking in developing nations; however, this tendency is waning as affluence rises. Furthermore, because biomass resources are renewable and widely spread, many technologies are being developed to convert biomass to other energy services, such as electricity, process heat, and transportation fuels. However, energy development initiatives have been hampered by the restricted availability of biomass resources, pricing, and land usage. The availability of feedstock has a considerable impact on transportation costs and operational times for large-scale enterprises. Using locally accessible agricultural wastes as fuel in small-scale power production in rural farming communities might circumvent these concerns [84]. Because raw biomass cannot be utilized in a generator, it must first be transformed to biogas via a process known as gasification. Gasification is a process that converts carbonaceous materials into syngas by the interaction of raw materials at high temperatures with a regulated amount of oxygen and steam [85]. Biogas is a flammable gas made up mostly of methane and carbon dioxide, with minor amounts of other gases and trace components. Anaerobic digestion of organic materials produces methane-rich biogas, which is a flexible source of renewable energy. Methane may be utilized to replace fossil fuels in both heating and electricity generation, lowering greenhouse gas emissions and mitigating climate change. A biomass power plant is comparable to a steam-fired turbine in operation. Biogas produced by anaerobic digestion of organic waste powers a biogas generator. The yearly energy (kWh) generated by the biogas generator is stated mathematically as [83];

$$E_{BM} = P_{BM} \times C_{uf} \left[365 \left({}^{operating\ hours}/_{day}\right)\right]$$

Where C_{uf} is the capacity utilization factor and P_{BM} is the maximum rating of the biomass gasifier expressed as;

$$P_{BM} = B_T \times 1000 \times C_V \times \eta_{BG}$$

B_T is the available biomass in tons/year, η_{BG} represents overall conversion efficiency from biomass (fuel wood) to electricity, and C_V denotes the calorific value of biomass measured in MJ/kg [45, 83, 86]**.** Various applications of biomass as RES abound in literature [49, 83, 84, 87-93]; these include rural electrification, waste to energy conversion, cooking, and reduction of GHG emissions.

2.3.5 University campus load profile and management

A good understanding of energy use in universities is important to meet the SDG-7 leading to the development and deployment of energy-efficient technologies. The use of energy in universities are for various purposes around the globe; these include lighting, operation of equipment and instruments in laboratories, heating, cooling, transportation, etc. The library is one of the essential buildings in every educational institution that requires electrical energy to ensure the quality of indoor air temperature and the comfort of occupants. A study carried out at the library of Universiti Teknologi Mara (UiTM), Bertram, Malaysia showed average daily energy consumed as 394 kWh (Monday – Thursday) and 330 kWh on Fridays, of which 55% was used for air-conditioning and the remaining for lighting and other loads [94]. For example, 40% of the energy used at the Victoria University of Wellington, Australia is for hot water and space heating; the same is applicable in the United States, where space heating accounted for the large amount of energy used from natural gas [66]. Smart technologies are being applied in universities for energy efficiency; for instance, at the campus of the University of Parma, Italy, the peak thermal load (16MW) as a result of direct heating and cooling of buildings was reduced using a modified energy management scheme. In this scheme, the start-up of the boiler was delayed for 2 hours on Mondays and one hour remaining days of the working week, resulting in an energy saving of 104 MWh, approximately 1.5% of total energy consumed on campus [95]. The authors of [96] reported that buildings contributed to 40% of overall energy usage in Europe and accounted for 36% of CO_2 emissions. In addition, a new method was proposed to evaluate the historical use of energy and renewable self-generating capacity of buildings in the university. As a case study, this methodology was applied using an average university, the University of Lleida, in the Catalonia region of Spain. The buildings used belong to four campuses with PV arrays installed on their roofs; the results showed large variations in the energy use of the buildings, spanning from 50 to 470 kWh/m^2 in a year. Figure 2.7 shows the 24-hour (31st October 2018) load profile of the Howard College campus of UKZN and the solar irradiance for the same day. The load data was obtained with permission from the UKZN energy management office, and the solar irradiance was measured by the Southern African Universities Radiometric Network (SAURAN) weather station equipment (pyranometer) located on the campus.

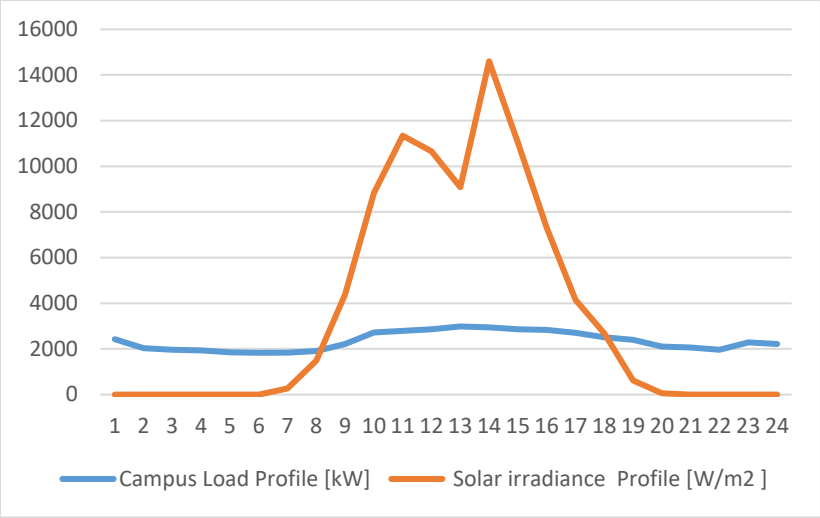

Figure 2. 7: Typical 24-hour solar irradiance and campus load profiles

As it can be seen that the peak load occurred throughout high irradiance, and with adequate investment and good technical design of solar PV, the energy cost of the campus can be reduced. The city of eThekwini electricity office has designed a solar mp that calculates and estimates possible costs and potential savings for residents in the city of Durban, South Africa, who want to install PV panels on their roofs. University campus electricity demand can be reduced through demand-side management (DSM) schemes, as demonstrated in [93]. The load data set was separated into two groups, one for weekend/holiday demand and the other for weekday demand. The related typical load patterns were developed by averaging data from the same month to characterize the load profile of the campus at that time. A total of 24 yearly load curve profiles were developed, one for each month, corresponding to 12 working and 12 non-working day curves. Smart sensors, lighting control systems (LCS), electric heat pumps (EHP), and building energy management systems are used to implement the DSM idea (BEMS). The later related assumptions and installation costs were based on measurement data gathered from previous microgrid project, the Internet-of-Things (IoT)-based campus microgrid at Seoul National University (SNU), South Korea, with a peak load of 912 kW [22]. DSM helped in the overall demand reduction and demand shifting, which transfered a portion of the load from times when energy costs were at their highest to times when they were at their lowest. The load control using DSM assumptions for the study was built based on the performance of the SNU microgrid. The overall demand was lowered by 8.9%, and 5% of the load from 11:00 a.m. to 5:00 p.m. was consistently relocated to the time between 00:00 a.m. and 06:00 a.m. every weekday because this was when power rates were the lowest. The demand did not change throughout the weekend [97].

2.4 Other Components in UCM application

Apart from the major RESs, other components are important for the successful operation of the microgrid. For example, the technical benefits of energy storage system (ESS) application in a microgrid, as stated in reference [94], include serving as a standby power source, reducing peak load, and enhancing power quality.

2.4.1 Energy storage system

The energy storage system provides significant support to the operation of microgrids with high RES penetration. The power generated by RES, such as wind turbines and solar PV, is intermittent in nature, and due to the sensitivity of microgrids to change in load or generation, microgrids must have a storage system with high power and energy densities. The utilization of DER in microgrid can be increased by integrating ESS. The purpose or objective of ESS in a microgrid is to balance energy demand and RE produced or generated, especially in islanding mode. In essence, any shortfall in meeting the load demand would be solved either by discharging the batteries and/or capacitor and activating the fuel cell and/or importing from the main grid. ESS has several benefits to different stakeholders (distribution system operator, transmission system operator, independent system operator) in deregulated power systems. However, the benefits for the end-users are improved power quality and reliability, reduction of demand charges, and time of use. Apart from providing system reliability, ESS can be used to optimize distributed generator or on-site generation to reduce the total cost of energy purchased from the main grid. The ESS stores energy during the off-peak period (less expensive tariff) and use it during the peak period (high tariff). In a microgrid with RES, ESS provides load capacity and reduces the need for VAR generation from the RESs. In addition, ESSs provide energy leveling to source variations, energy buffering to load changes, and ride-through advantages for microgrid applications. ESSs are either chemical or mechanical, common examples include; supercapacitors, batteries of different types, flywheels and superconducting magnetic energy storage, pumped hydro storage, and hydrogen fuel cells [20]. The energy storage system has great potential for microgrid power regulation applications and is an essential microgrid component. Electrochemical systems (or batteries), kinetic energy storage systems (or flywheel storage), and potential energy storage systems are the three primary kinds (pumped hydro and compressed air storage). In the design and operation of microgrids, ESS is critical. It serves as a power-quality regulator, ensuring that supply and demand are balanced, reliable, and stable [98]. ESS can be used for demand response, storing excess energy, and supporting island mode operation. The study in [99] showed that the gains from using battery storage increase with the battery size.

2.4.2 Electric vehicle

A vehicle that is propelled by one or more electric motors or traction motors is known as an electric vehicle (EV). Studies have encouraged the growth of numerous categories of clean energy transportation systems,

such as hybrid electric vehicles (HEVs), battery electric vehicles (BEVs), plug-in electric vehicles (PEVs), and plug-in hybrid electric vehicles (PHEVs), as rising petroleum costs strain the global economy and environmental distresses (PHEVs). Plug-in electric vehicles (PEVs) and electric vehicles (EVs) are gaining popularity as a result of their potential to reduce fuel consumption, emissions and the ability to increase the penetration of renewable energy sources into the transportation sector. Similarly, plug-in hybrid electric vehicles are already playing an important role in reducing greenhouse gas emissions, which are dangerous and the primary cause of global warming. In the future years, electric vehicles are expected to account for a significant portion of car sales. The additional energy required to charge their batteries may impact network stability and dependability, particularly when they are connected during system peak demand. In some cases, such as when EV owners plug in their vehicles as soon as they get home from their last daily commute, the charging needs of an EV fleet may be synchronized. This creates a high peak demand that can disrupt network operations, particularly when EV demand is timed with system peak demand. If the charging method for electric vehicles (EVs) is left unmanaged, grid capacity may be insufficient, and distribution networks may experience significant feeder voltage excursions and equipment overloads. Referenc [98] examined a control system hierarchy that allows EVs to be integrated into electrical distribution networks to address this issue. The control strategy is based on MAS, with a vehicle controller (VC) agent capable of providing either complicated or simple functionality for regulating the power flow between EVs and the power grid. In the most basic example, the VC agent serves as an ON/OFF switch, permitting full power flow at a level determined by the capacity of the power line or no power flow at all. In such a situation, the agent would be stationed at the charging station and would only require the bare minimum of memory and computing power. It informs the MG Aggregation Unit (MGAU) about the driver's charging preferences, which determines the charging schedule (Le. charge or not) for each EV. The goal of [99] was to look at how a number of dispersed EVs engaging in V2G technology, principal frequency control service affected the MG's short-term dynamic behavior. Even if a large number of EVs or an infinite number of EVs participated, it was determined that the frequency deviation would not be zero. The frequency deviation was used to estimate the output power of each EV. The output power of each EV, on the other hand, has an impact on the frequency deviation value. Intelligent solutions for monitoring charging sites and grid impact will be required to integrate electric vehicles into distribution networks. By shifting electric load to off-peak hours and storing extra energy from renewable sources, electric cars offer a way to regulate power demand. Furthermore, if a vehicle to grid (V2G) is implemented, electric cars might be utilized to increase dependability and power quality. In microgrids, electric vehicles (EVs) may be thought of as mobile battery storage. A microgrid (figure 2.6) that combines renewable generating and vehicle energy storage has several benefits, including (1) energy security, (2) cost savings, and (3)

dependability. The charging stations will act as energy management gateways, allowing unidirectional and bidirectional power transfer while storing energy in the vehicles [100-105].

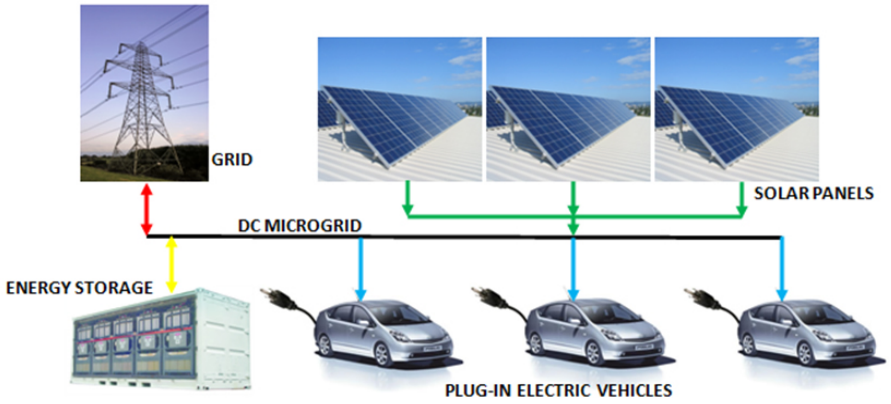

Figure 2. 8 A microgrid for charging PEVs [104].

To minimize power exchange spikes between the multi microgrid system and the main grid, coordinated charging and discharging schedule is necessary for several microgrids in a given region. Reference [100] offered a two-stage integrated energy exchange scheduling technique for a multi microgrid system, in which EVs were treated as storage devices. A price-based decentralized scheduling strategy was used to control the operation of the microgrid; the results showed a reduced cost of electricity and limited transitions between battery charging and discharging states. The utilization of second-hand electric-vehicle batteries to boost resilience, provide better degrees of energy independence, maintain grid stability, and cut energy costs by up to 40% was another application of EV in a microgrid. According to the article "Old electric-vehicle batteries for microgrid," using used Nissan Li-ion batteries extends the life of electric-vehicle batteries, decreasing the need to manufacture new batteries. [106].

2.4.3 Diesel generator

A diesel generator (DG) blends a diesel motor with an electric generator (alternator) to produce electrical energy. Diesel generators are commonly utilized as backup power supply to restore and sustain loads during grid outages, which are a serious issue in many nations worldwide. They are also useful for more complex applications, such as peak-lopping and grid support. The diesel generator's power regulation role is as follows: when renewable energy is in short supply, the load demand in the microgrid system may be fulfilled by turning on diesel generators to balance the system's power. In order to maintain the operating temperature and prolong the service life of the generator, the minimum power output of the diesel generator should be 30% of its rated power. The fuel consumption of a diesel generator $f_{con}(t)$ is related to the power dispatched from it $P_{disp}(t)$ and its rated power $P_{r.}$ as follows:

$$f_{con}(t) = \begin{cases} AP_{disp}(t) + BP_r, & if\ S_{dgi}(\mathrm{t}) = 1 \\ 0 & otherwise \end{cases} \quad (2.13)$$

Where A (per kWh) and B (per kW) are constants (cost coefficients), and S_{dgi} (t) represents the status of the diesel generator switch at time t.

A battery-less PV-diesel microgrid with multiple diesel generators was developed in [107] to supply the loads during outages instead of using diesel generators only. The results showed (i) a significant reduction in the fuel consumption with multiple DGs compared to a single DG, (ii) the total dispatched energy cost was reduced considerably, and (iii) the proposed microgrid can supply the load without loss of supply [107-109].

2.4.4 Power converter

Power electronic interfaces are used to facilitate the overall integration of major RESs in a microgrid. Power converters are designed and customised to achieve economic performance. Their applications can be significantly enhanced by making them rugged, reliable, cheap, and interchangeable [35]. A converter is an electronic device that maintains energy continuity between AC and DC electrical components in hybrid power generation. It is made up of an inverter and a rectifier that converts AC to DC and vice versa.. The converters utilized for microgrid operation can be categorized as grid feeding, grid forming, and grid supporting converters [25]. Power electronics circuits used in microgrids applications can be classified as;

a. AC/DC Converters (Rectifiers): The microgrid requires AC-DC converters between the grid and the DC bus in grid-connected mode. In a single-phase system, a single-phase diode or single-phase thyristor is used and for a three-phase, three-phase thyristor, or three-phase diode rectifier circuits are used.
b. DC/DC Converters: Most devices in DC microgrids require varied voltage levels; DC-DC converters are employed to obtain voltage at different DC levels as required by the loads. DC-DC converters aim to achieve a controlled voltage and extract the most power possible from renewable energy sources. MPPT controllers are used to extracting the greatest amount of power from the source. The basic goal of MPPT systems is to track the renewable source's maximum power (PV panel or fuel cell).
c. DC/AC Inverters: DC-AC power electronics converters or inverters are needed when loads that require AC voltage are fed from a DC source.

A power electronic converter, such as a Voltage Source Inverter, is commonly used to link DGs to the network (VSI). The most significant function of an interface inverter is to regulate the active and reactive powers injected by the DG by adjusting the phase angle and amplitude of the output voltage [110].

2.5 Benefits of microgrids

With a good operation strategy, a microgrid can provide various benefits ranging from technical, environmental, social to economical for every stakeholder. For a university offering an R&D test-bed, maximizing campus thermal and electrical energy use, and limiting CO_2 emissions, constructing a Microgrid intends to accomplish economic and environmental throughputs. One major challenge of implementing microgrids is their financial feasibility because of high capital costs. The utilities and government address this problem through renewable energy incentive programs such as feed-in tariff [20]. Most of the benefits highlighted below apply basically to grid connected microgrids, however, off-grid microgrids share some of the benefits. For instance, optimal sizing of local RES, battery energy storage and energy management system of an off-grid microgrid will result in both economic and environmental benefits.

2.5.1 Technical

In microgrids, the proximity of distributed generators to the load being served could offer the following benefits to both utility and consumers [29].

a. Improved power quality
b. Better voltage stability
c. Peak shaving (using storage)
d. Lower power losses
e. Higher reliability (reduced number of outages)

A demand response scheme was proposed in [111] for the campus microgrid of the University of Connecticut, Storrs in the US, to shave peak load. The campus electrical load varies from 9.5 to 20 MW, with a peak of 17MW occurring approximately 10% of the year. The results show a decrease in the peak load to average consumption, reduced electricity bill and decreased consumers' dissatisfaction caused by load shedding. The campus microgrid in [112] was set by integrating DGs such as wind turbines, biomass, solar PV, and energy storage system into the distribution network of a college campus. The results obtained prove that microgrids can improve the stability, reliability, and quality of supply in grid-connected and islanded modes with load increment of up to 1.25p.u in both modes.

2.5.2 Economic

From a macro-economic point of view, a microgrid can operate as a market maker in the local retail and service market and a hedge against price volatility, load increase, outages, and other hazards. It is assumed that the end consumers enjoy the overall economic benefits of a microgrid when they own and operate multiple micro source units as an aggregated prosumer entity. The economic benefits of microgrids are majorly based on the use of renewable energy resourses, which are free, available and inexhaustible. As the costs of production of renewable energy generation, energy management systems and storage technologies reduce microgrid deployment becomes economically viable[113]. Other economic benefits come from the postponement or deferral of investments in expanding generation and transmission systems. Cost is also saved in transmission and distribution (T&D) by integrating several micro sources (e.g., electric vehicles) as they are operated in plug-and-play mode, hence there is avoidance or deferral of T&D investment costs. Economic benefits also come in terms of unit commitment and economic dispatch of microgrid resources resulting in cost saving. This cost-saving benefit of a microgrid is achieved through economic dispatch. The master controller dispatches the microgrid generation once the electricity price is high, charges the battery when the electricity price is low, and discharges the battery storage as the price of electricity increases. Also, through economic operation, as in the case of UCSD, saving eight hundred thousand dollars(US$800 000) monthly when disconnected from the main grid [67]. The economic benefits of a microgrid are not limited to saving the cost of electricity but also in earnings from the feed-in tariff. The feed-in tariff is a premium rate that is more than the electricity rate and is usually guaranteed for a fixed term. Utilities buy back power at the premium rate from local generation to encourage investment into RE generation [36]. Implementing a microgrid with RES reduces the amount of energy imported from the grid; hence energy costs are minimized drastically. One of the challenges of the Federal University of Rio de Janeiro (UFRJ) is its electricity expenses. Hence the university sought to reduce these expenses by implementing microgrids. Six microgrid configurations were simulated to determine the most viable solution economically and technically. The results showed that a combination of the grid and the natural gas (NG) generator would be the most appropriate, whereby the NG generator operates during peak periods (high rate) [114]. Economic and environmental evaluations were carried out to determine the benefits of the SPM at the University of Geneoa; the calculated results showed that potential savings are achievable by reducing operating costs and energy usage [115]. Economic benefit of microgrid is also reflected directly or indirectly from employment opportunities generated in the construction and maintenance of microgrid. In other words, these opportunities may increase domestic product, relocation of skilled workers to microgrid sites thereby increasing goods and services demands from new and existing businesses[116].

2.5.3 Environmental

Power generating stations and highway vehicles are the largest producers of pollutants such as nitrogen dioxide (NO_2), carbon monoxide (CO), sulphur dioxide (SO_2) and lead (Pb). The deployment of microgrid with RESs will significantly reduce these GHG emissions by using intelligent control or algorithms for environmental-economic dispatch of microgrid microsources. Universities play an essential role in addressing climate change by generating information and incorporating climate problems into teaching and research programs and direct and indirect operational actions. Universities have a critical role to play in combating climate change [117]. The microgrid project of the University of Southampton located on the Highfield Campus was designed to help protect the environment by generating electrical and thermal energy more sustainably instead of burning natural gas that produces GHG. Although the results obtained were not huge, but showed that the proposed designs were feasible economically and technically [68].

2.5.4 Research and development

Establishing university Microgrids has several advantages: they will be an ideal small-scale research project and a test-bed for measuring and optimizing power use through the construction of Microgrids [115]. One of the objectives of the smart microgrid located at the Savona campus of the University of Genoa, Italy, is to operate as a laboratory facility for research, testing, and development of management strategies and power components. The research activities include implementing and validating techniques for the best operation of storage elements and dispatchable sources, modelling, and simulation, application and authentication of algorithms to forecast the generation from RES using forecasting tools, new communication protocols, and paradigms [118].

2.6 Conclusion

This chapter has presented a review of related literature to this thesis. A general overview of microgrid architecture, control, and protection and a comprehensive review of renewable energy sources used in university campus microgrid have been described. As reported in some literature reviewed, RESs present huge benefits when intergraterd into the distribution network through a microgrid. However, due to their unpredictability and intermittent nature, there is need for backup or secondary energy sources (battery storage, diesel generator) during islanding or off-grid applications. Among the various RESs, solar and wind are prominent and widely used in most microgrid applications because they are free and contionus technology developments for their integration resulting in low installation costs. Hence, solar PV, wind turbine, battery and diesel generators are major energy sources considered in this study. Both grid connected and off-grid applications of AC microgrid were investigated with a view to determine the viability and feasibility of UCM operating in an islanded mode during load shedding. Most existing UCMs were developed with the aim to meet the local energy demands using available RESs and to serve as a test bed

for carrying out research. Apart from financial benefit, continuous power supply on university campus is critical to successful completetion of academic activities such as lectures, practical and laboratory experiments. The technical, economic and environmental study of a hybrid renewable energy system for university campus microgrids is presented in the next chapter.

CHAPTER THREE

TECHNICAL, ECONOMIC AND ENVIRONMENTAL ANALYSIS OF A HYBRID RENEWABLE ENERGY SYSTEM FOR UNIVERSITY CAMPUS MICROGRID

3.1 Introduction

Hybrid renewable energy system can be described as an integration of several renewable sources in a microgrid for electricity supply in an area. In other words, HRES aggregates and consolidates different energy generators and energy storing device together to meet the local energy demand. Technical, economic and environmental analysis is crucial for efficient utilzationof a HRES in a microgrid. HOMER softwareis selected among other software tools such as RETScreen, iHOGA, H2RES, EnergyPlan etc to size and optimize a HRES for UCMs. The results of the simulation show that the optimal configuration is cost effective to reduce the energy demand cost on each campus with low CO_2 emission. Sensitivity analysis is also carried out to determine the effects of changing variables such as inflation rate and discount rate on the cost of energy.

3.2 Review of Microgrid Applications on University Campuses

Universities are characterized by many buildings; offices, classrooms, laboratories, residences, sports centres, and large populations of students; hence, university campuses are smaller models of cities or towns. As a result of diverse university activities, many resources are being consumed daily during which electricity is utilized. Most electricity consumed on university campuses is generated from fossil fuels such as coal, gas, oil, which produce greenhouse gases that cause environmental pollutions [66, 119-121]. In the year 2015, the united nation set seventeen sustainable development goals (SDGs). The seventh goal is "Affordable and clean energy," designed primarily to guarantee economic, reliable, and sustainable energy access or all by 2030 [122]. Thus, universities must promote energy sustainability through research, transmitting requisite knowledge, creating awareness within and outside the universities, and developing a practical model of sustainable energy concept on their campuses to be successful [2, 123]. In Tu [1], many universities in the United States are promoting the idea of sustainability among faculty staff, students, and the community. Globally, several universities are designing appropriate schemes to improve their sustainability both in short and medium terms [124]. Other universities have critically reviewed their energy policies, advocating for energy efficiency on their campuses using different energy resources [125]. In the last decade, higher education institutions all over the world are investing in renewable energy sources (RESs) with obligations to reduce energy demand and greenhouse gas emissions, in agreement with the Nearly Zero Energy Buildings (NZEB) concept; this also facilitates the applications of the microgrid in university campuses. Figure 1 shows a 5 kW solar photovoltaic (PV) mounted on one of the buildings at the Steve Biko campus of Durban University of Technology (DUT). The complete system includes a 5 kW inverter (SYNAPASE 5.0k+) and 48V, 50Ah lithium-ion battery (SDA10-4850). This PV system is used

for a laboratory experiment and to power the laboratory during load shedding. The university campus can be regarded as a testbed for experiments to test, develop, and apply modern technology for new power systems through research activities carried out on campus.

Consequently, the universities can become models to reduce fossil fuel consumption and improve energy management through research, development, and small-scale implementation of energy-efficient solutions [120, 122, 126]. In addition, university campuses satisfy many constraints that could hinder the development of microgrids, such as techno-economic and geographical constraints. The implementation of a microgrid on a university campus is not only technically viable but also economically and geographically viable as a result of the following factors [127]:

- The same administration manages all distributed energy resources (DERs) and loads.
- All DERs and loads are nearby and connected to a similar network.
- There is a point of common coupling that connects the campus to the main utility grid.

HOMER (Hybrid Optimization of Multiple Energy Resources), freely accessible simulation software developed for distributed power, is selected for this research because of its widespread use in renewable energy supply for case studies and validation tests. The main contribution of this study is the proposition of an optimal hybrid renewable energy system for university campuses (microgrids) , considering economic, environmental, financial, and technical implications. To the best of the authors' knowledge, this is the first work that comprehensively presents the analysis of optimal hybrid microgrid system configurations for five university campuses considering the peculiarity of each campus. The proposed microgrid model was based on bi-objective optimization, which maximizes annual utility bill saving and minimizes CO_2 emissions. While HOMER ranks the optimal hybrid system using the net present cost (NPC), this study considered the two objectives in its recommendation for the five campuses. The results show the different configurations of an optimal hybrid system for each campus as a result of different load profiles and meteorological data. Also, it is noted that annual savings are directly proportional to the campus load while the CO_2 reduction is approximately 50% for four campuses.

Several studies have been published on making university campuses green and smart. To minimize load interruption at the University of Connecticut, the authors of [111] applied a distributed demand response (DR) algorithm to the university campus microgrid. The result shows a decrease in the peak-to-average consumption ratio and reduces in general consumers' dissatisfaction level. In [112], using the microgrid concept, RESs such as wind, PV, and biomass are integrated into the distribution network of a college campus and analyzed for small signal stability. The case study shows improved reliability, stability, and supply quality in both grid and off-grid modes. A smart energy system for heating and cooling is developed and applied at the University of Parma campus, comprising PV panels, windmills, heat pumps, etc. The proposed model yields 1.5% savings in the cost of energy [95]. The main objectives of the Smart

Polygeneration Microgrid (SPM) at the University of Genoa are to generate clean energy to meet the university demands and to serve as a prototype for testing, research, and development of power components [118]. The project reported in [68] investigated the technical design of an off-grid solar PV system able to generate sufficient power to meet the electrical loads of the Highfield Campus of the University of Southampton. The design solution comprised of 5016 PV panels generating 1.325 GWh, which amounted to 3.76% of the campus's yearly electrical loads. This was preferably a small fraction; however, the payback period of the project was 5.6 years. Elenkovav *et al*. [2] investigated and analyzed a smart microgrid at one of the campuses of Democritus University of Thrace (DUTH) in Xanthi, Greece. The smart microgrid was optimized to reduce electricity costs, manage campus energy, and load. In addition, the developed model could be used as a teaching aid, a tool for creating awareness of sustainable energy technologies, building efficiency, and energy-saving. In [97], a tool called Microgrid Decision Support Tool (MDSTool) was used to evaluate both the technical and economic feasibility of a university campus microgrid. The project received federal government incentives and consisted of technologies like fuel cells, solar PV, and energy storage systems. The overall result showed significant savings in the cost of electricity and concluded that incentives strongly determined optimal design of a microgrid and its financial feasibility. The goal of [96] was to present a creative method for estimating the historical energy demand and renewable self-generation potential of university buildings (University of Lleida) and then related it to a test case for typical campus buildings in the Catalan region .

According to [114], the initial purpose of adopting microgrids in universities such as Princeton, the University of Texas, Cornell University, and New York University was for reliability. However, climate change, energy costs, and research have inspired modern microgrid development with RES. A test case by the Universidad Federal de Rio de Janerio was presented, whereby six different microgrid architectures were simulated to determine the most viable solution both economically and technically. The contribution of a high-reliability distribution system(HRDS) in relation to the microgrid operation was assessed at the Illinois Institute of Technology to reduce the operation cost and raise the reliability of the load point [128]. The authors of [129], using specific economic indices such as simple payback period, net present value, and lifecycle, evaluated the financial feasibility of designing a grid-tied campus microgrid at Seoul National University (SNU), South Korea. The design also considered the economic benefits of energy storage by the application of a battery that charged during the off-peak (low cost) period and discharged during the peak (high cost) period resulting in a cumulatively low demand charge. The smart microgrid design's principal aim at the University of Brasilia, Gama campus (with 220 staff members and 1200 students) was to set up a laboratory prototype for research, teaching, analysis, practical test, and meet the laboratory's energy demand [130]. In [8], a model approach for designing an expansive grid-tied PV system (2 MWp) was developed and applied to the Technical University of Crete campus to make it energy independent. The

study reported in [131] considered the possibilities of using a hybrid of solar PV and fuel cells to meet the electrical energy demand of the Kavakli campus of Kirklareli University and to reduce carbon emission significantly on the campus. Reference [132] reported the strategy carried out at Palermo University targeted to foster its campus's energy performance to use further funds saved through energy efficiency schemes to finance more energy efficiency interventions. The results could be useful in the energy planning of metropolitan cities on a larger scale. Implementing a smart grid technology, a green campus smart grid (GCSG), was introduced in [125]. The GCSG was at the Lappeenranta University of Technology, consisting of distributed generation units (solar PV and wind turbine), energy storage, electric vehicle, and energy management system. The project provided a platform for open research to develop major components of smart grid technologies. The University of California San Diego (UCSD) has a vast campus with various DERs used in a microgrid to meet approximately 80% of its electrical loads. Some of the major benefits realized from the UCSD campus microgrid included [133, 134];

- Lower operating cost
- Improved reliability of the system
- Reduction of greenhouse gases
- Integration of faculty research with microgrid operation.

In [135], the electrical energy demand of the University Polytechnic of Bucharest campus is analyzed. A micro smart grid comprising a solar PV power plant is proposed to operate in an autonomous mode most of the time. The primary objective is to limit the national grid supply to the barest minimum and take as much as possible from the micro smart grid. The authors of [136] proposed a design to transform the Eindhoven University of Technology campus distribution network (DN) into a smart grid, thereby integrating RESs, creating awareness for staff and students to enhance the campus energy efficiency, increase the reliability and efficiency of the distribution network. The recommended UCM in [137] comprised of a rooftop PV array (300kWp), a 130 F supercapacitor, 100kWh battery storage (Li-Ion), 15 kW fuel cell, and hydrogen electrolyte. The objectives of the UCM included, among others;

- Charging of electric vehicles of staff
- Peak shaving during high demand
- Supplying to some extent the residential loads on campus.

Different types of DERs such as wind turbines, PV, biogas, electric vehicles, and energy storage system were combined to form a microgrid in a university campus by the faculty of technical sciences in Novi Sad, Serbia. The study [39] conducted an ecological analysis and a techno-economic to determine the possible annual energy generation, cost of investment, and CO_2 emission reduction through DER use. The results obtained gave the payback period of 12 years, justifying the investment and the proposed concept. A hybrid energy system in [40] consisting of a biomass gasifier, solar PV, fuel cell, and a battery was optimized for

Maulan Azad National Institute of Technology (MANIT) Bhopal, Madhya Pradesh, using HOMER Pro©. The optimal hybrid system was a solar PV, fuel cell, and biomass gasifier with 5 kW capacity each, which can meet the fluctuating load throughout the year without any power outage. The results obtained gave 15.064 Rs/kWh as the COE and Rs 5 189 003 as the total NPC

From these studies, university campuses are suitable platforms for implementing microgrid systems, particularly with the integration of RESs [20]. Presently, electricity generation in most African countries is predominantly from fossil fuel; for instance, 82.34% of the total power generated in South Africa is from coal despite a moderate average daily solar radiation of 4.5 kWh/m^2 to 6.5 kWh/m^2 that is available in the country [138]. However, the high cost of renewable energy technologies reduces their integration; consequently, it is crucial to consider the economic, technical, and in some cases, environmental impacts of RES in microgrid applications [139]. For RES to oust the traditional sources, a detailed analysis of renewable energy penetration effects in terms of reliability, cost, and greenhouse gas (GHG) emission is needed [140]. Therefore, techno-economic analysis is vital for efficient and effective usage of RESs in microgrids; it guarantees the entire system's economic feasibility and technical viability. Among several economic indices used to assess the economic viability of RES based microgrid projects include;

- Cost of electricity (COE)
- Net present cost (NPC)
- Payback period (PP)
- Internal rate of return (IRR)

It has been shown in literature that a 100% renewable power system is expensive in terms of NPC and COE but environmentally friendly, hence the need for a hybrid power system.

3.3 HRES Microgrid

One of the major drawbacks of RESs is their intermittency, that is, erratic behavior due to their dependency on weather or climatic conditions. This obstacle can be overcome by combining various RESs, conventional sources, and energy storage for a hybrid power system to meet the varying load demand at all times. The major objective of designing a hybrid renewable energy system (HRES) is the power supply system's reliability under unpredictable weather conditions and the cost of energy (COE). Studies have been carried out to determine the size and the mix of HRES, especially for off-grid microgrid applications. Most of these are for rural or remote areas electrification projects where RESs such as solar, biomass, and wind are available free of charge and friendly to the environment. In most of these HRES, conventional sources (non-renewable) such as diesel generators, microturbines, and energy-storing devices (battery, supercapacitors) are used as a backup to meet the load demand [45, 91, 141-145]. This section presents a brief review of some applications of HRES found in the literature, especially on microgrids. According to [45], HRES has evolved globally as a better option to meet the growing energy demand because of the

sustainability and utilization of resources effectively in terms of cost. The authors of [146] used dispatch strategies to analyze the performance of an HRES (PV, Wind, Hydro, diesel generator, and battery) for rural electrification using HOMER. The COE and NPC under various dispatch strategies ranged from 0.1 $/kWh – 0.162 $/kWh and $465 790 - $ 716 658 respectively. The hybrid system of [147] employed solar PV and fuel cell (FC) as the primary energy sources and a supercapacitor (SC) as the supporting energy source. The hybrid system, PVFC-SC, was applied in an islanded microgrid using a multilevel inverter that promises higher power quality and uninterrupted supply under irregular and unbalanced load conditions. The authors of [148] demonstrated the use of HRES to reduce the intermittency of RES (PV and Wind turbine) in an isolated microgrid. A diesel generator was used as a supporting source to meet the load demand during shortage; hydrogen fuel cells and batteries were considered as storage. Using HOMER, a comparison of two hybrids (PV-biomass hybrid and wind-biomass hybrid) was made in [146] based on environmental and economic factors. The study concluded that the PV-Biomass hybrid was more economical, dependable, reliable, and ecologically safe for localized electrification than the wind-biomass hybrid. According to [149], HRES can be employed to reduce losses in the network and boost efficiency. A smart method based on multi-objective particle swarm optimization was deployed to design an AC-DC smart microgrid to increase network availability and reduce the costs of the network. In addition to rural electrification, [150] concluded that HRES could offer domestic job opportunities to rural dwellers through wasteland development; this was also validated in [151]. A hard and soft constraint-based optimization model was developed and applied at three rural locations in southern India. The optimization was performed to minimize the NPC, maximize the renewable fraction, and maximize power exported into the main grid. A feasibility study of off-grid HRES was carried out in [152] to supply water to a community toilet in a rural village of Odisha, Cuttack district, India using a hybrid of biogas and solar PV. The NPC, capital cost, operating cost, and COE were determined for different configurations using HOMER. Using HOMER, [153] designed a flexible hybrid system that comprised of both RES and conventional generator. Using a secluded village in Malaysia, the study investigated all possible combinations of PV, batteries, diesel generators, power converters, and grid for utmost economic and environmental benefits. In determining the best design, a sensitivity analysis was carried out considering changes in power purchased, sell back, load growth, fuel price, and other variables. An HRES was optimized in [154] to power a base transceiving station (BTS) for 5G mobile network applications at a site in Akure, Nigeria. The optimal configuration for the selected site comprised of PV (60%), wind turbine (30%), and diesel generator (10%) using HOMER. Two different energy demand profiles, a residential load (75 apartments) and an industrial load, were used to analyze the influence of HRES component sizing on performance in [155]. The results showed (i) exceptional efficacy of the microgrid management for the residential load rather than the industrial and (ii) accurate sizing of the solar PV allows for intelligent use of the storage system (battery) and reduces the

energy imported from the main grid. Kumar [156] considered a microgrid with HRES connected to a distribution network to reduce losses and improve the load's voltage profile. The paper suggested a hybrid Nelder Mead-Particle Swarm Optimization algorithm to optimize the system using 12-bus, 69-bus, and a simple radial distribution system (84 bus) as case studies. The result showed a simultaneous reduction in distribution energy loss and profile improvement in the voltage. The schematic diagram of a typical HRES based microgrid (Figure 3.1) is made up of different components such as RES (solar, wind, hydro), energy storage system (battery, supercapacitor, flywheel), converter (inverter), conventional energy source (diesel generator, utility grid), etc. The mathematical modeling of each component used in this present study is given below.

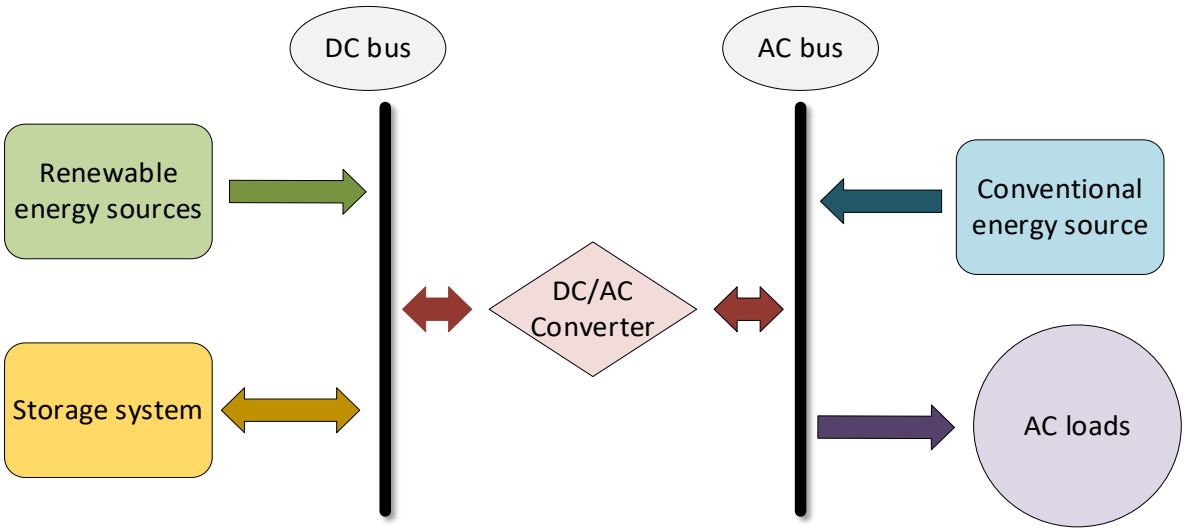

Figure 3. 1: A simplified block diagram of a typical HRES

A. Solar PV (PV)

Photovoltaic panels or arrays are employed to generate electrical energy by converting solar radiation into electrical power. The output of the PV panel can be obtained from equation (3.1) [45, 138].

$$P_{PV} = C_{PV} D_{PV} \left(\frac{I_T}{I_{T,STC}}\right) [1 + \alpha_P (T_C - T_{C,STC})], \quad (3.1)$$

Where C_{PV} represents the rated capacity of the PV panel or array (kW), D_{PV} is the derating factor (in %) of the PV array, I_T denotes the solar radiation incident on the PV array (kW/m^2) in the current time step, α_P is the temperature coefficient of power (%/°C). $I_{T,STC}$ is the incident solar radiation under standard test conditions (1kW/m^2), T_C represents the PV cell temperature (°C), and $T_{C,STC}$ denotes the temperature of the

PV cells in normal test conditions (25 ° C). If the influence of temperature on the PV array is to be ignored, i.e., if the temperature coefficient of power is zero, thus equation (3.1) can be interpreted as;

$$P_{PV} = C_{PV} D_{PV} \left(\frac{I_T}{I_{T,STC}}\right), \quad (3.2)$$

HOMER uses the derating factor to accommodate for variables such as panel soiling, cabling losses, shading, snow cover, aging, etc. PV manufacturers evaluate their PV modules' power output under standard test conditions (STC), which are 1kW/m^2, 25°C cell temperature, and no wind. Unfortunately, standardized test conditions do not indicate normal operational conditions since full-sun cell temperatures exceed 25 ° C [86].

B. Wind Turbine (WT)

Wind turbines are designed to convert rotational kinetic energy to electrical energy. The mechanical power produced by the wind turbine is proportional to the area of the blade (A) in m^2, the density of the air in kg/m^{2,} and the velocity of the wind in m/s at hub height. Therefore, the power of the wind turbine can be calculated as [157, 158].

$$P_{wind} = \frac{1}{2}\rho A V^3, \quad (3.3)$$

HOMER depends on the wind turbine's power curve (Figure 3.2) to calculate the estimated wind turbine power output at that wind speed under normal temperature and pressure conditions. The red dotted line shows the hub-height wind speed in Figure 3.2, and the blue dotted line shows the wind turbine power production estimated by the power curve for that wind speed. When the wind velocity at the turbine hub height is not in the ranges stated in the power curve, the turbine does not generate power, on the basis that wind turbines do not generate power at wind speeds below or above the maximum cut-out wind speeds.

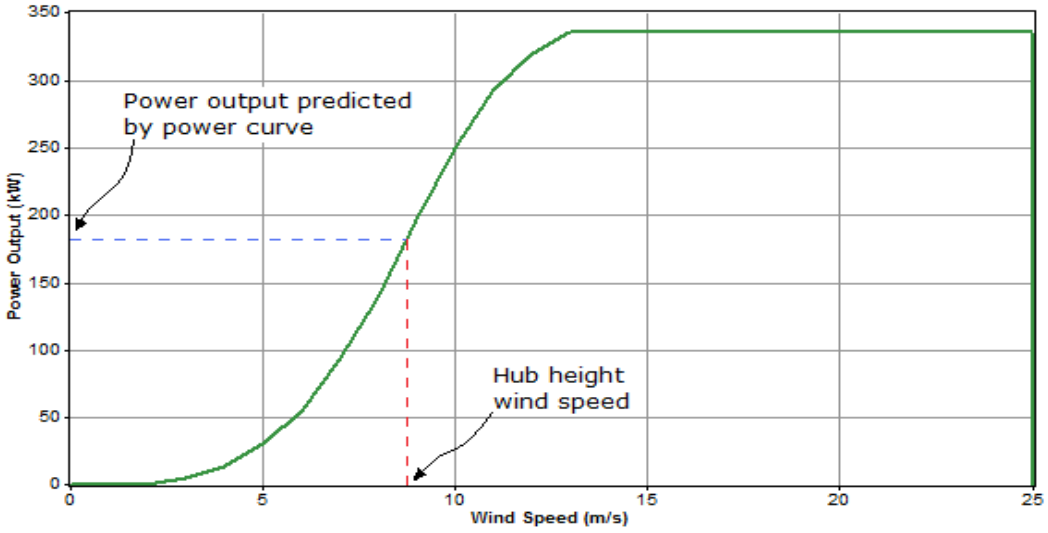

Figure 3. 2: Wind turbine power curve [86]

HOMER significantly increases the power value expected by the power curve by the air density ratio, by equation (3.4) for calculating the performance of the wind turbine, P_{WT} in kW.

$$P_{WT} = \left(\frac{\rho}{\rho_0}\right).P_{WT,STP}, \quad (3.4)$$

$P_{WT,STP}$ is the output of the wind turbine at the normal temperature and pressure in kW, ρ is the real air density (kg / m^3), and ρ_0 represents the air density at the maximum temperature and pressure (1,225 kg/m^3), respectively.

C. Diesel Generator (DG)

Diesel generators are often included in HRES, especially for off-grid applications or during islanding to overcome the intermittency of RES and increase system reliability by increasing its output to recompense the power deficiency. The diesel generator is made up of diesel engines and a control system. The relationship between the output power, synchronous AC generator, $P_{engine(t)}$ of a single diesel engine, and its fuel consumption at a time t, $V_{fuel(t)}$ in liter/hour can be expressed as [159].

$$V_{fuel}(t) = \alpha + \beta P_{engine}(t), \quad (3.5)$$

Where α is the no-load fuel consumption in litre/hour, and β is the relationship curve slope between diesel fuel and power output in litre / kWh. In HOMER, it is assumed that the fuel curve is linear. Equation (3.6) gives the relationship between the fuel consumed by the generator, F in litre/hour, and the generator's electrical output in kW.

$$F = F_0 Y_{gen} + F_1 P_{gen}, \quad (3.6)$$

F_0 is the intercept fuel curve coefficient (litre / hour / kW), F_1 is the slope of the fuel curve (litre / hour / kW), Ygen is the estimated generator power (kW) and P_{gen} represents the generator electrical output (kW)[86].

D. Battery Energy Storage (BES)

Batteries are essentially employed as backup resources and to keep steady voltage during peak demand or shortage in a generation. HOMER makes use of a battery bank/string made up of 24 batteries connected in a series-parallel configuration [160]. HOMER calculates the total amount of energy stored in a battery at any time by adding available energy and bound energy, and each is defined in equations (3.7) and (3.8)[86].

$$Q_{1,end} = Q_1 e^{-k\Delta t} + \frac{(Qkc-P)\left(1-e^{-k\Delta t}\right)}{k} + \frac{Pc\left(k\Delta t-1+e^{-k\Delta t}\right)}{k}, \quad (3.7)$$

$$Q_{2,end} = Q_2 e^{-k\Delta t} + Q(1-c)\left(1-e^{-k\Delta t}\right) + \frac{P(1-c)\left(k\Delta t-1+e^{-k\Delta t}\right)}{k}, \quad (3.8)$$

Where k is the rate constant, c is the capacity ratio, P is the power(kW) of the storage bank (positive) or of the storage bank (negative), and t is the time stage (hour). Q_1 and $Q_{1,end}$, respectively, are the usable

energy(kWh) at the start and end of the time step. Q_2 and $Q_{2,end}$ are the bound energy(kWh) at the beginning and end of the time step, respectively.

E. Power Converter

A bidirectional power converter is attached between them to sustain energy transmission between the AC and DC buses, as illustrated in Fig. 6 [146]. A converter is an electronic system used in hybrid power generation to preserve the energy continuity between the electrical components AC and DC. It consists of an inverter and rectifier to perform AC to DC conversion respectively. In Homer, the rectifier is proportional to the inverter as defined by the input of Relative Power. So the power rating of the converter can be measured [45, 86];

$$P_{conv} = \frac{P_D}{\eta_{conv}}, \tag{3.9}$$

P_D is the peak demand of the load, and η_{conv} represents the efficiency of the converter.

3.4 Description of Case Study

South African university campuses are powered primarily by the national utility company, ESKOM, which has 83.5% of its electricity generated from coal-fired stations due to the availability and low cost of coal in the country [161]. The burning of coal accounts for most CO_2 emissions in the country, ranking her among GHG's largest emitters, hence the significant shift towards RES. Some universities have solar PV installed on their campuses (rooftop, standalone) but not planned or coordinated to meet the campus electrical load. Therefore, there is a need for large-scale grid-connected renewable energy (PV) systems on university campuses.

The University of KwaZulu-Natal (UKZN) was founded in January 2004 following the merger of Durban-Westville University and Natal University. The university has five campuses, Edgewood campus, EC (29.817ºS, 30.847ºE), Howard campus, HC (29.868ºS, 30.981ºE), Westville campus, WC (29.818ºS, 30.943ºE), Pietermaritzburg campus, PC (29.617ºS, 30.394ºE), and Medical school campus, MC (29.874ºS, 30.99ºE) all in the KwaZulu-Natal (KZN) province of South Africa. The university has a student population of over 46 000 across the five campuses for both undergraduate and postgraduate studies. Figure 3.3 shows the aerial view of each campus. It is observed that there are potentials for installing solar PV panels on the roofs of most of the campuses' buildings. In addition, some of the campuses have facilities to develop a solar farm in the range of 10 MW.

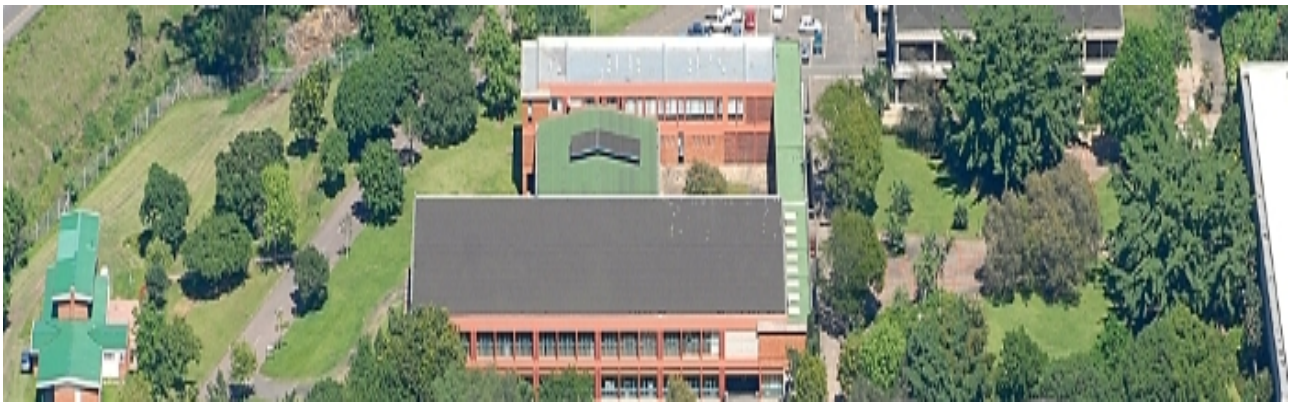

(a)

(b)

(c)

(d)

(e)

Figure 3. 3: Aerial views of each campus (a) Edgewood Campus (b) Howard College Campus (c) Medical School Campus (d) Pietermaritzburg Campus (e) Westville Campus

3.4.2 Weather Data of UKZN Campuses

University campuses have substantial potential and capacity for deploying RES to meet energy needs and reduce carbon footprints on campus [20]. The weather data, as seen in Figure 3.4 and Figure 3.5 were obtained from the National Aeronautics and Space Administration (NASA) website using the campuses' GPS coordinates. The meteorological data (wind speed, temperature, and solar irradiance) are the same for EC, HC, MC, and WC due to their proximity within the city of Durban, while PC is located in the city of Pietermaritzburg (approximately 75 km from Durban). The yearly average wind speed and yearly average temperature for Durban and Pietermaritzburg are 4.78 m/s and 18.53°C and 3.80 m/s and 16.15°C, respectively. The annual average solar global horizontal irradiance (GHI) is 4.71 kWh/m_2/day, the same for Durban and Pietermaritzburg.

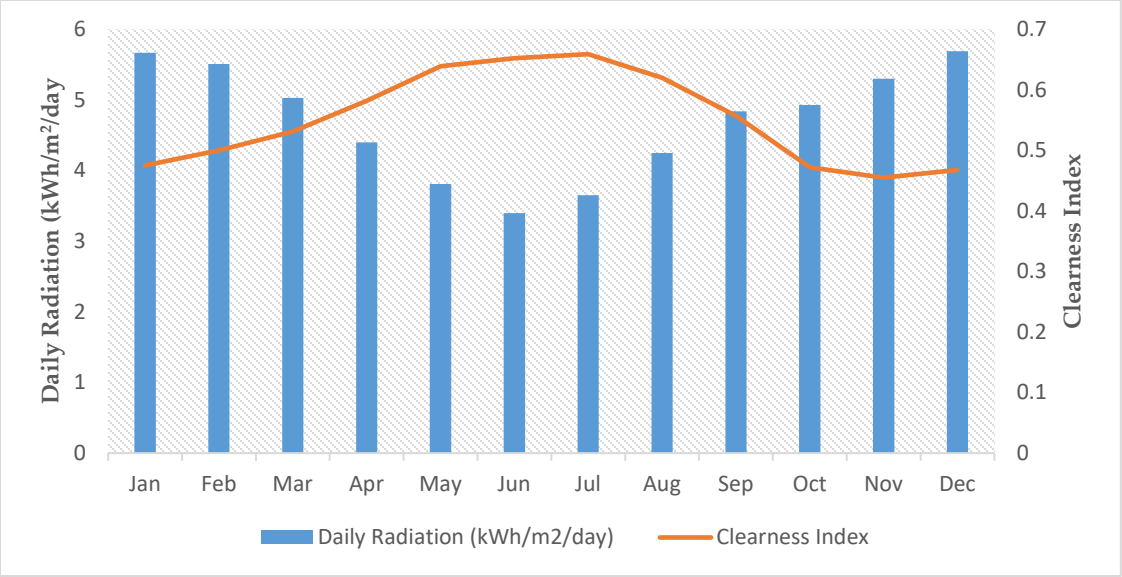

Figure 3. 4: Global horizontal solar radiation, Durban and Pietermaritzburg

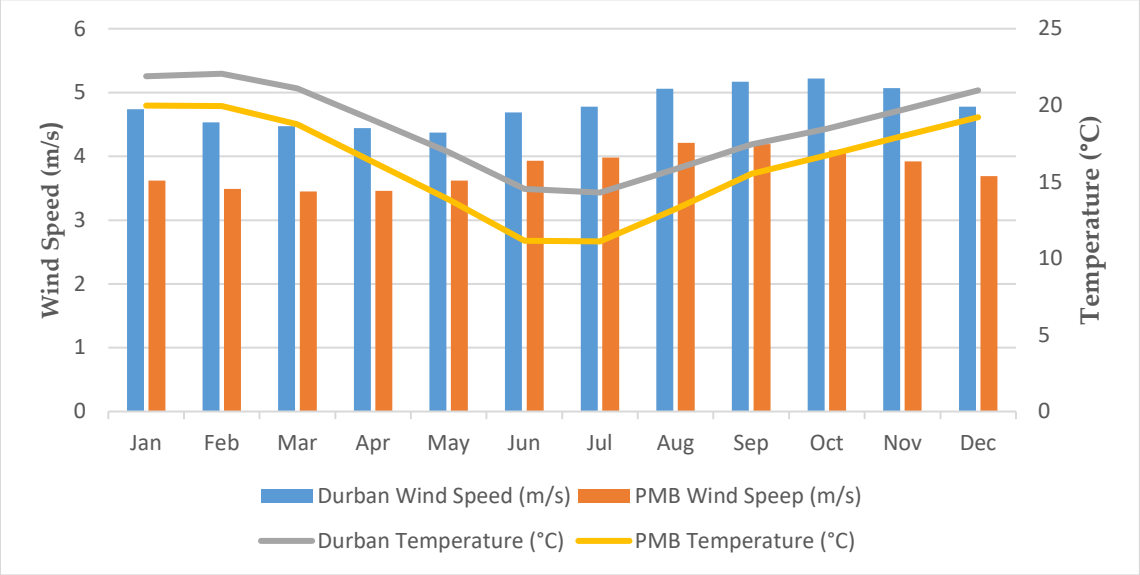

Figure 3. 5: Wind speed and temperature, Durban and Pietermaritzburg.

3.4.3 Load Data

Energy demand on university campuses varies per academic discipline for instance, faculties of engineering and sciences are equipped with experimental facilities and large-scalemachinery that consume a substantial amount of power. Also, campuses with student hostels have large thermal and electrical loads. Other loads are for lighting, cooling, and heating [3]. The total energy used by each campus in 2019 is given in Table 3.1, while the daily (a specific week day) load profile for the campuses is shown in Figure 3.6. The half-

hourly load data of each campus for 2019 obtained from the university energy management database is used for the simulation in HOMER

Table 3. 1: The total energy usage in 2019

Campus	Energy Used (GWh)
HC	18.84
EC	4.76
WC	22.59
PC	15.45
MC	6.18

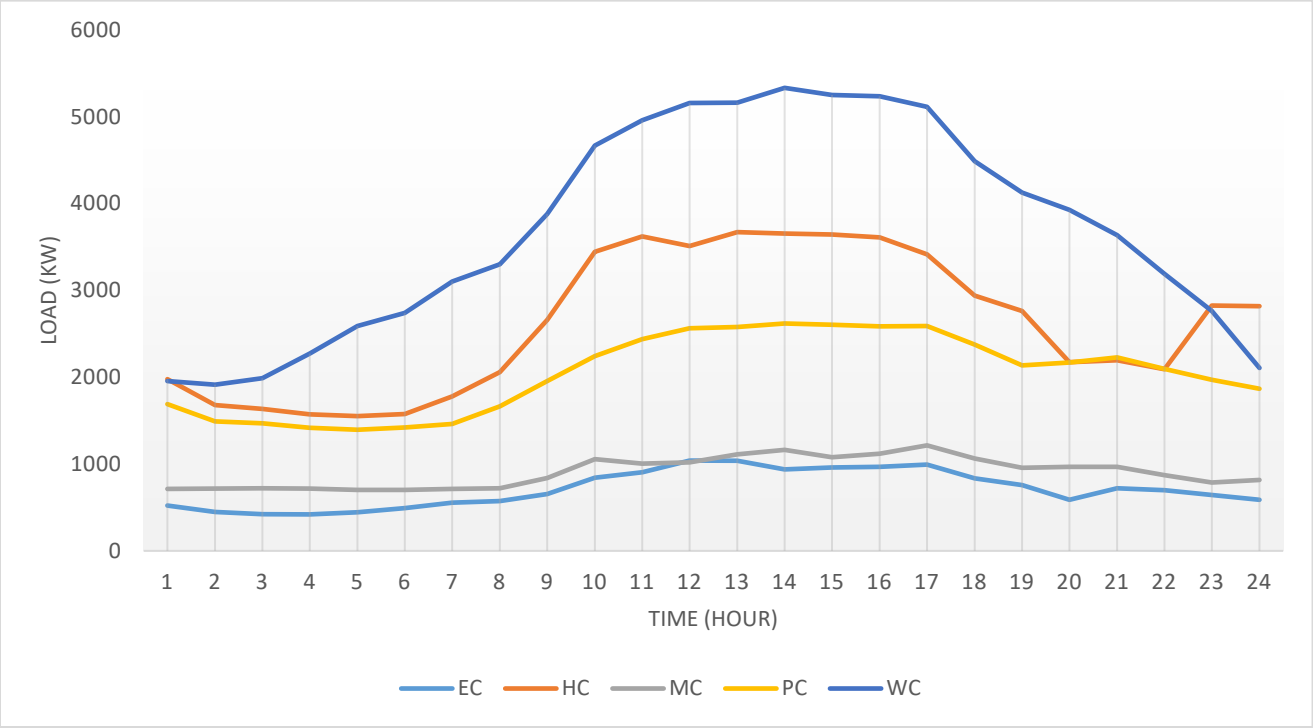

Figure 3. 6: Daily load profile of the five campuses

3.4.4 Tariff Structure

Except for PC, the remaining campuses are fed by eThekwini electricity on a time of use (TOU) tariff structure. TOU tariff allows utility customers to schedule their load voluntarily (manually or automated) to reduce their energy costs. The price of electricity is time-varying and depends on the season as well. This allows power utility to cost electricity at different amounts during the day to encourage energy consumption during off-peak periods [60]. The periods of the TOU tariff for low demand season (1 September to 31 May inclusive) and high demand season (1 June to 31 August inclusive) are shown in Table 3.2 and Table 3.3,

respectively, while the rates for both seasons are given in Table 3.4 (100 cents equal 1 rand) [61]. HOMER has custom tariff options to choose from, but for this work, the eThekwini electricity TOU tariff structure is built into the user library and applied for the simulation.

Table 3. 2: Time of use tariff structure for low demand season

Periods	Mon-Fri	Sat	Sun
22h00 – 06h00	off-peak	off-peak	off-peak
06h00 – 07h00	standard	off-peak	off-peak
07h00 – 10h00	peak	standard	off-peak
10h00 – 12h00	standard	standard	off-peak
12h00 – 18h00	standard	off-peak	off-peak
18h00 – 20h00	peak	standard	off-peak
20h00 – 22h00	standard	off-peak	off-peak

Table 3. 3: Time of use tariff structure for high demand season.

Periods	Mon-Fri	Sat	Sun
22h00 – 06h00	off-peak	off-peak	off-peak
06h00 – 07h00	peak	off-peak	off-peak
07h00 – 09h00	peak	standard	off-peak
09h00 – 12h00	standard	standard	off-peak
12h00 – 17h00	standard	off-peak	off-peak
17h00 – 18h00	peak	off-peak	off-peak
18h00 – 19h00	peak	standard	off-peak
19h00 – 20h00	standard	standard	off-peak
20h00 – 22h00	standard	off-peak	off-peak

Table 3. 4: Seasonal energy rates

Energy Rates (cent/kWh)			
Season	**Peak**	**Standard**	**Off-Peak**
Low (Summer)	111.67	79.67	53.81
High (Winter)	323.88	104.38	60.76

3.4.5 Economic indexes

The success of any HRES project depends on accurate technical design and economic analysis. The technical design talks about the correct sizing of the HRES components to meet the load all through the year. HOMER software (Pro and Grid) is being used by researchers, investors, and project managers as an optimization tool to model and analyze HRES with a view to reduce electricity costs through demand charge reduction and maximize the available RES in the location, thereby reducing the emission of GHG. The economic feasibility is evaluated based on certain financial performance indicators (FPIs), such as net present cost (NPC), internal rate of return (IRR), cost of energy (COE), simple or discounted payback period (PBP), return on investment (ROI)[162]. The FPIs used in this work are among the most popular and are discussed below.

a. Net Present Cost (NPC)

The NPC is the total system cost (initial capital cost, annual operating cost, replacement cost, fuel cost, and maintenance cost) through the project's lifetime minus the total cost incurred over the project lifetime [20, 142, 144, 145]. The NPC can be calculated as;

$$C_{NPC} = \frac{C_{AT}}{CRF(i_r P_L)}, \tag{3.10}$$

$$CRF = \frac{i_r(1+i_r)^N}{(1+i_r)^N - 1}, \tag{3.11}$$

C_{NPC} is the NPC, C_{AT} represents total annualized cost, CRF is the capital recovery factor, PL is the project lifetime, i_r is real interest rate, and *N* is the year number [163, 164]. The NPC is HOMER's major economic output used to rank all the optimization results based on possible configurations [86].

b. Cost of Energy (CoE)

The CoE generated by the electricity distribution company or customer is the ratio of the annualized system components cost of the generated energy. The generated energy used for calculating CoE incorporates energy used to supply the demand alone. This allows the economics of different renewable energies with their arrangements to be set side by side. CoE can be calculated as follows:

$$CoE = \frac{ACS}{Energy_{used}}, \tag{3.12}$$

where *ACS* is the annualized cost of the system (Rand/yr) and $Energy_{used}$ is the energy served (kWh/yr) [20, 144, 145, 163]. HOMER specifies CoE as the mean price per kWh of generated system electricity and uses it to compare systems but not to rank them [86]. Table 3.5 shows the summary of previous studies on the optimization of a hybrid system using HOMER software.

Table 3. 5: Summary of some studies on the optimization of a hybrid system using HOMER software

Year	Case Study	Location	Configuration	Mode	(COE)	Reference
2020	Rural village	Bolivia	PV-DG-BS	OG	$0.778/kWh	[165]
2019	Small island	Thailand	PV-BS	OG	$0.247/kWh	[47]
2018	Transceiver station	Nigeria	PV-DG	OG	$0.172/kWh	[166]
2018	Local community	South Africa	PV-WT-MT-BS	GC	$0.095/kWh	[167]
2018	Remote household	Iran	WT-FC	OG	$0.760/kWh	[91]
2018	University campus	Malaysia	PV-BS	GC	$0.104/kWh	[168]
2018	Rural village	Namibia	PV-WT-DG-BS	OG	$0.248/kWh	[169]
2018	Electric Vehicle	Banglade sh	PV	GC	$0.012/kWh	[170]
2017	University hostel	India	PV-WT-BS	GC	$0.044/kWh	[171]
2017	Rural area	South Africa	WT-DG-BS	OG	$0.320/kWh	[172]
2016	University campus	India	PV	GC	$0.082/kWh	[173]
2016	University campus	Republic of Korea	PV-WT-DG-BS	GC	$0.509/kWh	[174]
2016	Small Island	Greece	PV-WT-DG-BS	OG	$0.230/kWh	[140]
2021	University campus	South Africa	PV-WT-DG-BS	GC	$0.081/kWh	This work
2021	University campus	South Africa	PV-WT-DG	OG	$0.220/kWh	This work

c. Payback Period (PBP)

A payback period (PBP) is the number of years in which the total costs expended on the HRES project to generate thermal energy and electricity are recuperated. From the HOMER perspective, SPP is when the aggregate nominal cash flow of the difference between the current and base case system changes from negative to positive. Hence, SPP signifies the number of years for the project to breakeven [20, 86, 163].

$$SPP = \sum \frac{I_C}{Y_b - Y_c}, \tag{3.13}$$

I_c is the investment costs, Y_b is the yearly benefits (return), and Y_c is the annual costs (expenses).

d. Internal Rate of Return (IRR)

The internal rate of return (IRR) is the rate of discount at which the systems under review and current case studies have the same NPC. The discount rate at which the base case and the current system have the same NPC.

$$IRR = \frac{\sum B_n - \sum C_n}{(1+i)^n}, \quad (3.14)$$

B_n is the year n benefits, C_n is the year n costs, n is the number of years, and I is the discount rate [20, 86].

3.4 Simulation and Optimization

HOMER Grid (Pro Edition) is used in this work to simulate HRES microgrid for each campus. HOMER performs a simulation of a system by ensuring the energy balance between the power sources and the load for every hour of the year (8760 hours). In other words, it compares the total load (electric and thermal) at a particular hour to the available system energy for that hour and decides for each hour. For systems with storage elements (batteries or fuel cells) and or diesel generators, HOMER decides at every hour whether to charge or discharge the storage and or to operate the generators [86] [175]. HOMER utilizes two optimization algorithms, a search algorithm that simulates all suitable system architectures defined by the search space and a proprietary derivative-free algorithm to look for the most economical system. HOMER then shows a list of configurations and arrangements, sorted by minimum NPC or lifecycle cost, that can be used to compare system design options [176]. HOMER considers unforeseen circumstances; specific input parameters such as inflation rate, fuel price, interest rate, solar radiation, and wind speed are subject to change. Sensitivity variables are defined before the optimization, multiple values of such variables are entered, HOMER replicates the optimization operation for every value of the sensitivity variable and shows how the results are influenced [86]. Sensitivity variables defined in this work include diesel fuel price and inflation rate. The parameters of components used for the simulation are as stated in table 3.5 while figure 3.7 shows the setup of the simulation in HOMER for the WC.

Table 3. 6: Parameters of the HRES microgrid components

System Component	Description	Capital Cost (R)	Replacement Cost (R)	O&M cost (R/yr)	Operating lifetime(Years)	Other details
PV	Fronius Symo 20.0-3-M	35 000	35 000	700	25	Efficiency: 17.3% Operating temperature: 45°C Capacity: 5kW
Wind Turbine	Norvento nED 24	1 000 000	1 000 000	20 000	20	Capacity:100 kW Hub height:36 m
Diesel Generator	Generac 100 kW	250 000	250 000	250	15 000 hours	Minimum load: 30%
Battery	Lead Acid (ASM)	16 000	16 000	160	5	Initial SOC:90% Minimum SOC: 40% Max charge current: 167A Max discharge current: 500A
Power Converter	System Converter	30 000	30 000	300	15	Efficiency: 95% Relative capacity: 100%

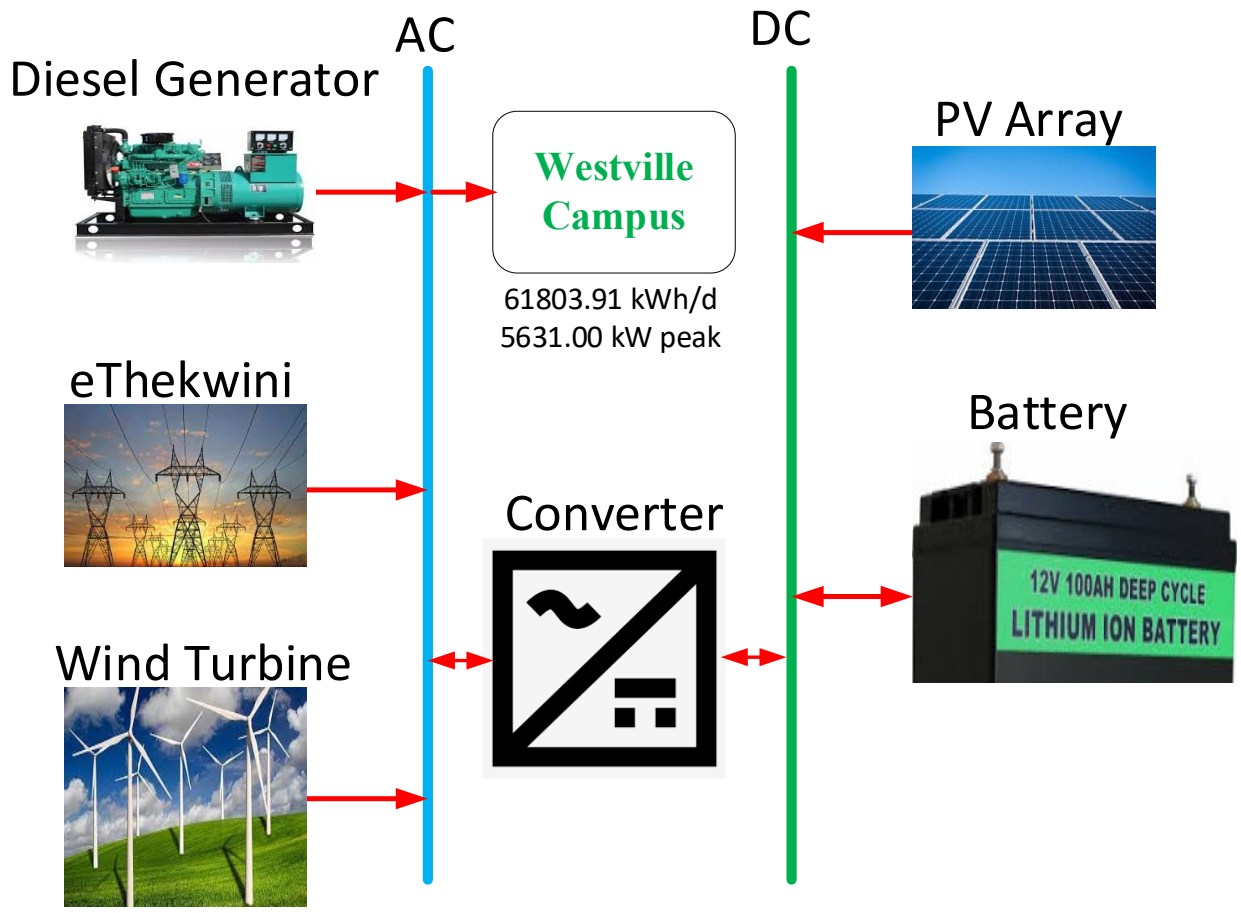

Figure 3. 7 : HRES model for Westville campus in HOMER

3.5 Results and Discussion

Using the HOMER Grid software package, an HRES microgrid is modeled and simulated for each of the campuses with the same technical and economic parameters of components shown in Table 3.6. All costs are in the South African rand (R) and for the year 2019, including all meteorological data. The Utility was used as the base case for comparison with the hybrid system. In addition, the inflation rate (4%) and discount or interest rate (9%) for South Africa in 2019 were used. The costs of equipment were obtained from similar projects done recently as well from actual market costs. This study seeks to design an HRES microgrid for UKZN campuses to reduce the electricity utility bill (maximizing utility bill saving) and reduce the GHG emissions on campus. Among the six GHG reported in the simulation results, the value of CO_2 emission is significantly high compared to others (Nitrogen Oxides, Carbon Monoxide, Sulfur Dioxide, etc.). Therefore, an emission penalty (R120/ton of CO_2) based on the South African carbon tax for 2019 [177] was included; hence only CO_2 emissions were considered in this study. To rank the feasible solutions, HOMER was set to size each component using the NPC value (the least being optimal). The peak shaving dispatch strategy was selected to reduce customers' electricity bills by limiting imports from the grid during

the peak period, thereby reducing monthly demand charges. The results for the five campuses are comprehensively discussed in the next subsections[1].

3.5.1 Edgewood campus

The Edgewood was previously a College of Education; it became UKZN's School of Education in 2001. The peak load for the campus was 1143 kW (which occurred midday 26 February 2019) with an average daily energy demand of 13033.71kWh. The highest consumption for this campus occurs between 09h00 and 16h00 during weekdays, which is quite beneficial for the solar PV system. The simulation results show that the W-D-G hybrid with the lowest NPC (R98 265 130). It also has the least COE of R1.069/kWh. However, the CO_2 emission (1 511.1 metric ton/year) is the highest. Next to the W-D-G is P-W-D-G with NPC value of R98 407 820, a COE of R1.07/kWh, and a CO_2 emission of 1 504.6 metric ton/year. Table 3.6 shows the comprehensive results of the simulation. The main objective of this work is to maximize utility bill saving and minimize CO_2 emissions. The hybrid system that meets this objective is P-W-D-B-G, with the highest annual utility bill saving (R4 010 968) and the least CO_2 emissions (1 499.1 ton/year), resulting in a 50% reduction. This hybrid system is made up of 33.9 kW solar PV, 1 500 kW wind, 55 kWh battery, and 105 kVA diesel generator. The project lifetime savings over 25 years is R100 272 200, which is quite significant and can be invested in sustainable projects.

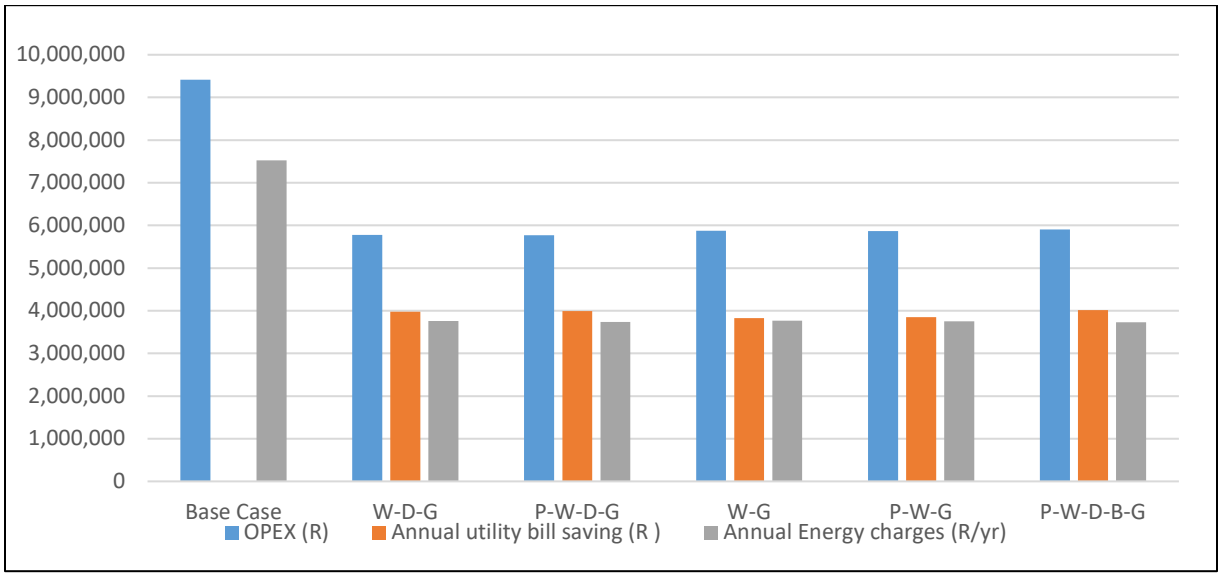

Figure 3. 8: Financial indices for Edgewood campus

[1] The following abbreviations are used specifically to explain the results only:
P-Solar PV;W-Wind Turbine; D-Diesel Generator; G-Utility Grid; B-Battery

Table 3. 7: Financial and environmental indices for Edgewood campus

HRES Configuration						
	Base Case	**W-D-G**	**P-W-D-G**	**W-G**	**P-W-G**	**P-W-D-B-G**
Economic Metrics						
Simple payback time (yrs)		4.0	4.1	4.0	4.1	4.4
LCOE (R/kWh)	1.997	1.069	1.070	1.082	1.082	1.101
IRR (%)		24.59	24.19	24.3	23.96	22.1
NPC (R)	135 297 000	98 265 130	98 407 820	99 421 520	99 558 220	101 247 600
Environmental Impact						
CO_2 emissions (metric ton/yr)	3 006.6	1 511.1	1 504.6	1 510.1	1 503.7	1 499.1
Annual fuel consumption (L/yr)	n/a	1 789	1 721	n/a	n/a	1 820

3.5.2 Howard campus

The Howard College was until 2004 part of the University of Natal. The Howard campus houses a range of qualifications in science, Engineering, Environmental (Architecture) Law, Management Studies, Humanities, and Social Sciences. The annual peak demand for the campus in 2019 was 3 896 kW (19 March 2019), average daily consumption of 68 428.1 kWh and an annual demand of 24 976.3 MWh (approximately four times of the Edgewood campus). Table 3.7 gives the simulation results showing five hybrid systems ranked by the NPC. The optimal hybrid system is the W-D-G having an NPC of R374 855 300, R1.044 as COE, and an annual utility bill saving of R15 579 110, however, with a high CO_2 emission (5 827.9 ton/year). Considering the amounts of annual utility bill saving and CO_2 emissions, the P-W-D-G hybrid is recommended for this campus, having the same COE as W-D-G, higher saving, and lower emission.

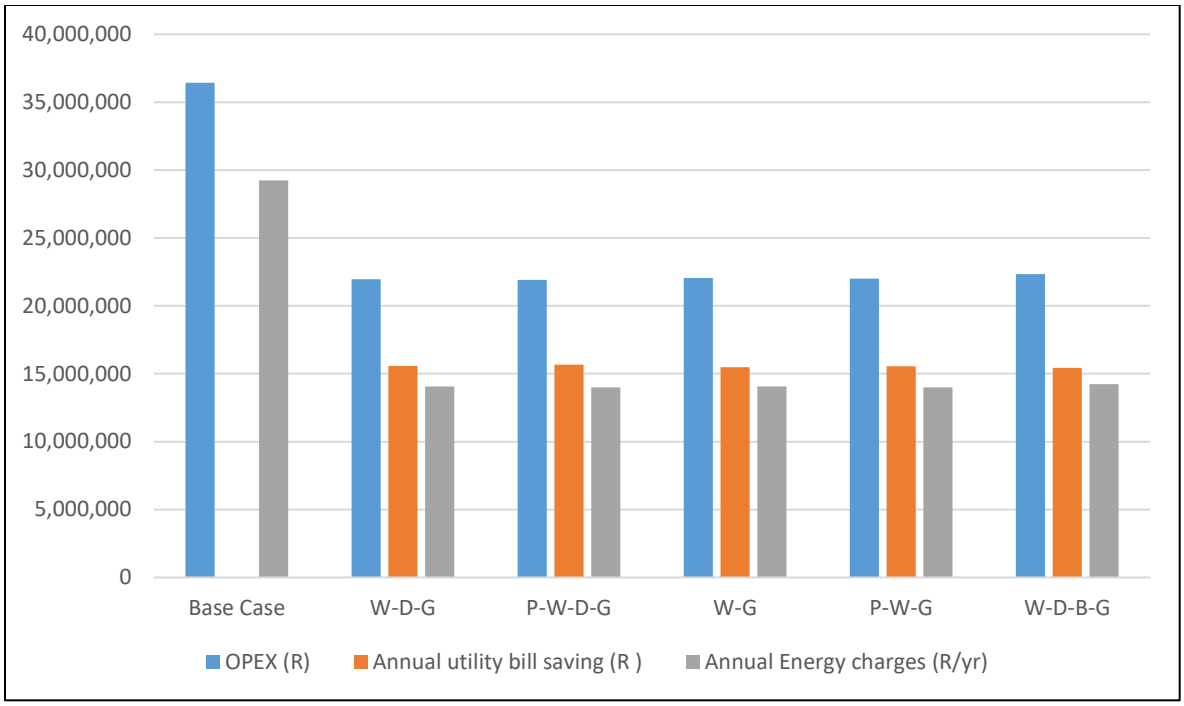

Figure 3. 9: Financial indices for Howard campus

Table 3. 8 Financial and environmental indices for Howard campus

HRES Configuration						
	Base Case	**W-D-G**	**P-W-D-G**	**W-G**	**P-W-G**	**W-D-B-G**
Economic Metrics						
Payback time (yrs)		3.9	4.0	3.9	4.0	4.1
LCOE (R/kWh)	1.932	1.044	1.044	1.048	1.047	1.084
IRR (%)		25.2	24.83	25.16	24.78	23.91
NPC (R)	523 447 300	374 855 300	375 167 800	375 957 300	376 294 700	382 357 200
Environmental Impact						
CO_2(metric ton/yr)	11 918.2	5 827.9	5 805.2	5 827.6	5 804.9	5 895.0
Fuel consumption (L/yr)	n/a	610	617	n/a	n/a	616

3.5.3 Medical school campus

The Medical school campus, known as Nelson Mandela medical school (named after the former South African President), was founded in 1950. The campus, among other facilities, has three student residences that accommodate close to 2160 students, one of which is a six-story building. The daily, monthly, and annual energy consumption for the campus were 22 546.9 kWh, 685.8 MWh, and 8 229.6 MWh, respectively, while the peak load (1 264 kW) occurred 25 February 2019. Like EC and HC, the optimal hybrid system is W-D-G with an NPC of R123 538 300, COE of R1.05, and an annual saving of R4 977 698, enabling a payback period of 4 years as shown in Figure 8 and Table 8, respectively. The optimal system is made up of a 19 kW wind turbine, 100 kW diesel generator connected with the grid. Although, with this hybrid system, 38.3% (3 153 051 kWh) of the total energy was purchased from the grid, 61.7% (5 073 758 kWh) supplied by the wind turbine, the diesel generator operated only for 60 hours in the year producing just 2 799 kWh.

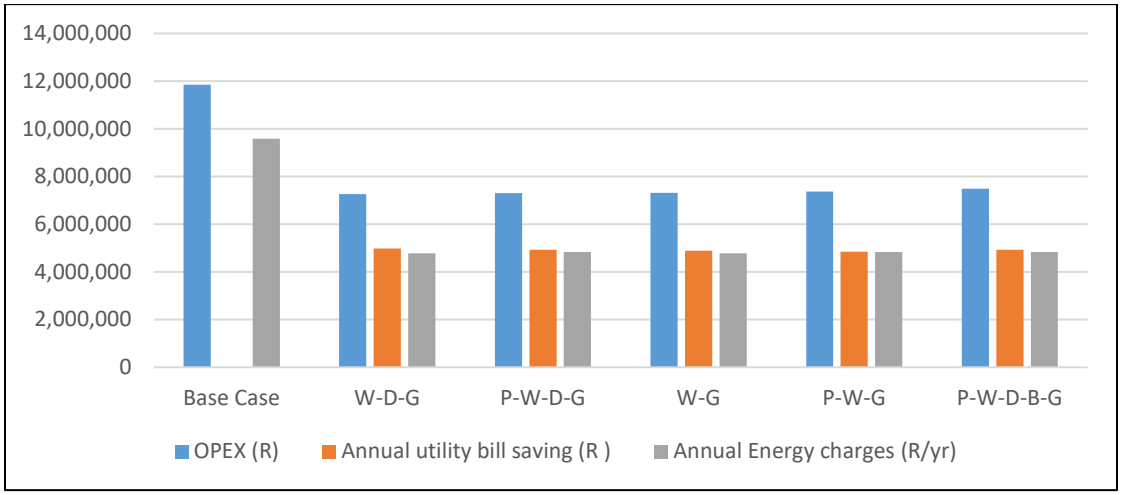

Figure 3. 10: Financial indices for Medical school campus

Table 3. 9: Financial and environmental indices for Medical school campus.

HRES Configuration						
	Base Case	**W-D-G**	**P-W-D-G**	**W-G**	**P-W-G**	**P-W-D-B-G**
Economic Metrics						
Simple payback time (yrs)		4.0	4.0	4.0	4.0	4.2

LCOE (R/kWh)	1.904	1.045	1.073	1.050	1.078	1.104
IRR (%)		24.63	24.72	24.65	24.75	23.03
NPC (R)	170 356 400	123 538 300	123 931 500	124 188 700	124 561 500	127 378 000
Environmental Impact						
CO_2 emissions (metric ton/yr)	3 934.2	1 995.0	2 020.3	1 994.5	2 019.7	2 020.5
Annual fuel consumption (L/yr)	n/a	866	937	n/a	n/a	888

3.5.4 Pietermaritzburg campus

This campus is located in the city of Pietermaritzburg, the official headquarters of the KwaZulu Natal province. Academic programs on this campus are in the fields of Agriculture, Science, Education, Human and Management Sciences. The peak load (2 865 kW) occurred on 16 March 2019, the daily, monthly, and annual energy consumption for the campus was 46 269.6 kWh, 1 407.4 MWh, and 16 888.4 MWh, respectively. The optimal hybrid system (W-D-G) for this campus is made up of a 100 kW diesel generator and 45 kW wind turbine reducing the annual utility bill from R27.2 million to R19.1 million. This is because of the low annual average wind speed for Pietermaritzburg (3.80 m/s). Hence, the campus has the highest COE (R1.45/kWh), payback period (5.9 years), the least CO_2 emission reduction (33.7%), and the lowest renewable fraction (41.5%) as shown in Table 9

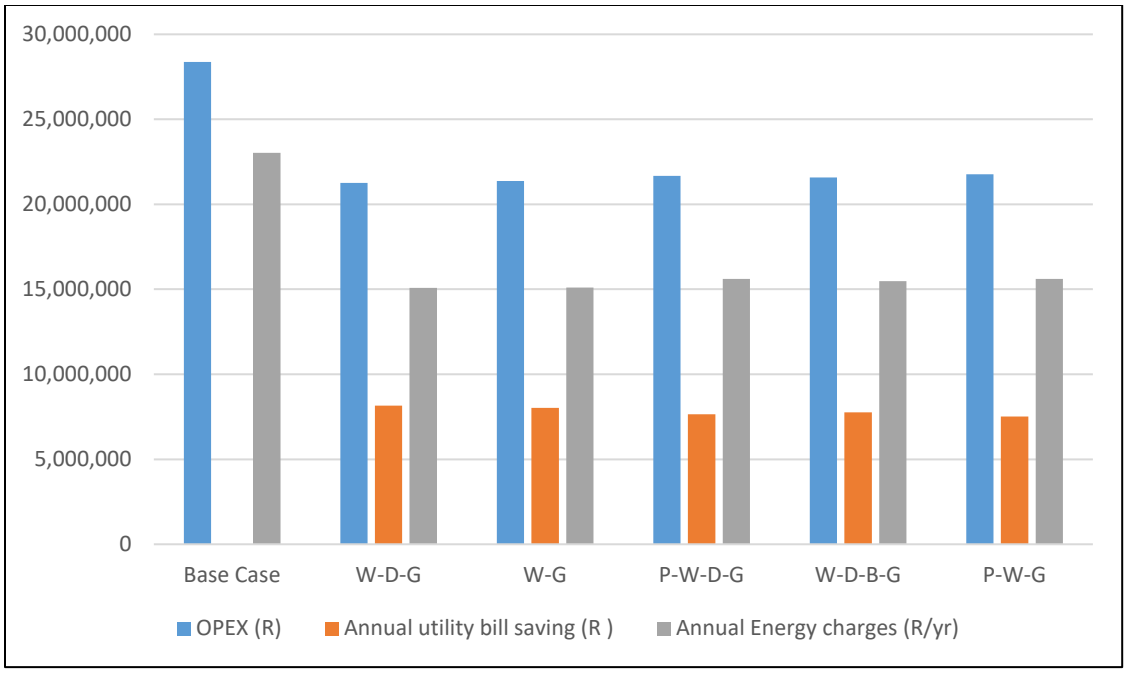

Figure 3. 11: Financial indices for Pietermaritzburg campus

Table 3. 10: Financial and environmental indices for Pietermaritzburg campus

HRES Configuration						
	Base Case	**W-D-G**	**W-G**	**P-W-D-G**		**P-W-G**
Economic Metrics						
Payback (yrs)		5.9	6.0	5.8	5.8	5.8
LCOE (R/kWh)	1.903	1.445	1.451	1.500	1.486	1.505
IRR (%)		15.88	15.71	16.49	16.18	16.34
NPC (R)	407 774 000	350 646 500	352 053 900	352 522 300	352 607 300	353 761 800
Environmental Impact						
CO_2 emissions (metric ton/yr)	9 425.3	6 248.1	6 247.6	6 461.5	6 407.6	6 461.0
Annual fuel consumption (L/yr)	n/a	925	n/a	931	936	n/a

3.5.5 Westville campus

The Westville campus is the official address of the UKZN, accommodating the offices of the Vice-Chancellor, executive members, and administrative divisions. Programs offered on the campus include Engineering, Science, Management, Law, Social Sciences, Commerce, Humanities, and Health Sciences, making it the biggest of the five campuses (this is also reflected in the campus load profile). The campus recorded its peak load (5 631 kW) on 25 February 2019. Daily, monthly and annual energy consumption for the campus were 81 720.2 kWh, 2 485.7 MWh, and 29 827.9 MWh, respectively. Similar to other campuses' results, the optimal hybrid system for this campus is W-D-G, that is an installed capacity of 6 800 kW wind turbine and 100 kW diesel generator.

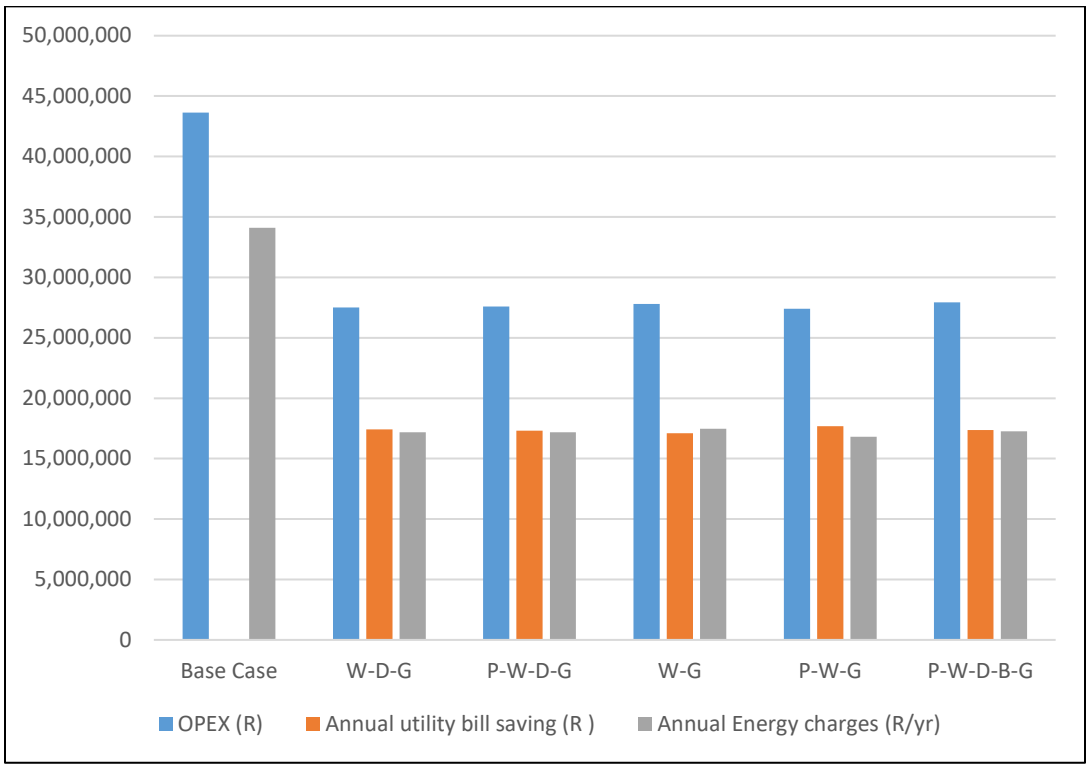

Figure 3. 12: Financial indices for Westville campus

Table 3. 11: Financial and environmental indices for Westville campus

HRES Configuration						
	Base Case	**W-D-G**	**W-G**	**P-W-D-G**	**P-W-G**	**P-W-D-B-G**
Economic Metrics						

Simple payback time (yrs)		4.0	4.1	4.1	4.3	4.3
LCOE (R/kWh)	1.934	1.081	1.084	1.118	1.068	1.119
IRR (%)		24.39	24.35	24.33	22.64	22.71
NPC (R)	626 933 700	463 469 100	464 528 000	466 604 200	467 659 400	473 226 700
Environmental Impact						
CO_2 emissions (metric ton/yr)	14 256.9	7 375.1	7 374.9	7 508.4	7 232.2	7 412.0
Annual fuel consumption (L/yr)	n/a	332	n/a	337	n/a	340

3.5.6 Overall Analysis

The campuses' energy consumptions vary per student population and physical size; Figure 3.13 shows the monthly peak load for all campuses in 2019. Considering the daily load profiles, it was observed that the peak demand period is between 08h00 and 16h00, while the annual peak load occurs between 12h00 and 13h00. The campuses consumed the maximum amount of electricity in February and March because of the summer heat, whereas the energy consumed in June and December was minimal due to the winter and end of the year vacations, respectively. The optimization results show that the optimal hybrid system for all the five campuses based on the least NPC value is a combination of the wind turbine, diesel generator, and grid (W-D-G). Although, as observed from the results, all the campuses require a 100 kW diesel generator, the power supplied by the wind turbine varies from campus to campus ranging from 1.5 MW to 6.8 MW, while the balance required to meet the load is imported from the grid.

The wind turbine is the prominent RES for all campuses; hence the low wind speed of PC affects the results obtained on that campus. The simple payback period for PC is six years, while the average payback period for the remaining four campuses is four years. In addition, PC has the highest COE, R1.45/kWh for the selected system configuration, while COE for other campuses ranges from R1.04/kWh to R1.08/kWh. It is observed that the NPC is directly related to the peak load; that is, the NPC increases with the load. Reviewing the individual campus results by considering the objective of this work, i.e., to maximize utility bill saving and minimize CO_2 emission, the hybrid systems that meet this objective are recommended as in

Table 3.13. The P-W-D-B-G produces the most negligible CO_2 emission (1 499.1 metric ton/yr) and gives the highest annual utility bill savings of R4 010 968 for the Edgewood campus. The P-W-D-G has lower CO_2 emissions (5 805.2 metric ton/yr) than W-D-G (5 827.9 metric ton/yr) for the Howard campus, with the highest annual utility bill saving R15 668 490. The W-D-G hybrid has the least CO_2 emission and highest annual utility bill savings for both the Medical school and Pietermaritzburg campuses. The P-W-G produces the least CO_2 emission (7 232.2 metric ton/yr) and the highest annual utility bill saving of R17 684 010 for the Westville campus. The project lifetime savings over 25 years for all campuses are significant and can be invested in sustainable projects within the university.

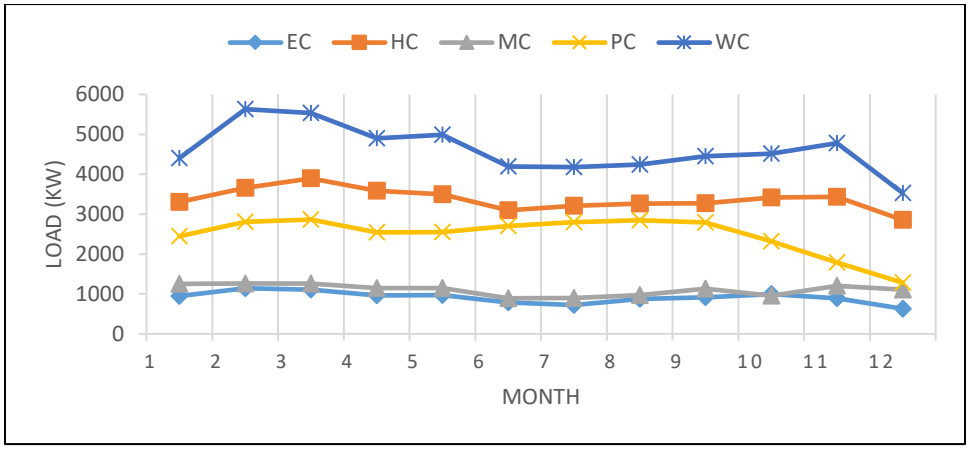

Figure 3. 13: Monthly peak load for all campuses in 2019

Table 3. 12: Summarized optimization results for all campuses

Campus		**W (kW)**	**D (kW)**	**G**	**NPC (R) X10^6**	**COE (R/kWh)**	**Peak Load (kW)**	**Payback (Years)**	**Annual Savings (Rx10^6)**	**Emission Reduction (%)**
EC		1500	100	1	98.27	1.07	1 143	4.0	3.97	49.7
HC		5900	100	1	374.86	1.04	3 896	3.9	15.58	51.1
MC		1900	100	1	123.54	1.05	1 264	4.0	4.98	49.3
PC		4500	100	1	350.65	1.45	2 865	5.9	8.16	33.7
WC		6800	100	1	463.47	1.08	5 631	4.0	17.42	48.3

Table 3. 13: Recommended HRES architectures

Campus	**Recommended HRES Architecture**
Edgewood	P-W-D-B-G

Howard	P-W-D-G
Medical School	W-D-G
Pietermaritzburg	W-D-G
Westville	P-W-G

3.6 Sensitivity analysis

In reality, certain parameters are not constant over the project lifetime; hence, a sensitivity analysis is needed to see how the variations of some input parameters will affect the feasibility of the project. From the real-time energy data for one of the campuses (Howard), it is observed that the annual peak load did not change significantly between 2011 and 2019 (Table 13); hence the electrical load demand was not considered in the sensitivity analysis. Also, considering the negligible annual production of the diesel generator (less than 0.01% of total annual production), the change in fuel (diesel) price will have no significant effect on the results. Furthermore, the inflation rate in South Africa has been on the decline since 2016. Likewise, the interest rate is decreasing. These are two economic indicators that will affect the objective of this study and, hence, the viability of the project. Therefore, three inflation rates (2%, 3%, and 4%) and three discount rate values (7%, 8%, and 9%) based on current market trends were chosen. Two campuses were considered, Howard and Pietermaritzburg, for the sensitivity analysis considering the variation in their weather parameters. The sensitivity analysis results presented in Table 3.15, Table 3.16 , Figure 3.14 and Figure 3.15, show similar trends for both campuses. The NPC increases as the inflation rate increases while the COE reduces, resulting in more annual utility bill savings. On the other hand, as the discount rate increases, the COE increases, NPC reduces, and the annual utility bill savings decreases.

Table 3. 14: Annual peak load for Howard College campus (2011-2019)

Year	**Peak load (kW)**
2011	4092
2012	4090
2013	4022
2014	4494

2015	4057
2016	3918
2017	4310
2018	3955
2019	3896

Table 3. 15: Sensitivity analysis for Howard college campus

Inflation Rate (%)	**Discount Rate (%)**	**NPC Million (R)**	**COE (R)**	**Utility Bill Savings Million (R/yr)**
2	7	371.85	1.05	15.58
3	7	406.55	1.00	15.82
4	7	446.03	0.96	16.12
2	8	342.81	1.08	15.38
3	8	373.36	1.05	15.58
4	8	407.93	1.00	15.86
2	9	317.39	1.12	15.07
3	9	344.39	1.08	15.38
4	9	374.86	1.04	15.58

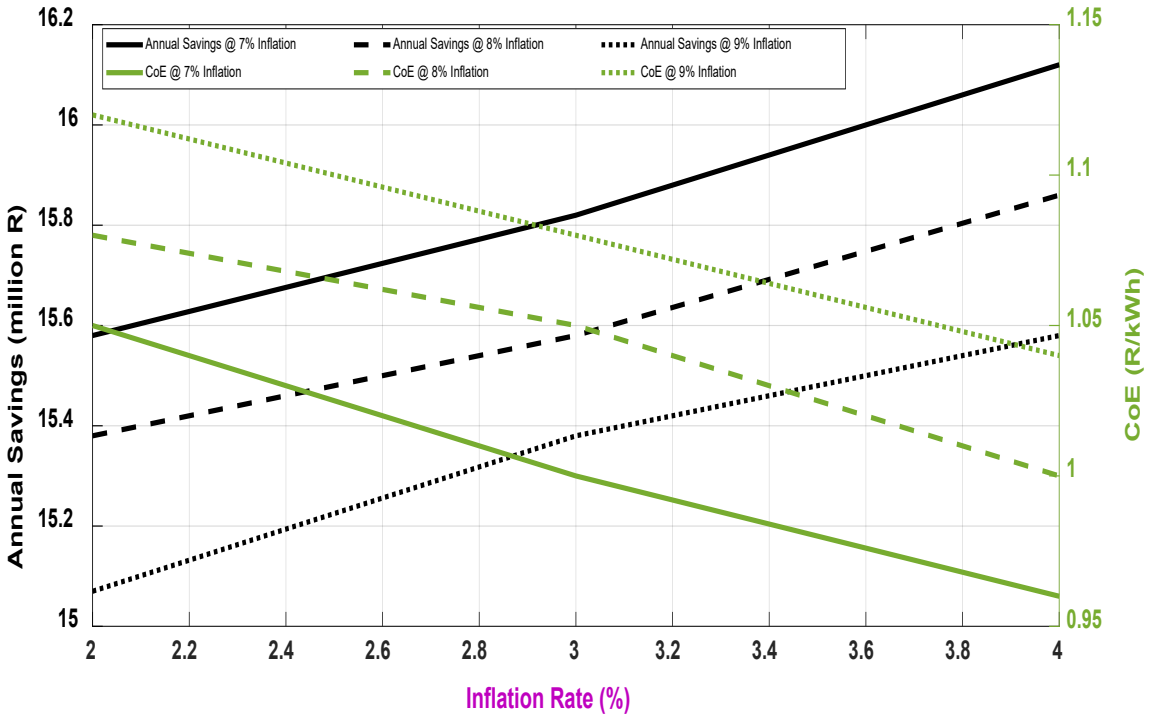

Figure 3. 14: Sensitivity analysis for Howard campus

Table 3. 16: Sensitivity analysis for Pietermaritzburg campus

Inflation Rate (%)	**Discount Rate (%)**	**NPC (R)**	**COE (R)**	**Utility Bill Savings (R/yr)**
2	7	347.74	1.45	8.16
3	7	381.41	1.41	8.35
4	7	419.69	1.36	8.69
2	8	319.61	1.49	7.87
3	8	349.20	1.45	8.16
4	8	382.74	1.41	8.35
2	9	295.02	1.54	7.45
3	9	321.14	1.49	7.87
4	9	350.65	1.44	8.16

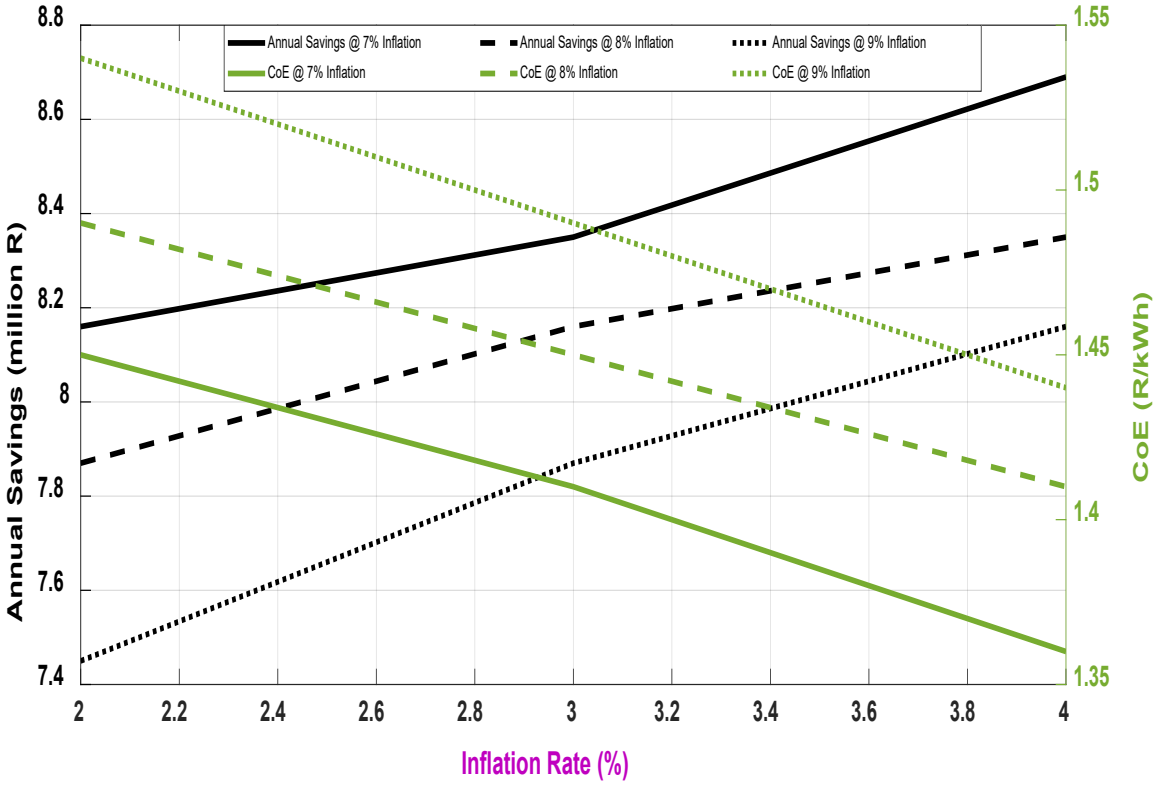

Figure 3. 15: Sensitivity analysis for PMB campus

In other words, the highest annual utility bill savings (R16.12 million and R8.69 million for Howard and Pietermaritzburg respectively) is obtained at the lowest discount rate (7%) and the highest inflation rate (4%).

3.6 Conclusion

A comprehensive techno-economic, environmental and feasibility analysis of the UKZN campuses microgrids has been carried out. This study proposes a university microgrid model that capitalizes on DERs to reduce energy import from the grid resulting in huge savings from the utility bills. The results show that the integration of DERs in the university energy mix could reduce the energy costs and the emission of CO_2 significantly. Furthermore, the amount saved from utility bills can be reinvested into renewable energy projects on the campuses, for instance, the installation of rooftop PV on all buildings and energy storage. This work can be benchmark for universities to be self-sustaining and testbed for renewable energy integration projects. Furthermore, the following summarizes the outcome of this study:

i. University campus load profile is unique; for all campuses, the peak load (Figure 3.13) in 2019 occurred between February and March since academic activities began in February, and both months are the peak of the summer in South Africa. Besides, the least load was in December for all campuses because of vacation except the Medical School campus.

ii. The COE varies from R1.04/kWh to R1.45/kWh, using the average exchange rate of rand to the dollar in 2019 ($1 = R14.45), the COE varies from $0.072/kWh to $0.1/kWh, this result is comparable to similar studies on university campus microgrid in references [35] and [77].

iii. The least consumption across the campuses was in June because of the winter vacation hence the highest utility bill savings despite the high tariff during winter (June to August).

iv. It is observed that the annual utility bill savings range from R3.97 million to R17.42 million and are directly proportional to the peak load.

v. The payback period is approximately 4 years for all campuses except Pietermaritzburg, which is 6 years because of low wind speed.

vi. The average emission reduction for all campuses is 49.6% except Pietermaritzburg (33.7 %) for the same reason stated in (V) above.

Considering the erratic load shedding experienced in South Africa in recent years, there is a need to consider the feasibility of the off-grid operation of university campuses for self-sustainability during load shedding. Lectures and practical experiments were disrupted, and the entire university internet network (IP phones off) might be down because of load shedding. One of the objectives will be to ensure continuous supply to critical loads using a hybrid system of diesel generator, solar PV, and battery storage (Tesla Power wall). Given the above, investigating an optimal hybrid system for off-grid application in university campus is considered future work.

CHAPTER FOUR

OPTIMIZATION OF HYBRID RENEWABLE ENERGY SYSTEM FOR OFF-GRID APPLICATION: A CASE STUDY OF UNIVERSITY CAMPUS MICROGRID

4.1 Introduction

Considering the erratic load shedding experienced in South Africa in recent years, there is a need to consider the feasibility of the off-grid operation of university campuses for self-sustainability during load shedding. Lectures, practical experiments are disrupted, and the entire university internet network (IP phones off) might be down because of load shedding. This study aims to ensure continuous supply to critical loads using a hybrid system of diesel generator, solar PV, and battery storage. Therefore, the main goal of this work is to investigate the feasibility of an off-grid HRES microgrid to meet the electricity demand of a university campus at a minimum cost. The main contributions of this study is the investigation and optimal sizing of an off-grid hybrid system design proposed for a university campus that comprises of PV, WT, DG, and battery storage. This study considers variations of energy demands for summer study, summer vacation, winter study and winter vacation days with a view to compare the corresponding operating costs and evaluate the efficiency of the HRES daily. MATLAB function "quadprog" is used to optimize the HRES with priority given to the RES to meet the energy demand when available. Off-grid application of microgrid is common in remote or rural areas where connection to the main grid is impossible or not economical. Off-grid microgrid offers certain benefits, the quality of life of people dwelling in rural or remote communities can be improved significantly through access to electricity. Geographical limitations and the high cost of grid extension are major difficulties responsible for the lack of electrification in these communities. Hence, off-grid microgrids are suitable solutions to overcome these challenges, especially with the integration of RESs within the communities. According to [43], a network system of DER (wind turbine, solar PV, diesel generator, and battery storage) that is not connected to the grid is referred to as an off-grid microgrid. Off-grid application of microgrid does not only help to reduce energy costs but also makes consumers energy independent. As reported in [178], the head office of Winkelmann Group, based in Ahlen, Germany, went off the European power grid in December 2018. The off-grid microgrid can produce 9 MW and 10 MW of electrical and thermal output, respectively, using six CHP plants, thereby reducing electricity and grid usage costs. The off-grid application of microgrids is gaining more attraction for technical, environmental, and economic benefits. Most off-grid applications of microgrid reported in literature are for rural/remote area electrification [45-50], remote islands [64], military bases [65], and telecommunication base transceiver stations [176, 179, 180] while most university campus microgrids are grid-tied [68, 97, 112, 164].

4.2 Hybrid System Modelling and Configuration

The proposed hybrid system in this study comprises solar PV, wind turbine, diesel generator, battery, and power converter, as shown in Figure 4.1. For the purpose of power flow analysis, the control (communication) system has been omitted and is assumed to operate at an efficiency of 100%.

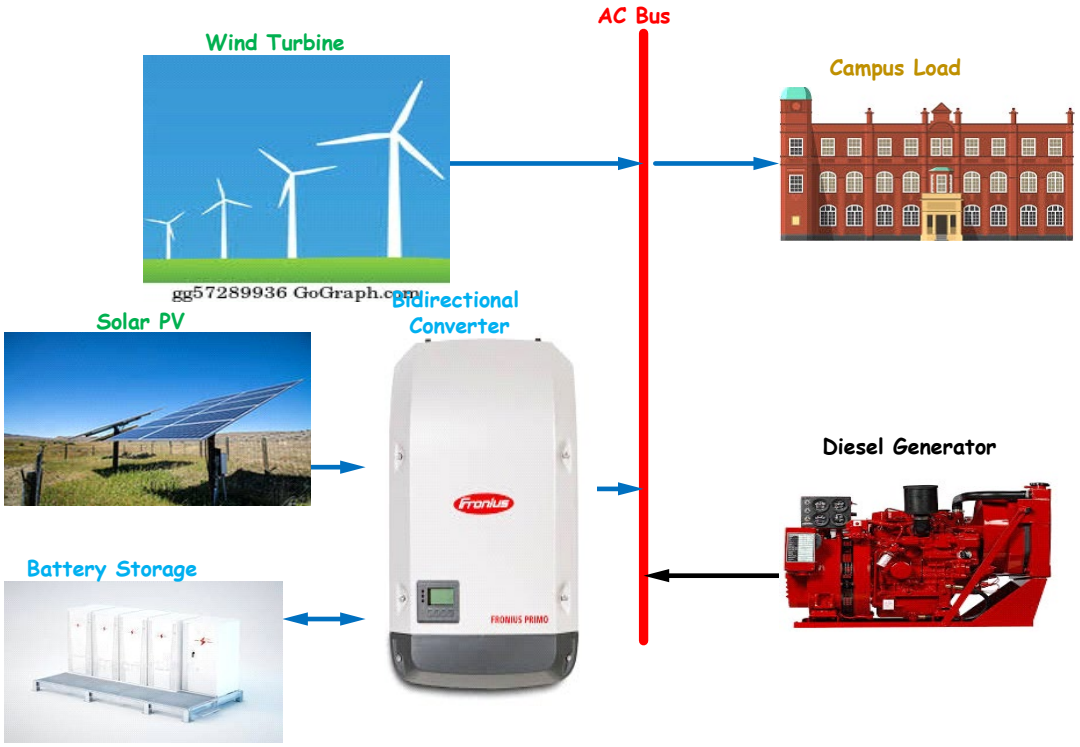

Figure 4. 1: Proposed Off-grid Hybrid Microgrid Configuration

4.2.1 Solar Photovoltaic Model

Several solar photovoltaic cells are linked in series to improve voltage output and in parallel to increase the current in a solar photovoltaic system. The product of a PV module's maximum current and maximum voltage is the maximum power output. However, equations (4.1) through (4.2) may be used to characterize the PV system's hourly energy production (4.3) [181, 182].

$$E_{PV} = A_{ARR}.H_{Rad}\eta_{PV} \quad 4.1$$

$$\eta_{PV} = \eta_{STC}(1-\beta(T_C - T_{STC}))\eta_{INV} \quad 4.2$$

$$T_C = T_a + \frac{SI}{SI_{NOCT}}(T_{NOCT} - T_{aNOCT}) \quad 4.3$$

In equation (4.1), η_{PV} represents the conversion efficiency (%) of the PV system, A_{ARR} is the PV array area (m^2), H_{Rad} is hourly solar irradiation (kWh/m^2) incident on the PV array. η_{STC} is the module efficiency at standard test condition (STC) (%), β is the temperature coefficient at the maximal power of the module (typically 0.004 – 0.005/°C), T_c is the PV cell temperature (°C), T_{STC} is the standard test condition temperature (25°C), η_{INV} is the inverter efficiency (%), T_a is the ambient temperature (°C), SI is the incident solar irradiance on the PV plane (W/m^2), SI_{NOCT} is the incident solar irradiance of $800W/m^2$, T_{NOCT} is the nominal operating cell temperature (°C), and T_{aNOCT} is the ambient temperature for the nominal operating cell temperature (20°C).

The output power of PV array can also be determined using equation (4.4) [183],

$$P_{Arr} = N_P N_S P_{\max} \eta_{MPPT} L \qquad 4.4$$

Where P_{max} represents the maximum power of the PV module, N_P and N_S are the numbers of parallel and series-connected modules, respectively. η_{MPPT} is the MPPT efficiency, and L is the loss in the system.

4.2.2 Wind Turbine

Wind turbines are categorized into two designs according to their orientation of the axis of rotation. Horizontal axis wind turbine (HAWT) has its axis of rotation parallel or horizontal with the ground while vertical axis wind turbine (VAWT) axis of rotation is perpendicular or vertical to the ground. The HAWT is preferred for electrical power generation due to its higher conversion efficiency and access to stronger wind at higher hub height [183, 184]. The major components of a HAWT and its configuration are shown in figure 4.2. Therefore, this work is considered a HAWT with three blades. The power output of a WT is a function of certain parameters such as air density, wind speed at a particular location, the area swept by the rotor blade, and energy conversion efficiency. Therefore, the mechanical power output, P_{mech}, of a WT, is given by:

$$P_{mech} = 0.5 C_{cp} \rho A V^3 \qquad 4.5$$

Where C_{cp} is the power coefficient and is a function of the tip-speed ratio and the blade's angle, V is the wind speed (m/s), A is the area swept by the blade (m^2), and ρ is the air density (kg/m^2). However, it should be noted that the effective wind speed is usually at 50-100m above ground level. Hence, the wind speed measured by the anemometer at a reference height must be converted to a new value at the actual hub height using equation 4.6 [70, 183].

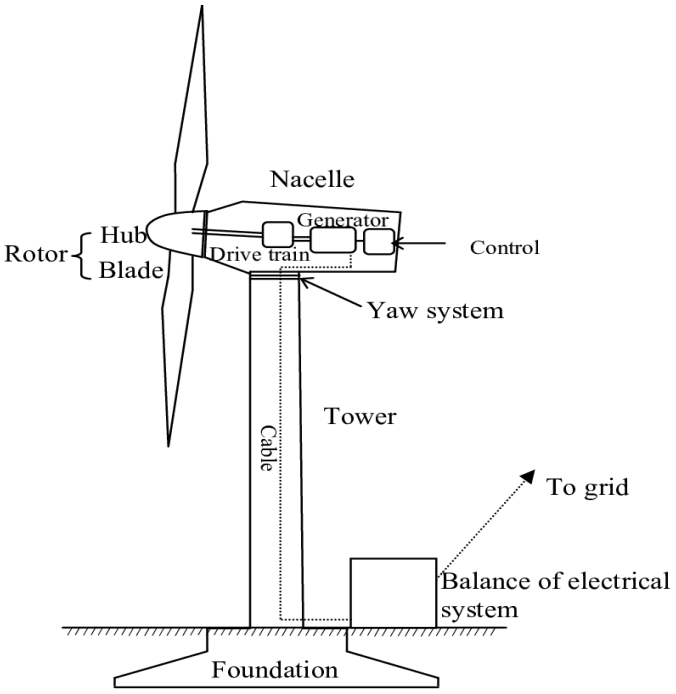

Figure 4. 2: Components of HAWT [185]

$$V_{new} = V_{ref}\left(\frac{h_{new}}{h_{ref}}\right)^{\alpha} \tag{4.6}$$

Where V_{new} and V_{ref} are the wind speeds at the desired hub height h_{new} and at the reference height h_{ref} respectively, and α is the power-law exponent, representing the friction coefficient of the ground surface. V_{new} is used to model the power output to calculate the power generated by the wind turbine. Equation 4.7 gives an approximation of power generated from the wind turbine depending on the performance curve of the wind turbine.

$$P_w = \begin{cases} 0 & ;\mathrm{V} \le V_{in} \ge V_{out} \\ V^3\left(\frac{P_{rated}}{V_{rated}^3 - V_{in}^3}\right) - P_{rated}\left(\frac{V_{in}^3}{V_{rated}^3 - V_{in}^3}\right) & ;\mathrm{V}_{in} \le V \le V_{rated} \\ P_{rated} & ;\mathrm{V}_{rated} \le V \le V_{out} \end{cases} \tag{4.7}$$

Where P_W represents the power generated by the wind turbine, V is the wind speed, V_{in} and V_{out} are the cut-in wind speed and the wind turbine's cut-out wind speed, respectively. P_{rated} and V_{rated} are respectively the rated power and rated speed of the wind turbine. This work adopted a mathematical model proposed in [183]to determine the electrical power from the hourly wind speed as given by equation (4.8).

$$P_{elect} = 0.5\eta_{wt}C_{cp}\rho A V^3 \tag{4.8}$$

Where η_{wt} represents the efficiency of the wind turbine as stated in the manufacturer's data sheet.

4.2.3 Diesel Generator

Without the connection to the local electricity grid, supply reliability is crucial for the operation of the off-grid microgrid. Therefore, DGs are included in hybrid systems to act as a backup during the period when the RESs cannot meet the load demand, thereby ensuring system reliability. However, in order to deploy DG in the hybrid system, it is important to consider the operating limits of the DG as recommended by the manufacturer. Therefore, the operation of the DG at any instance must be within the rated power and stated minimum value (considering the fact that maximum efficiency of the DG correlates with its rated power); this constraint is expressed in equation (4.9).

$$P_{dg}^{\min} \leq P_{dg}(t) \leq P_{dg}^{\max} \tag{4.9}$$

The rate of fuel consumption (directly proportional to fuel cost) is modelled using equation 4.10

$$FC(t) = \alpha P_{dg}(t) + \beta P_{dg,rated}(t) \tag{4.10}$$

FC(t) is the fuel consumption rate(l/h), $P_{dg}(t)$ represents the power output of DG and $P_{dg,rated}$ is the DG rated capacity (kW). α and β are the fuel curve intercept coefficient (l/h/kW) and the diesel curve intercept coefficient (l/h/kW). For the economic operation of the hybrid system, a load-following dispatch strategy is used whereby the DG is turned on when the RES and/or the battery cannot supply the load.

4.2.4 Battery Storage

Battery energy storage systems are included in the hybrid system due to the following:

- Stochastic and intermittent nature of RES
- Reduction of fuel cost and CO_2 emission
- Maintenance of system stability i.e., balance between load and supply
- Storage of excess energy produced by RES

The battery system (battery bank) in this work is designed to be charged during excessive production of RES and discharged when the RES output cannot meet the load demand. For off-grid application, the battery must be operated within the minimum and maximum limits of their state of charge (SoC) as stated by the manufacturer. SoC of a battery simply expresses the battery charge level relative to its capacity at a specific time (hour). The SoC of the battery at any time (hour) is given by equation (4.11).

$$B_{soc}(t) = B_{soc}(t-1) + \eta_c P_{bc}(t) - \eta_d P_{bd}(t) \tag{4.11}$$

Where η_c and η_d are the battery charging and discharging efficiencies, respectively. P_{bc} and P_{bd} are the power received and emitted by the battery at a time, t, respectively. Considering the battery dynamics, equation 4.11 can be simplified further as:

$$B_{soc}(t) = B_{soc}(0) + \eta_c \sum_{t=1}^{N} P_{bc}(t) - \eta_d \sum_{t=1}^{N} P_{bd}(t) \quad 4.12$$

Where $B_{soc}(0)$ is the initial battery SoC.

In order to increase the life span of the battery, the battery operation must be governed by these constraints:

$$B_{cap}^{\min} \le B_{cap}(t) \le B_{cap}^{\max} \qquad \text{and} \qquad \mathrm{B}_{cap}^{\min} = (1 - DoD) B_{cap}^{\max}$$

Where DoD is the depth of discharge in percentage.

4.3 Optimization model

The hybrid system is designed such that priority is given to the RES (PV and WT) in meeting the load, when and if the RES output is not adequate to supply the load, the battery discharges provided that it is within its operating limits. The diesel generator is switched on only if the RES and battery are unable to meet the power demand, meaning that the diesel generator is kept at the least demand. In the case whereby the maximum demand is met only by RES, then the surplus energy generated by the RES is stored in the battery. Figure 4.3 shows the flow chart that illustrates the simulation and optimization process.

4.3.1 Formulation of the objective function

The hybrid system is optimized to minimize the power supplied by the DG. This is achieved by formulating the optimization problem to minimize the cost of fuel consumed by the DG during the operating time. The fuel cost, F_{cost} of the DG, is a non-linear quadratic function as in equation 4.13

$$F_{\cos t} = C_f \sum_{k=1}^{N} (aP_{dg(k)}^2 + bP_{dg(k)} + c) \quad 4.13$$

Where a, b and c are the generator cost coefficient (available in the manufacturer datasheet), C_f is the price per litre of diesel fuel, N represents the number of DG. Therefore, the objective function is expressed as:

$$\min F_{\cos t} = C_f \sum_{k=1}^{N} (aP_{dg(k)}^2 + bP_{dg(k)} + c) \quad 4.14$$

Subject to the following constraints:

$$P_{pv}(k) + P_{wt}(k) + P_{bd}(k) - P_{bc}(k) + P_{dg}(k) = P_d(k) \quad 4.15$$

$$P_{pv}(k) \geq 0, P_{wt}(k) \geq 0, P_{bc}(k) \geq 0, P_{bd}(k) = 0, P_{dg}(k) \geq 0 \quad 4.16$$

$$B_{soc}^{\min} \leq B_{soc}(0) + \eta_c \sum_{k=1}^{N} P_{bc}(k) - \eta_d \sum_{k=1}^{N} P_{bd}(k) \leq B_{soc}^{\max} \quad 4.17$$

For all k = 1,…., N, where N is 24, i.e., a number of hours in a day. $P_{pv(k)}$, $P_{wt(k)}$, $P_{bd(k),}$ and $P_{dg(k)}$ represent variables of energy flowing from the solar PV, wind turbine, battery, and diesel generator respectively to the load at any time (k) while $P_{bc(k)}$ is the energy flow to the battery.

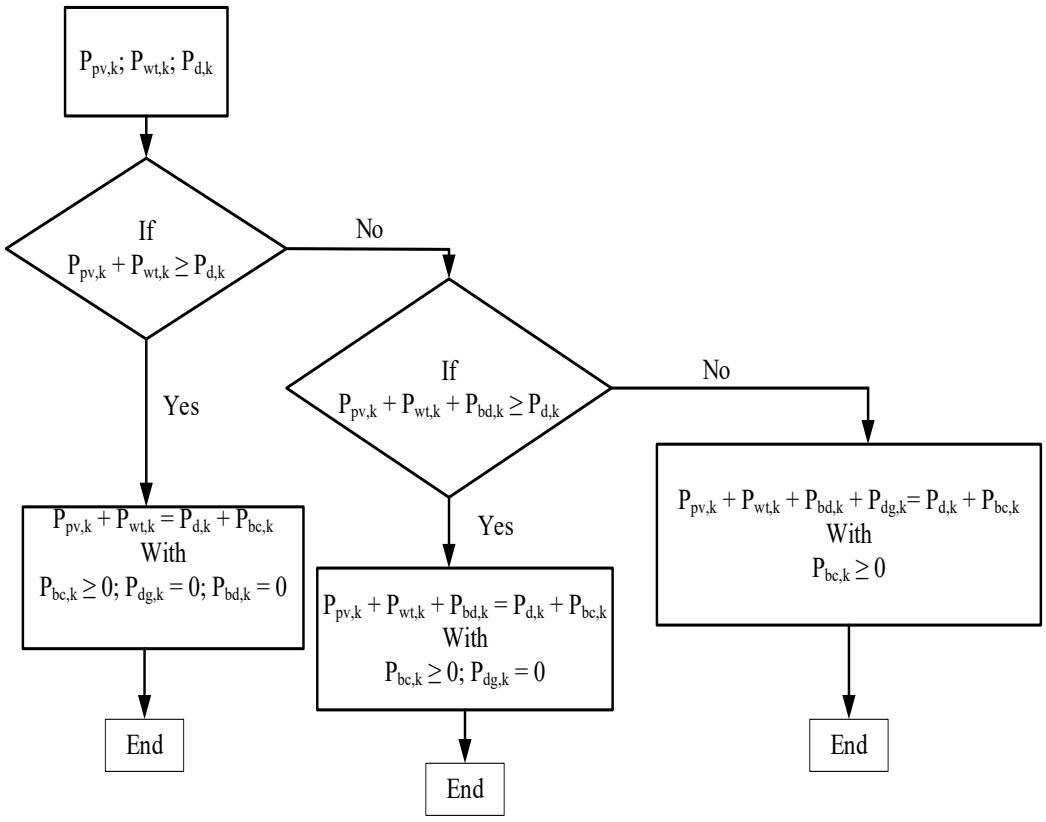

Figure 4. 3: Flow chart for optimization process

The non-linear optimisation is solved by deploying the "quadprog" function in MATLAB. This function finds the minimum for problems in the form:

$$\min \frac{1}{2} x^T Hx + f^T x \text{ such that } \begin{cases} A.x \leq b, \\ Aeq.x = beq, \\ lb \leq x \leq ub. \end{cases} \quad 4.18$$

H, A, and *Aeq* are matrices, and *f, b, beq, lb, ub,* and x are vectors.

4.3.2 Load model

Four load models of two campuses (Howard and PMB) are considered for this study; these are daily load profiles for typical days during summer and winter based on the 2019 university sessional calendar.

4.3.3 Levelized cost of energy

Levelized cost of energy (LCOE) is a useful economic tool to estimate the cost of energy across various energy generating sources (e.g., solar, wind, natural gas) that have an unequal lifetime, different investment costs, operation, and maintenance (O & M) cost, efficiency etc. Therefore, the value of LCOE is crucial to making an informed decision in implementing HRES projects. A lower LCOE value indicates a lower energy cost, which yields high financial gain to the investor, in this case, the university. In calculating LCOE, the power generating system's total lifetime costs ($) are divided by the estimated total energy (kWh) produced over its lifetime. This can be expressed mathematically according to equation 4.19 below [186-188].

$$LCOE = \frac{\sum_{t=1}^{n} \frac{I_t + M_t + F_t}{(1+r)^t}}{\sum_{t=1}^{n} \frac{E_t}{(1+r)^t}} \qquad 4.19$$

I is the initial investment cost (cost of constructing the power plant), M represents the O&M cost, which is fixed and variable costs for running the plant, and F is the fuel expenditures where applicable. E is the energy generated, r is the discount rate, and n is the project lifetime in years.

4.4 Simulation results and discussion

This section discusses the simulation results of the hybrid systems simulated under different load and climatic conditions. The costs of using only the DG to supply the load are also compared to the costs of using the hybrid system. The simulation model parameters are provided in Table 4.1 (the components were adapted from reference [182]), and the load data for the Howard College campus is presented in Table 4.2.

4.4.1 Howard College Campus

Table 4.3 presents the load data for the Howard campus; these are daily load data for selected days during the summer study period (4 February – 31 May 2019), summer vacation (13- 22 April 2019), winter study period (8 July -31 August 2019) and winter vacation (14 June – 7 July 2019). Figure 4.1 shows the four load profiles together (to illustrate the variations). It is observed that the demands begin to rise from 07h00, peak between 11h00 and 13h00, and start decreasing from 16h00 to 19h00 (closing hours); a small rise is observed between 21h30 and 22h30. The load demands for the selected days are met by a combination of energies supplied by the DG, solar PV, wind turbine, and battery.

Table 4. 1: Simulation parameters

Components			
Solar PV	Wind Turbine	Battery	Diesel Generator
A_{ARR}, PV array area - 1000m^2	Hub height – 80m	Battery charge efficiency – 85%	Fuel cost - \$1.2/litre
Geometric factor – 0.6	Reference height – 42m	Battery discharge efficiency – 100%	a - \$0.246/(kW)^{2}h
SI_{NOCT}, incident solar irradiance at nominal operating cell temperature – 0.8 kWh/m^2	Blade diameter – 1.5m	Maximum capacity – 500 kWh	b – 0.1/kWh
T_c, cell temperature - typically 45°C	Turbine efficiency – 95%		Capacity – 200 kVA
T_{aNOCT}, ambient temperature for the nominal operating cell temperature - 20°C	Cut out speed – 20m/s		Number of units - 18
T_{STC} , standard test condition temperature - 25°C	Cut in speed – 3m/s		
PV generator efficiency measured at reference cell temperature – 0.17	Rated speed – 10m/s		
β, temperature coefficient at the maximal power of the module – 0.004/°C	Rated power – 500kW		
	Friction coefficient – 0.25		
	Number of units – 10		

It is observed that the two demands during summer are higher than the two demands during winter. However, this is contrary to what is expected as the utility regards the winter period as a high-demand period hence higher tariff as shown in Tables 3.2 and 3.3. The obvious reason is the use of air conditioners in most offices and lecture rooms during the summer; moreover, it is easier for staff members and students to dress warmly during winter. In addition, the city of Durban has temperate weather during winter compared to other cities in South Africa.

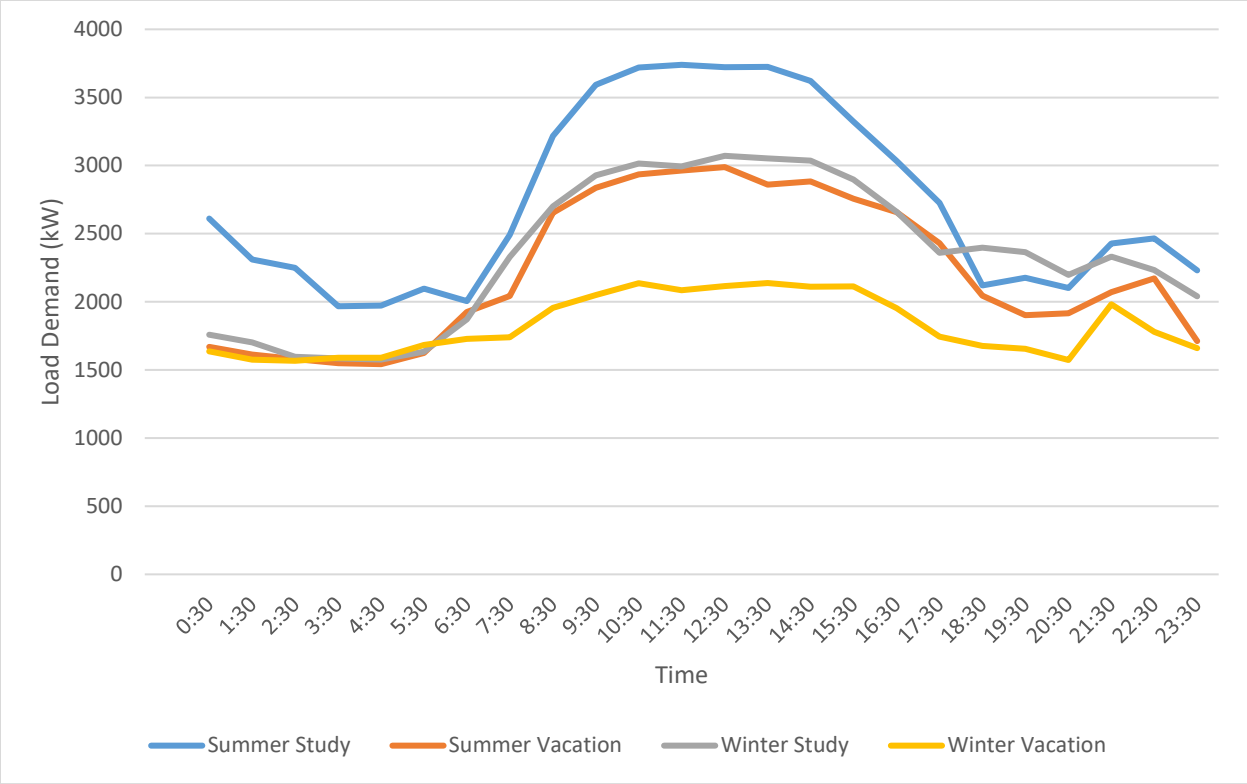

Figure 4. 4: Howard campus load profiles

The energy flow during each selected day (24-hour) is shown in Figs 4.5 to 4.8.

i. Summer Study day

During the early hours of the day between 00h00 and 08h00, the load was met by the DG and battery; the PV started generating from 08h00 while the WT started at 12h00. As observed in fig 4.5, as the wind speed increased and the PV continued to produce energy, the load was met majorly by the WT and PV between 12h00 and 20h00. For instance, at 15h00, the load demand was 3622 kW; this was supplied by the WT (3335.09 kW) and PV (286.91 kW). The DG switched off (15h00 – 20h00) when the RES output was enough to meet the load, and the battery was charged during this period. The setup ensures that the operating time and output of the DG depend on the power produced by the RES (PV and WT). Therefore, the more the output of the RES, the less the DG output hence lower operating (fuel) cost. The PV started generating earlier than the WT; however, the WT continued to generate after the sunset. With this pattern, the RES was able to compliment the energy supply for about 15 hours of the day.

Table 4. 2: Demand Profiles for Howard Campus

Time	Summer Load (kW)		Winter Load (kW)	
	Study	Vacation	Study	Vacation
00:30	2,612.06	1,670.39	1,758.59	1,636.91
01:30	2,310.82	1,613.54	1,702.42	1,574.54
02:30	2,249.62	1,579.61	1,595.80	1,567.30
03:30	1,967.64	1,549.60	1,584.86	1,589.80
04:30	1,971.71	1,542.62	1,576.28	1,590.22
05:30	2,096.10	1,625.54	1,633.67	1,684.50
06:30	2,005.98	1,924.85	1,870.40	1,728.78
07:30	2,491.91	2,043.71	2,328.35	1,739.16
08:30	3,216.86	2,652.66	2,700.31	1,957.18
09:30	3,593.82	2,836.68	2,929.39	2,049.89
10:30	3,720.29	2,935.10	3,015.71	2,137.07
11:30	3,739.58	2,964.55	2,993.03	2,084.26
12:30	3,721.79	2,988.95	3,071.75	2,114.97
13:30	3,724.31	2,861.23	3,052.78	2,138.02
14:30	3,622.14	2,883.00	3,037.42	2,110.50
15:30	3,322.96	2,757.83	2,898.32	2,112.95
16:30	3,034.11	2,659.24	2,661.63	1,954.27
17:30	2,726.58	2,430.02	2,359.38	1,745.69
18:30	2,119.60	2,045.60	2,397.89	1,677.28
19:30	2,176.31	1,901.37	2,364.23	1,654.56
20:30	2,102.51	1,916.17	2,197.84	1,573.03
21:30	2,428.05	2,072.12	2,332.27	1,981.02
22:30	2,464.73	2,170.98	2,232.38	1,779.10
23:30	2,231.77	1,712.30	2,041.67	1,661.08

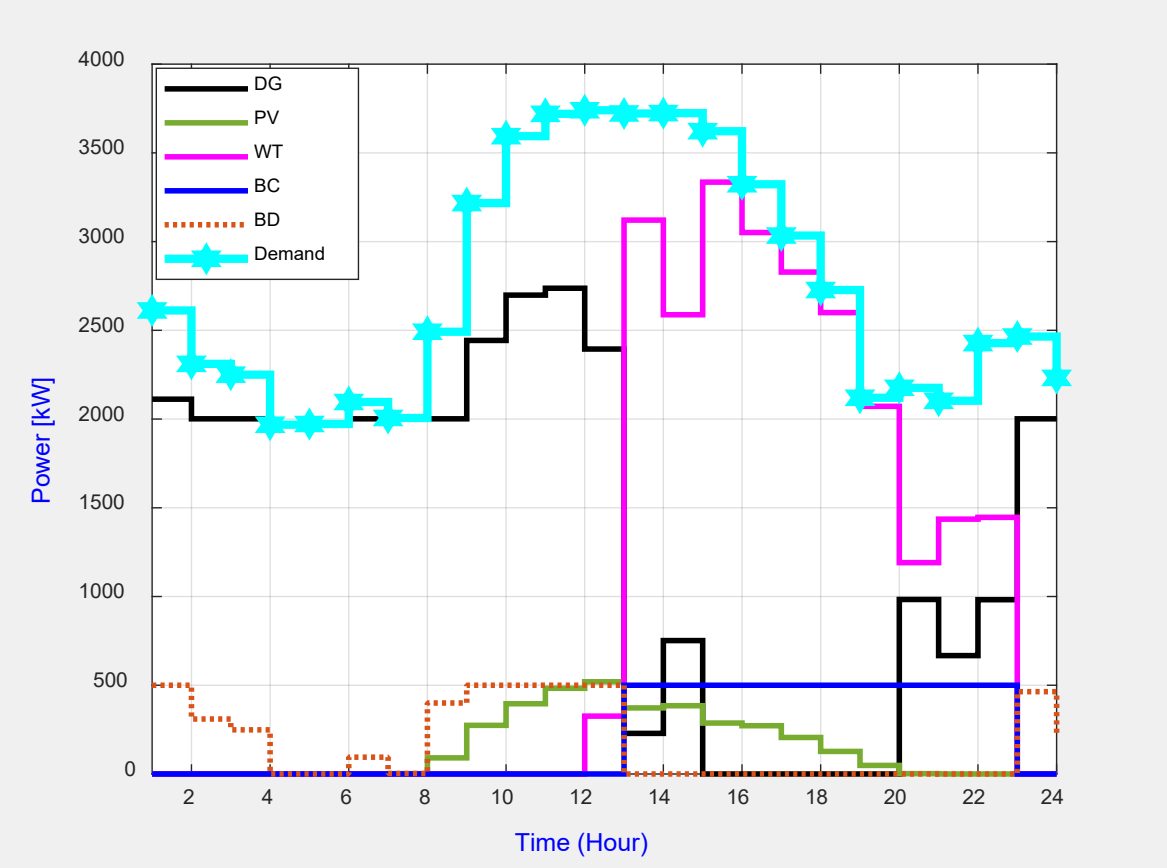

Figure 4. 5: Summer Study day (13 March 2019) Power Flow

ii. Summer Vacation day

The energy flow for this day is shown in Figure 4.6; the load profile for the day shows a decline in the load demand throughout the 24 hours compared to a typical study day, confirming less academic activities on campus. The wind speed throughout the day was below the cut-in speed (3.5 m/s); the maximum speed on the day was 2.157 m/s; hence there was no generation from the WT. The DG supplied the load only in the early hours of the day until the sun rose at 09h00. As the PV started generating, the output of the DG reduced gradually until the sun went down, and the DG supplied the load for the remaining hours of the day. The peak load (2989 kW) on the day occurred at 13h00 and was supplied by the DG (2317.41 kW) and PV (671.59 kW). As observed, the PV could supply part of the peak load period and serve as peak shaving.

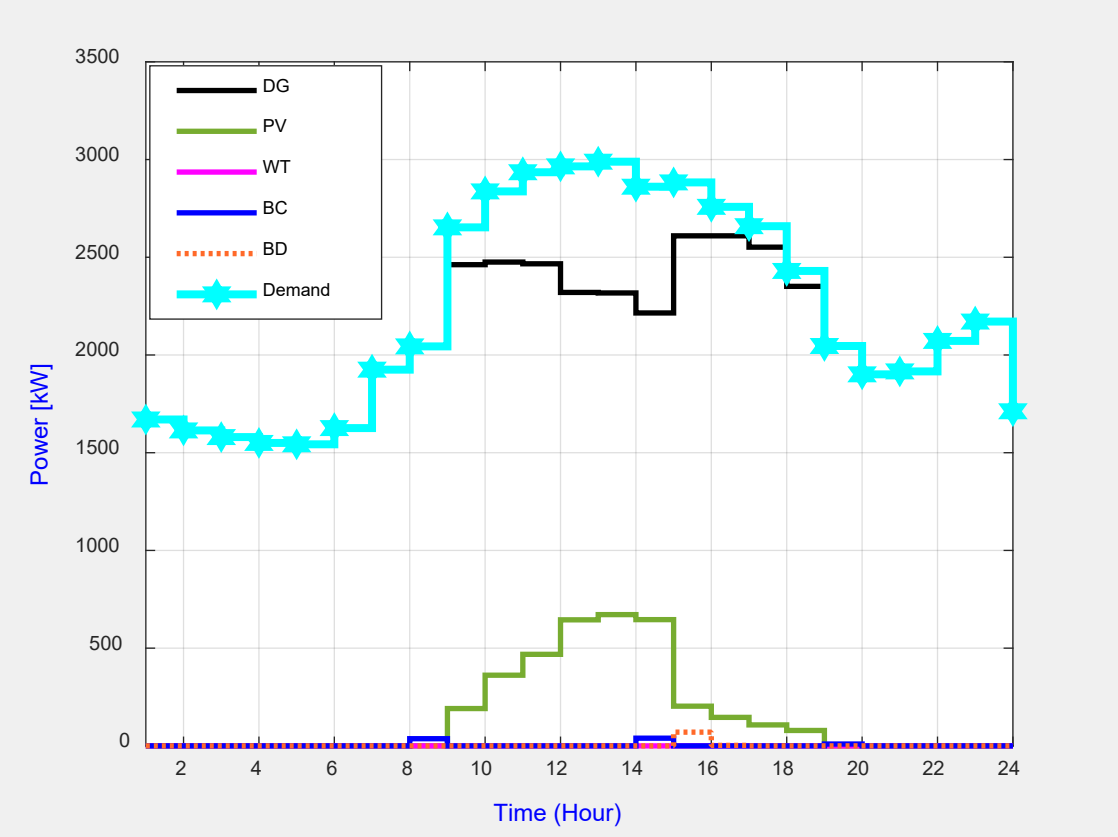

Figure 4. 6: Summer Vacation day (17 April 2019) Power Flow

iii. Winter Study day

The generation-demand profile for this scenario is shown in Figure 4.7. It is generally observed that the DG supplies the bulk of the power required to meet the load throughout this period. Likewise, the demand is lowest in the day's first-third (00h00 to 08h00), highest in the second-third, and median in the final third of the day. It is also observed that the PV generation begins to ramp up at 09h00 till 15h00, reducing the DG generation within this period, and the PV generation declines gradually after 15h00. The WT has a zero generation for most of this scenario; however, a short-spanned generation is between 16h00 to 18h00 and 19h00 to 20h00. It can be concluded that fuel cost resulting from the bulk DG generation in this scenario would be higher than the summer study period that experienced higher PV and WT generation to offset the demand.

iv. Winter Vacation day

The winter vacation day scenario is a peculiar scenario that experiences the least renewable energy generation and net demand when compared to the previous scenarios. Figure 4.8 is observed for most of the day, and the DG supplies all the demand with near-zero generation from the WT. The PV generation in

this scenario has a gaussian distribution with peak generation between 13h00 to 15h00. Similar to the winter study day, this scenario has a higher fuel cost and CO_2 emissions when compared to the summer vacation day.

The summary of the fuel cost of these scenarios comparing the 'DG only' and 'hybrid' modes is represented in Table 4.3. It can be inferred that the summer study day has the highest fuel cost in the DG only mode; however, in the hybrid generation mode, the summer vacation day has the highest fuel cost. Therefore, it can be concluded that the summer period incurs more fuel costs than the winter period at the Howard campus. However, the summer study period has the least fuel cost in the hybrid mode, indicating the highest penetration of PV, WT, and Battery sources. Consequently, the fuel-saving cost is highest in the summer study period. It can be observed that the generation in both modes for the summer vacation and the two winter scenarios are marginally different due to the low generation from the renewable energy sources; thus, the fuel savings are marginal in these scenarios.

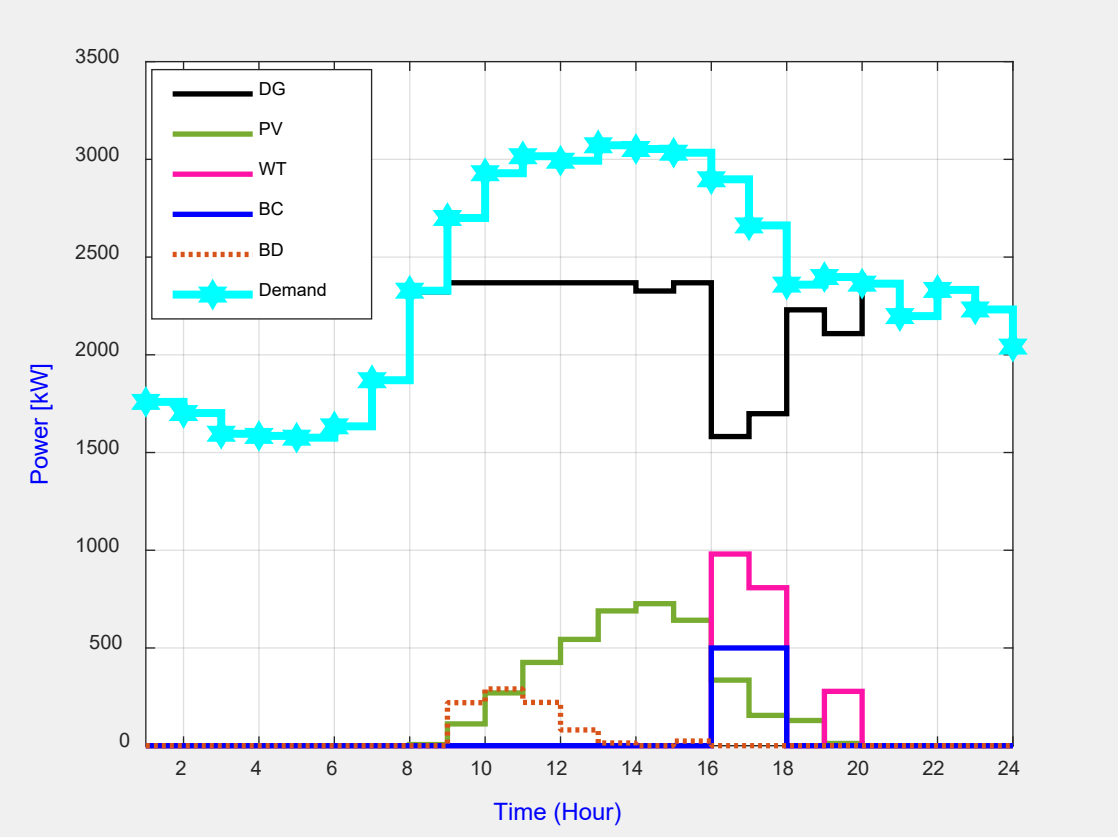

Figure 4. 7: Winter Study day (13 August 2019) Power Flow

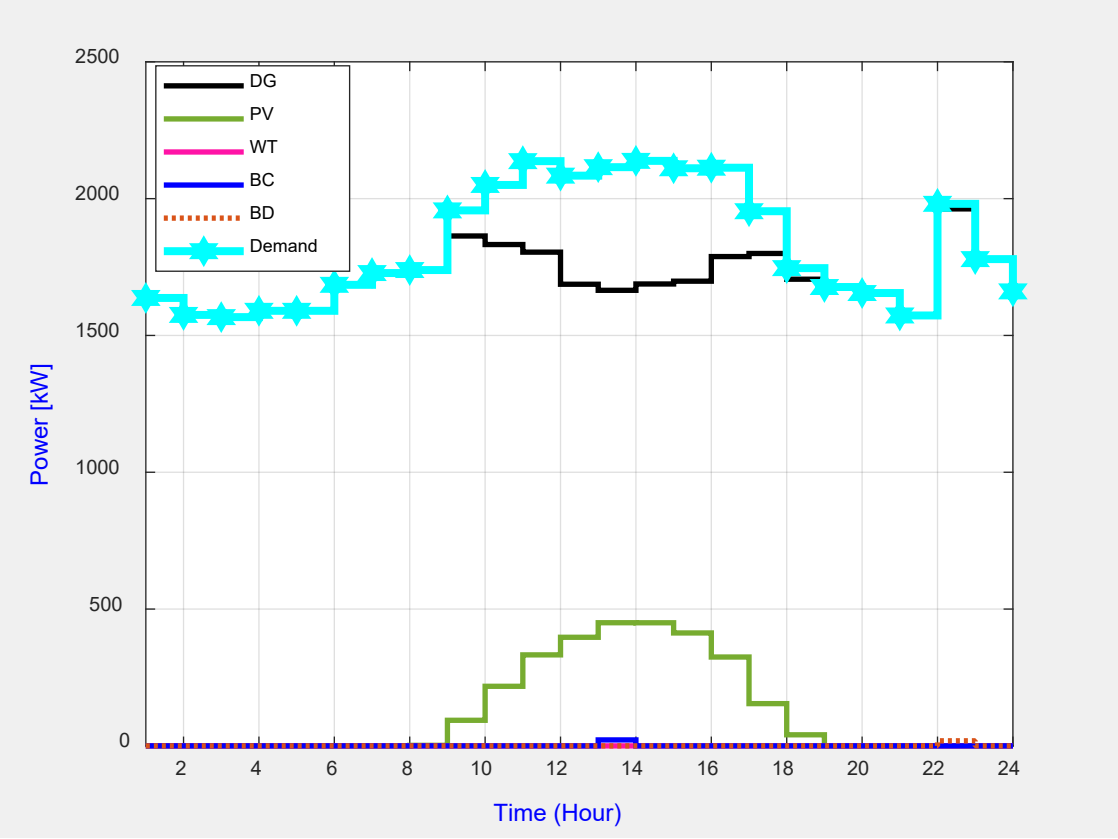

Figure 4. 8: Winter vacation day (25 June 2019) Power Flow

Table 4. 3: Fuel Cost Saving

	Summer ($/W)		Winter ($/W)	
	Study	Vacation	Study	Vacation
DG Only	65.65	53.34	56.33	43.84
Hybrid	33.95	49.75	49.37	40.95
Saving	**31.70**	**3.59**	**6.96**	**2.89**

4.4.2 Pietermaritzburg Campus

i. Summer study day

The generation-demand pattern for this scenario is depicted in Figure 4.9; it is seen that at the start of the day (00h00 to 08h00), all of the demands are met by the DG with a transient WT generation between 02h00 to 03h00. As the day begins to brighten, the PV starts to generate electricity, reducing the power supply from the diesel generator. The excess generation in this period is stored in the battery. During the peak demand (10h00 to 18h00) when several activities are ongoing at the campus, the PV and DG supply the load with relatively low support from the WT. Towards the end of the day, when the sun sets, the DG meets the demand operating maximum capacity; however, the total demand is greater than the DG power output.

Thus, the battery discharges power to offset the power shortage, leading to frequency instability or load shedding on campus.

Table 4. 4: Demand Profiles for PMB Campus

Time	Summer (kW)		Winter (kW)	
	Study	Vacation	Study	Vacation
00:30	1,718.00	1,586.00	1,847.00	1,492.00
01:30	1,630.00	1,445.00	1,811.00	1,512.00
02:30	1,582.00	1,354.00	1,674.00	1,487.00
03:30	1,530.00	1,318.00	1,596.00	1,460.00
04:30	1,433.00	1,265.00	1,651.00	1,443.00
05:30	1,407.00	1,277.00	1,647.00	1,436.00
06:30	1,539.00	1,386.00	1,724.00	1,559.00
07:30	1,756.00	1,526.00	1,783.00	1,881.00
08:30	1,986.00	1,645.00	1,878.00	1,987.00
09:30	2,311.00	1,811.00	1,956.00	2,095.00
10:30	2,542.00	2,003.00	1,958.00	2,205.00
11:30	2,641.00	1,971.00	2,024.00	2,174.00
12:30	2,649.00	2,074.00	2,029.00	2,128.00
13:30	2,684.00	1,936.00	2,001.00	2,045.00
14:30	2,657.00	2,004.00	2,054.00	2,082.00
15:30	2,711.00	2,043.00	2,021.00	2,019.00
16:30	2,609.00	2,049.00	1,986.00	2,006.00
17:30	2,339.00	2,001.00	1,976.00	1,831.00
18:30	2,123.00	1,945.00	2,061.00	1,825.00
19:30	2,216.00	1,940.00	2,136.00	1,784.00
20:30	2,245.00	1,909.00	2,094.00	1,793.00
21:30	2,104.00	1,802.00	2,118.00	1,743.00
22:30	2,017.00	1,627.00	2,030.00	1,655.00
23:30	1,877.00	1,584.00	1,913.00	1,595.00

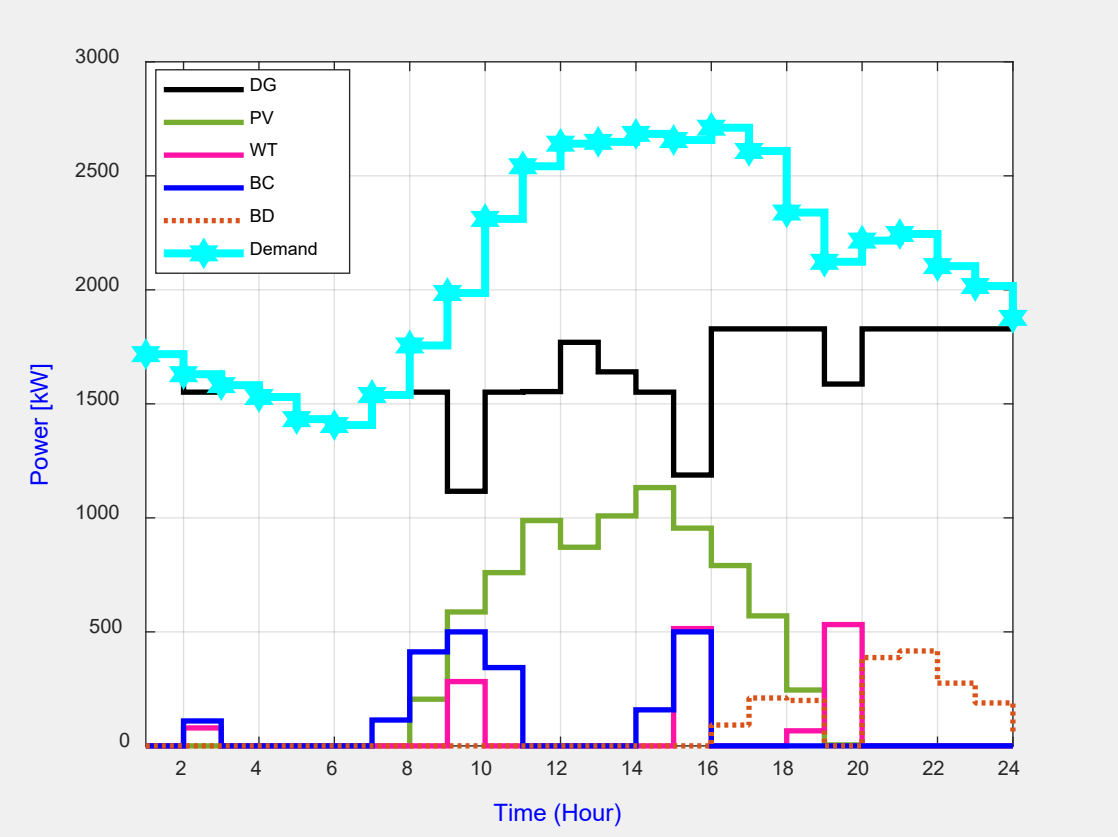

Figure 4. 9: Summer Study day (13 March 2019) Power Flow

ii. Summer vacation day

In contrast to the summer study day, the summer vacation day experienced a high penetration of WT generation in the energy mix with peak generation between 15h00 to 21h00, as depicted in Figure 4.10. To this effect, a high share of the demand is supplied by the WT with support from the DG when needed. The cumulative time for excess generation is 10 hours, part of which is stored in the battery. It is observed that there is intermittence in the PV and WT outputs; while the DG is already operating at full capacity to meet the demand, the battery supports during this scenario by dissipating power to balance the total generation and total demand. Another inference is the shut down of the DG for 7 hours when there is sufficient renewable energy penetration, thereby saving fuel cost and reducing CO_2 emissions.

iii. Winter study day

This day experiences a high share of WT generation, similar to the summer vacation day. As expected, the PV generation is low due to low irradiance in the winter season. Figure 4.11 shows the generation-demand pattern for a typical study period during the winter season at the Pietermaritzburg campus. The demand profile has an approximate uniform distribution with some deviation in the first third of the day. The bulk

of the demand is met by the DG and WT, with the DG meeting the demand in the morning and the WT generating power in the afternoon period. The excess power generated during the day is stored in the battery and dissipated at night (00h00 to 04h00 and 19h00 to 24h00) to support the DG output.

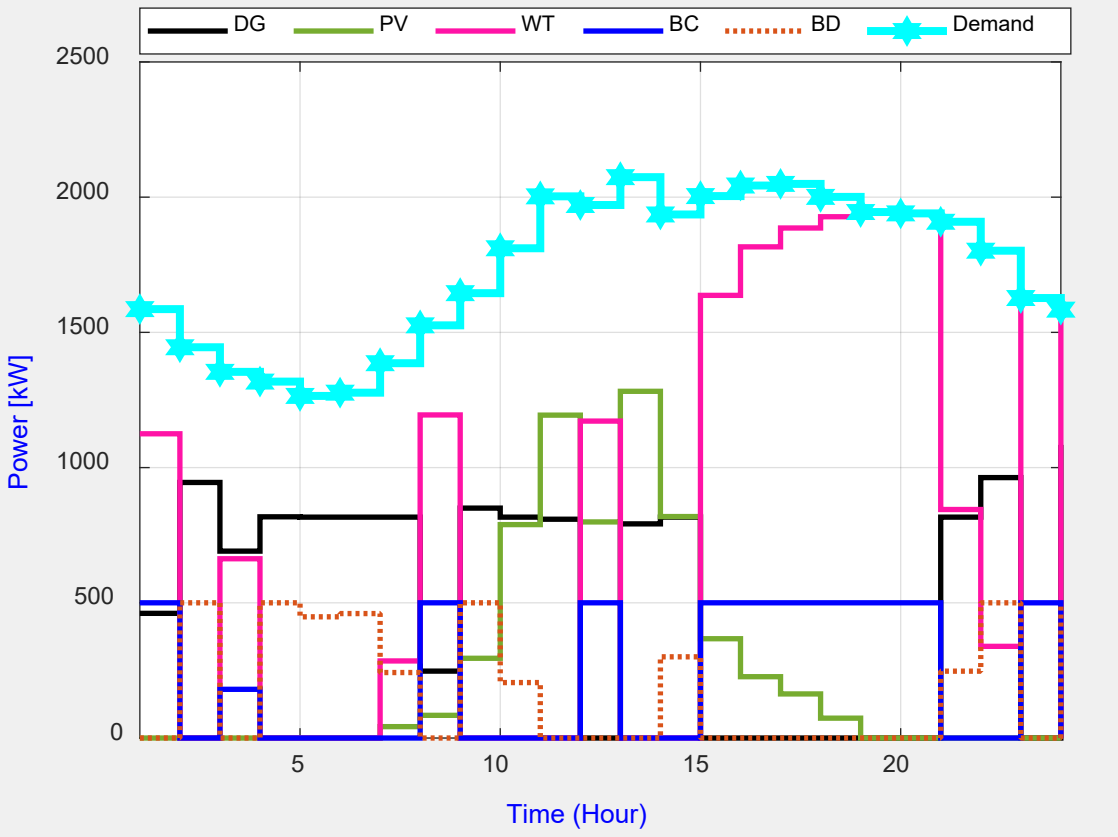

Figure 4. 10: Summer Vacation day (17 April 2019) Power Flow

iv. Winter vacation day

The winter vacation day on the Pietermaritzburg campus has a generation-demand profile shown in Figure 4.12. It is observed that is high WT generation on this day such that the DG is active for only 4 hours. Similarly, the excess generation is continually stored in the battery. The PV generation on this day is low due to the low irradiance in the winter season. In contrast to other scenarios where the DG is always active in the early hours of the day, it is observed that on the winter vacation day, the WT generates sufficient power needed to meet the load during this period and the support from the PV in the midday period is enough to balance the generation. The operation of the DG peaks at night when the WT and PV are unable to generate electricity; the power dissipation from the battery also ensures that there is net-zero active power deviation on the campus.

To investigate the fuel cost of the DG and fuel-saving cost during hybrid generation, Table 4.5 shows the financial implications of these two generation modes for the four scenarios analyzed on the

Pietermaritzburg campus. It is clear that the hybrid generation saves fuel cost than running the DG full-time; however, the winter vacation day, which experiences the highest penetration of WT, has the least fuel cost when compared with other scenarios. The least savings period is the summer study day due to the low generation from the renewable energy sources. A comparative investigation of Tables 4.3 and Table 4.5 shows a contrasting result between the summer study period and winter vacation period. While the summer study day is the highest fuel saving period at the Howard campus, it is the least fuel saving period at the Pietermaritzburg campus. Similarly, the winter vacation day at the Pietermaritzburg campus shows the highest fuel saving period due to the availability of renewable energy sources. The Howard campus has the least fuel-saving due to limited renewable energy available in the period.

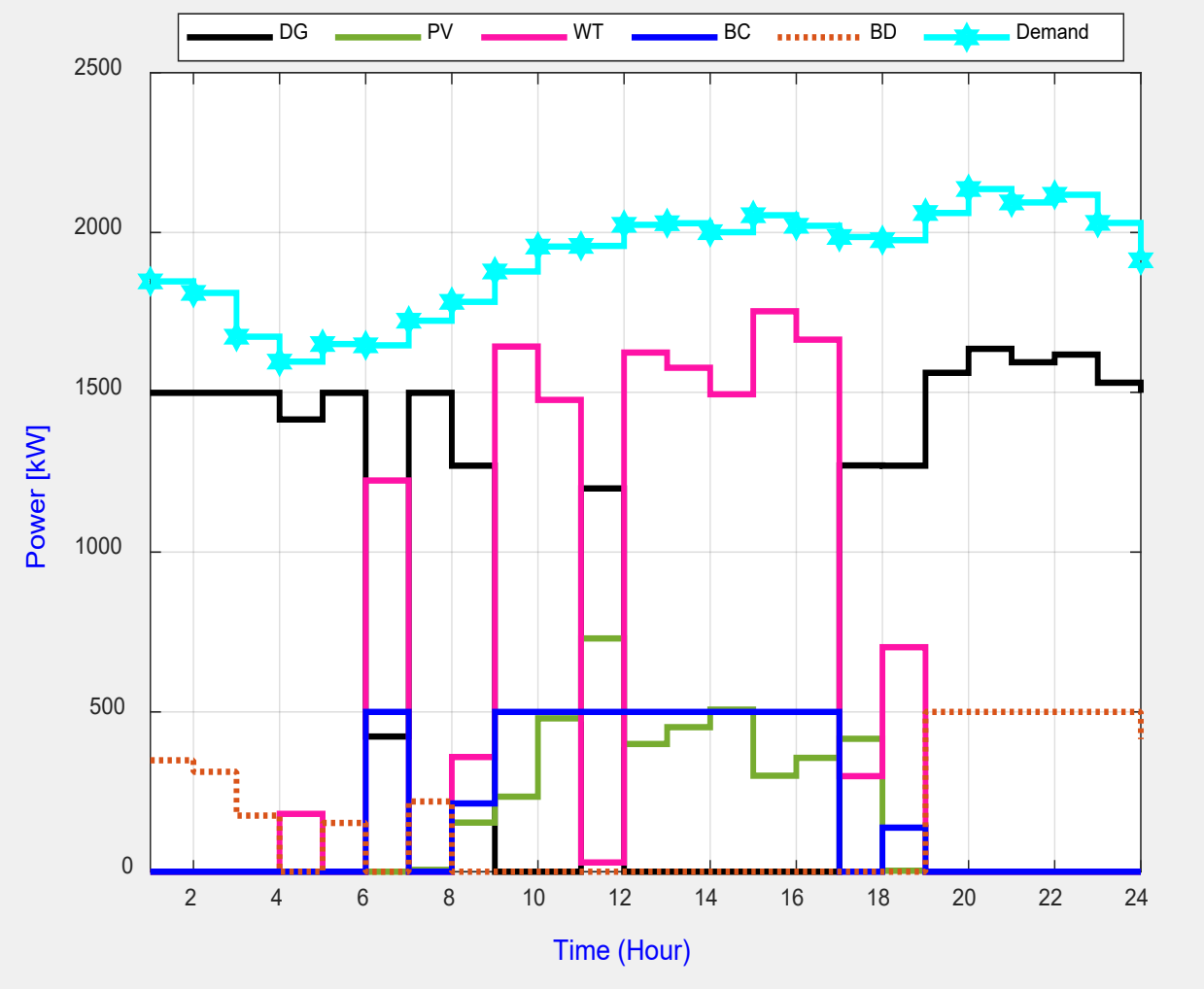

Figure 4. 11: Winter Study day (13 August 2019) Power Flow

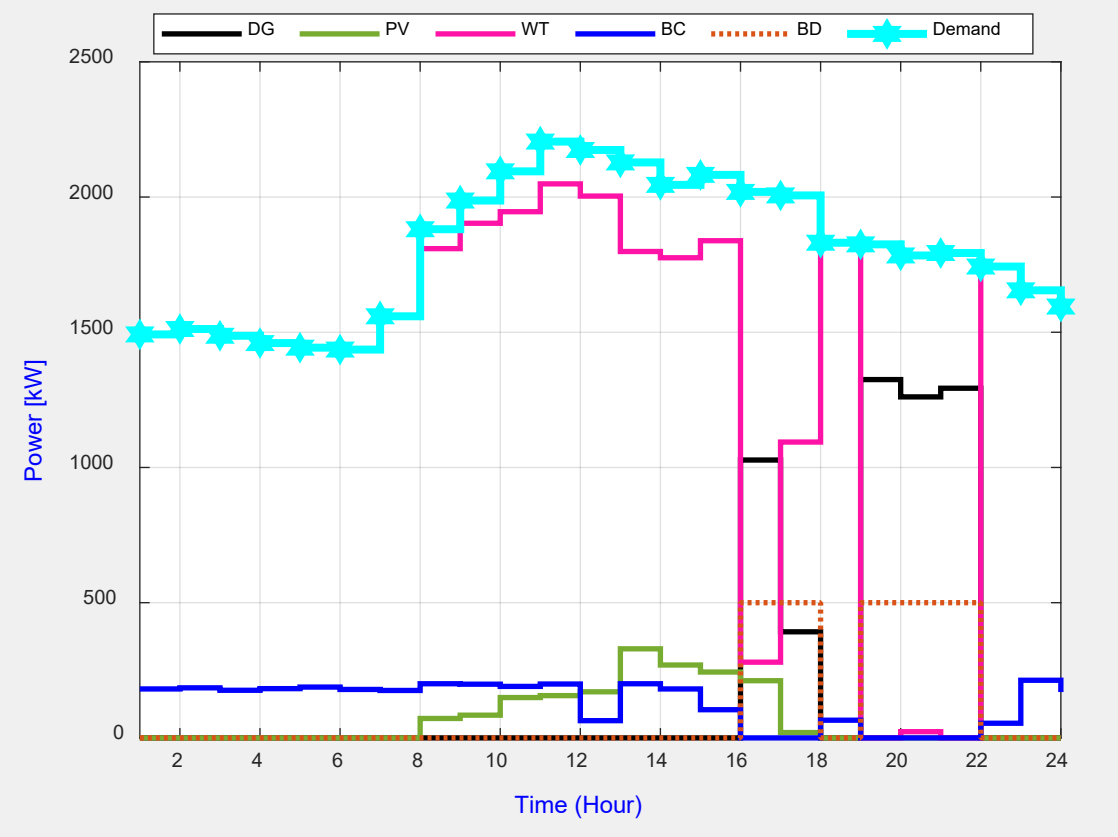

Figure 4. 12: Winter vacation day (25 June 2019) Power Flow

Table 4. 5: Fuel Cost Saving

	Summer ($/W)		Winter ($/W)	
	Study	Vacation	Study	Vacation
DG Only	50.31	41.50	45.97	43.24
Hybrid	38.90	12.56	23.78	5.30
Saving	**11.41**	**28.94**	**22.19**	**37.94**

4.5 Calculation of levelized cost of energy

Tables 4.6 – 4.8 show the calculations of the LCOE for the solar PV, wind turbine, and diesel generator respective. The data and assumptions made are based on the results obtained in chapter three. According to the simulation results, the total energy consumption (measured) on the Howard campus in 2019 was 18.8 GWh; this was shared among the three generating sources. The total LCOE for an off-grid hybrid of PV/WT/DG is found to be 0.2195 $/kWh, and this is almost three times the grid-connected hybrid of PV/WT/DG/BS in chapter 3. This is because the diesel generator was used to generate 62% of the energy used for the year.

Table 4. 6: Calculations of the LCOE for the solar PV

System Inputs	Value		Year	Production (kWh)	Investment Cost ($)	O&M Cost ($)
System Size (kW)	500					
Annual Production (kWh)	500,000		0		975,000	
Annual Degradation (%)	1%		1	500,000		1,000
			2	499,968		1,050
Cost Inputs			3	499,936		1,103
Initial Investment Cost ($/W)	1		4	499,904		1,158
Operations & Maintenance ($/W)	1		5	499,872		1,216
O &M Growth Rate (%)	5%		6	499,840		1,276
Discount Rate	8%		7	499,808		1,340
Incentive	25000		8	499,776		1,407
Annual Fuel Cost ($)			9	499,744		1,477
LCOE			10	499,712		1,551
10 Year	0.1976		11	499,680		1,629
20 Year	0.1009		12	499,648		1,710
25 Year	0.0819		13	499,616		1,796
			14	499,584		1,886
			15	499,552		1,980
			16	499,520		2,079
			17	499,488		2,183
			18	499,456		2,292
			19	499,424		2,407
			20	499,392		2,527
			21	499,360		2,653
			22	499,328		2,786
			23	499,296		2,925
			24	499,265		3,072
			25	499,233		3,225
				12,490,405		47,727

Table 4. 7: Calculations of the LCOE for wind turbine

System Inputs	Value		Year	Production (kWh)	Investment Cost ($)	O&M Cost ($)
System Size (kW)	4,000					
Annual Production (kWh)	6,675,997		0		7,975,00	
Annual Degradation (%)	1%		1	6,675,997		2,000
			2	6,609,237		2,100
Cost Inputs			3	6,543,145		2,205
Initial Investment Cost ($/W)	2		4	6,477,713		2,315
Operations & Maintenance ($/W)	0.5		5	6,412,936		2,431
O &M Growth Rate (%)	5%		6	6,348,807		2,553
Discount Rate	8%		7	6,285,319		2,680
Incentive			8	6,222,465		2,814
Annual Fuel Cost ($)			9	6,160,241		2,955
LCOE			10	6,098,638		3,103
10 Year	0.1253		11	6,037,652		3,258
20 Year	0.0661		12	5,977,275		3,421
25 Year	0.0858		13	5,917,503		3,592
			14	5,858,328		3,771
			15	5,799,744		3,960
			16	5,741,747		4,158
			17	5,684,330		4,366
			18	5,627,486		4,584
			19	5,571,211		4,813
			20	5,515,499		5,054
			21	5,460,344		5,307
			22	5,405,741		5,572
			23	5,351,683		5,851
			24	5,298,167		6,143
			25	5,245,185		6,450
				148,326,394		95,454

Table 4. 8: Calculations of the LCOE for diesel generator

System Inputs	Value		Year	Production (kWh)	Investment Cost ($)	O&M Cost ($)	Fuel Cost ($)
System Size (kW)	4,000						
Annual Production (kWh)	11,666,000		0		4,000,000		
Annual Degradation (%)	0.5%		1	11,666,000		75000	3,526,393
			2	11,607,670		78,750	3,702,712
Cost Inputs			3	11,549,632		82,688	3,887,848
Initial Investment Cost ($/W)	1		4	11,491,883		86,822	4,082,240
Operations & Maintenance ($/W)	0.5		5	11,434,424		91,163	4,286,352
O &M Growth Rate (%)	5%		6	11,377,252		95,721	4,500,670
Annual Fuel Cost Increase Rate	5%		7	11,320,366		100,507	4,725,703
Incentive	0		8	11,263,764		105,533	4,961,988
Annual Fuel Cost ($)	3,499,800		9	11,207,445		110,809	5,210,088
LCOE			10	11,151,408		116,350	5,470,592
10 Year	0.3353		11	11,095,651		122,167	5,744,122
20 Year	0.3183		12	11,040,173		128,275	6,031,328
25 Year	0.3149		13	10,984,972		134,689	6,332,894
			14	10,930,047		141,424	6,649,539
			15	10,875,397		148,495	6,982,016
			16	10,821,020		155,920	7,331,117
			17	10,766,914		163,716	7,697,673
			18	10,713,080		171,901	8,082,556
			19	10,659,515		180,496	8,486,684
			20	10,606,217		189,521	8,911,018
			21	10,553,186		198,997	9,356,569
			22	10,500,420		208,947	9,824,398
			23	10,447,918		219,395	10,315,617
			24	10,395,678		230,364	10,831,398
			25	10,343,700		241,882	11,372,968
				274,803,729		3,579,532	168,304,483

4.6 Conclusion

The optimal power dispatch of a hybrid power system (HPS) has been presented and analysed. The results reflect how changes in season, erratic nature of RES, and academic activities affect the campus load, power generated by RES, and hence the operational cost of the HPS. For instance, on the Howard campus, for both summer and winter vacation periods, the fuel costs for the HPS are close to the DG, only resulting in little saving; this is because the wind speeds are below the cut-off speed on those days. However, on the PMB campus, for both winter and summer seasons, fuel costs in the study periods are higher than that of vacation periods as a result of minimal academic activities on campus. In all, there are significant fuel cost savings in optimising the HPS.

CHAPTER FIVE

COMBINED ECONOMIC AND EMISSION DISPATCH (CEED) OF A UNIVERSITY CAMPUS MICROGRID USING QUANTUM-BEHAVED BAT ALGORITHMS (QBA) WITH CUBIC CRITERION FUNCTION

5.1 Introduction

The reliability of electrical power supply is vital for the successful operation of the university as major activities in the university such as teaching, learning and research are energy consuming. This study proposes a new metaheuristic optimization algorithm to solve the combined economic emission dispatch (CEED) problem using two university campuses as study cases. The proposed algorithm is the quantum-behaved bat algorithm (QBA) which is an improvement of the conventional bat algorithm. This bi-objective optimization problem is to simultaneously minimize the fuel cost and emissions from the power generators to meet the energy demand subject to linear and nonlinear system constraints. The CEED problem is formulated using the cubic function in place of the quadratic function to make the system more robust against nonlinearities of power system. The results show that the CEED objective function is superior at minimizing fuel cost as well as emission cost than the economic and emission dispatch objective functions. It is also shown that the proposed algorithm performs better with reduced total cost and emission levels when compared with the artificial bee colony algorithm. The incessant load shedding in South Africa has necessitated the need for universities to consider power autonomy inform of the microgrid. As stated earlier, university operations might be at risk when the power system is unreliable, considering that lecture theaters, libraries, laboratories, equipment, IT systems, and offices require power to function. Across the globe, most national grids are aged, overloaded (due to population growth), highly congested, and not reliable leading to unscheduled outages lasting for several hours or days. According to a report in [189], there was a power outage at the Boston campus of Northeastern University for about a week that affected the student residential halls. As an aftermath of this event, the university started exploring alternatives to improve its electric reliability. The university considered microgrid not only as a solution to ensure power reliability but also to minimize carbon dioxide emission on its campus (80% reduction by 2050). In other words, universities can own their power generating station within the campus and be totally off-grid with the advent of renewable and storage technologies, thereby providing energy at lower cost, less carbon, more efficient and reliable. According to a report in [190], four universities in Nigeria are to be disconnected from the national grid and operate as off-grid microgrids, estimated to generate 7.5MW. This becomes necessary because of the existing grid's poor quality, unavailability, and lack of reliability. The off-grid microgrid is designed to provide constant power that meets the universities' electricity demands, and the microgrid consists of solar PV, diesel generator and battery storage. In the same vein, a private university in Nigeria,

Covenant University is currently running off-grid through an independent power plant on campus with an installed capacity of 11.67 MW from a gas-fired turbine and diesel generators to ensure continuous power supply. However, the university is exploring the use of solar and waste to reduce greenhouse gas emissions and fuel costs [191]. Some universities in the United States have their own power plant (distributed generation) on campus in addition to the external grid to meet their energy demands. For example, the Princeton University, New Jersey powers, heats, and cools the campus through energy produced by onsite power plant (fueled by natural gas and diesel), a solar array (16,528 PV panels with a peak of 4.5 MW, producing 5-6 % of the university annual electricity) and public utility. The statistics from a live feed (14h00 on 21 July 2021) showed that the power plant and the solar plant produced 38% and 7 % of the energy needed while the remaining 55% was imported from the grid [192] [193]. It is important to note that lack of accessibility, power quality or reliability, and high tariff are not the only motivations for universities to be power-independent; reduction of emission and utility cost savings are significant factors to motivate every university to have power autonomy. With the increased penetration of RES, it is important to consider the impacts of RES on the CEED problem. However, most works reported in literature focused on the traditional power system, while only a few considered the CEED problem in a power system with RES. The present study considers a university microgrid's economic and environmental benefits by solving the CEED problem using two optimization algorithms.

5.2 Mathematical modelling of the CEED Problem

The CEED multi-objective problem can be modeled either as a second-order (quadratic) polynomial function or a higher-order polynomial function for economic (fuel cost) and emission functions. The higher-order function, for instance, a cubic function, can be adopted to improve the problem solution by reducing the nonlinearities of the current power system [194]. This work has used a third-order polynomial, cubic criterion function to formulate the CEED problem. Thus, the CEED problem can be viewed as an optimization problem having two objectives. On the one hand, to minimize the total fuel cost of the system and on the other to minimize the number of pollutants emitted into the environment [195]. Hence, CEED aims to operate the system to meet the load demand (along with operational constraints) at minimum costs and at least emission simultaneously without violating any system constraint [196].

5.2.1 Economical dispatch and minimization of fuel cost

Economic load dispatch can be defined as a process of finding an optimal combination of generation resources such that the system load demand is met totally in a most economical way and all other constraints are satisfied [194, 197]. Therefore, the economic dispatch objective is to minimize the total cost of the

system, including the fuel cost of generators and operational costs of RES [198]. The total fuel cost, F_c in ($/h) can be expressed as:

$$F_c(P) = \sum_{i=1}^{n} a_i P_i^3 + b_i P_i^2 + c_i P_i + d_i \quad (5.1)$$

Where n represents the total number of generators, P_i is the active power of generator i, and the fuel coefficients are represented by a_i, b_i, c_i and d_i.

Table 5. 1: Generator Coefficients and Limits

Unit	a ($/(MW)^{3}h)	b ($/(MW)^{2}h)	c ($/MWh)	d ($/h)	P_{gmin} (MW)	P_{gmax} (MW)
1	0.0010	0.0920	14.50	0.000002	0.3	0.9
2	0.0004	0.0250	22.00	0.000001	0.27	0.8
3	0.0006	0.0750	23.00	0.000002	0.21	0.7
4	0.0002	0.1000	13.50	0.000001	0.2	1.6
5	0.0013	0.1200	11.50	0.000003	0.17	1.8
6	0.0004	0.0840	12.50	0.000002	0.17	1.2

5.2.2 Emission dispatch

The emission dispatch objective is to minimize the total emission of pollutants produced by the generator [198].

$$F_e(P) = \sum_{i=1}^{n} e_i P_i^3 + f_i P_i^2 + g_i P + h_i \quad (5.2)$$

Where F_e is the emission value in (kg/h) and e_i, f_i, g_i and h_i are the emission coefficient of the ith generator.

Table 5. 2: Emission Coefficients and Price Penalty Factor

Unit	e	F	G	h	k
1	0.0015	0.0920	10.0	0.000001	1.0356
2	0.0014	0.0250	12.5	0.000001	1.7587
3	0.0016	0.0550	13.5	0.000002	1.7027
4	0.0012	0.0100	10.5	0.000001	1.0040
5	0.0023	0.0400	21.0	0.000003	0.5514

6	0.0014	0.0800	22.0	0.000002	0.5692

5.2.3 CEED

It is important to note that both economic dispatch and emission dispatch are two incompatible objectives; hence, CEED must be considered a multi-objective optimization problem to balance fuel cost and emission level. The Pareto-optimal solution is found by combining the two objective functions in (5.1) and (5.2) using a price penalty factor to give a single-objective function. The price penalty factor helps to combine the effect of fuel cost and emission, blending the generation and emission cost into a single objective function to minimize the system total cost, F_T in ($/h) as expressed in equation (5.3).

$$F_T = \sum_{i-1}^{n} \{F_c(P_i) + k_i F_e(P_i)\} \tag{5.3}$$

Where k_i is the price penalty factor in $/h. The Max-Max price penalty factor method is used in this work, it represents the ratio of the maximum fuel cost to the maximum emission as follows [198] [196] [199]:

$$k_i = \sum_{i=1}^{n} \frac{F_c(P_{i,\max})}{F_e(P_{i,\max})} \tag{5.4}$$

5.2.4 Constraints

The solution of equation (5.3) is subject to both equality and inequality constraints. The total real power generated by the generators must meet the system's total load demand and transmission losses. In addition, each generator's output is limited to its minimum and maximum values. These constraints are expressed as follows:

$$\sum_{i=1}^{n} P_{gi} = P_D + P_L \tag{5.5}$$

$$P_{gi}^{\min} \le P_{gi} \le P_{gi}^{\max} \tag{5.6}$$

Where

P_{gi} represents the real power output of generator i

$P_{gi}^{\min}$ and $P_{gi}^{\max}$ are the minimum and maximum values of generator i

P_D is the total load demand (MW)

P_L is the transmission loss in (MW) and is computed using the B matrix (loss coefficient). P_L can be expressed as:

$$P_L = \sum_{i=1}^{n}\sum_{j=1}^{n} P_i B_{ij} P_j + \sum_{n=1}^{n} B_{oi} P_i + B_{oo} \tag{5.7}$$

In equation (5.7), B_{ij}, $B_{oi,}$ and B_{oo} represent the loss coefficient of the generators, and their values are taken from [200].

B_{ij}= [0.1382 0.0299 0.0044 0.0022 0.0010 0.0008
0.0299 0.0487 0.0025 0.0004 0.0016 0.0041
0.0044 0.0025 0.0182 0.0070 0.0066 0.0066
0.0022 0.0004 0.0070 0.0137 0.0005 0.0033
0.0010 0.0016 0.0066 0.0050 0.0109 0.0005
0.0008 0.0041 0.0066 0.0033 0.0005 0.0244];

B_o= [0.0107 0.0060 0.0017 0.0009 0.0002 0.0030];

B_{oo}= 9.8573e-4;

5.2.5 Modelling of Renewable Energy Sources

Two RES (Wind turbine and Solar PV) are considered inform of generators to meet the load demands together with the conventional generators (CGs). The mathematical modelling of both renewable generators (RGs) is the same as stated in chapter 4. However, the RGs having intermittent sources cannot be dispatched. Hence, all CGs are set to run at minimum loading and at the same time maximize the RGs output to meet the load demand. Since the power generated by the RGs is uncertain or intermittent, their cost of generation can be modelled by considering two scenarios. The first case is when the output of the RGs is more than estimated or required, there is a penalty cost coefficient to be added to the generation cost. In Chapter 4, the excess generation is used to charge the battery, but there is no battery considered. In other words, the penalty cost is incurred for not using all the available power produced by the RGs. The second scenario is opposite to the first, and a reserve cost is added to compensate for overestimation or under-generation of the RGs, resulting in using reserved power from the CGs. In this work, the reserve cost coefficient is equal to zero because the CGs have enough capacity to meet the maximum load demand of the campuses considered. This is so designed for the reliability of the off-grid microgrid system. From the above, the total generation cost of the RGs can be obtained using a cost function as follows in equation (5.8) [70]:

$$F_{RG} = \sum_{i=1}^{N_{RG}} d_i(P_{RG,i}) + \sum_{i=1}^{N_{RG}} k_{p,i}(P_{RG,i}) + \sum_{i=1}^{N_{RG}} k_{r,i}(P_{RG,i}) \quad (5.8)$$

Where, d_i, $k_{p,i}$, $k_{r,i}$ and $P_{RG,i}$ represent the direct cost, the penalty cost coefficient, reserve cost coefficient, and power generation of the ith renewable generator, and N_{RG} is the total number of RGs.

5.3 Optimization Algorithm

Several methods have been used in the past to solve an optimization problems that is, finding the optimal solution among all suitable solutions. Many of these traditional or conventional methods have been applied to solve economic load dispatch problems in power systems; these include:

- Nonlinear programming
- Linear programming
- Dynamic programming
- Quadratic programming
- Newton-Raphson method,
- Gradient method
- Lamdha iteration

Due to the difficulty of finding initial solutions and convergence problems associated with these traditional methods (considering the nonlinearity of power system), new optimization techniques have been developed in recent years [201]. These new algorithms are inspired either by nature or animal behavior. Some of these heuristic and metaheuristic techniques are listed in [202]. The CEED problem is a real-world optimization problem, and many metaheuristic algorithms have been used to solve it, such as:

- Particle swarm optimization (PSO)
- Ant lion optimization (ALO)
- Gravitational search algorithm (GSA)
- Ant colony optimization (ACO)
- Grey wolf optimization (GWO)
- Firefly algorithm (FA)
- Cuckoo search algorithm (CSA)
- Differential evolution algorithm (DE)
- Bat algorithm (BA) and many more

However, these algorithms are not without shortcomings, especially when handling big and complex systems to prevent premature convergence, locate the global optimal solution, and avoid local optimal. In

order to address these limitations, modification of the original algorithm and hybridization of two or more algorithms have been proposed to enhance their performance [201]

5.3.1 BAT Algorithm

The bat algorithm (BA) is one of the recent metaheuristic methods developed in 2010 by Yang motivated by the behaviors of bats in their search of prey, foraging, their ability to avoid obstacles, their ingenious echolocation capacity, and at the same time, potential to compensate Doppler Effect in echoes [194, 201, 203]. Echolocation is a type of sonar that most bats use to keep away from obstacles, detect prey, and locate their roosting crevices in the dark by emitting a resounding pulse and listening for the echo's rebound as a result of surrounding objects. Yang [201, 204, 205], using the echolocation characteristics of bat developed BA following three approximate rules:

i) Each bat uses echolocation to estimate the distance between prey and other background and to know the difference between prey and neighborhoods.
ii) Bats fly to look for prey randomly with a velocity $\boldsymbol{V_i}$ at position $\boldsymbol{X_i}$ with a fixed frequency $\boldsymbol{f_{min}}$, varying wavelength λ, and loudness $\boldsymbol{A_0}$. Bats can spontaneously adjust the frequencies or wavelengths of their emitted pulses and adjust the pulse emission rate (in the range of 0 to 10 depending on the vicinity of their targets.
iii) The loudness is expected to vary for a position (large) $\boldsymbol{A_0}$ to a minimum constant value $\boldsymbol{A_{min}}$.

From the above and in order to formulate the mathematical equation for the algorithm, each bat i has a position X_i, a velocity V_i and a frequency f_i in d-dimensional space. These characteristics have to be improved iteratively to the current best position as shown below:

$$f_i = f_{\min} + r_1(f_{\max} - f_{\min}) \tag{5.12}$$

$$V_i(t+1) = V_i(t) + f_i(X_i(t) - X_{best}(t)) \tag{5.13}$$

$$X_i(t+1) = X_i(t) + V_i(t+1) \tag{5.14}$$

Assuming at t = 0, $\boldsymbol{V_i} = 0$

Where:

$\boldsymbol{r_1}$ is a uniformly distributed random number between 0 and 1

$\boldsymbol{f_{min}}$ is the minimum tolerable frequency

$\boldsymbol{f_{max}}$ is the maximum tolerable frequency

f_i is the frequency of the i^{th} bat

t is the iteration number

X_{best} is the location (solution) that has the best fitness in the current population.

Furthermore, every bat possess a new solution that can be generated locally as follows:

$$X_{i,new}(t) = X_{old} + \varepsilon A_i(t) \tag{5.15}$$

ε is a uniformly distributed random number between 0 and 1

$A_i(t)$ is the loudness

For effectiveness in controlling the exploration and exploitation, the loudness A_i and rate of pulse emission R_i must be varied during the iterations, hence, A_i and R_i are updated iteratively as follows:

$$A_i(t+1) = \alpha A_i(t) \tag{5.16}$$

$$R_i(t+1) = R_i(0)[1 - \exp(-\gamma t)] \tag{5.17}$$

In equations (5.16) and (5.17), α and γ are constants. For simplicity, α = γ can be used for the simulation. The pseudocode of the basic BA described by equations (5.12) to (5.17) is as follows [201]:

Initialize the bat population X_i *(I = 1, 2,……., N) and* V_i*;*

Define the pulse frequency f_i*, pulse rate* R_i *and loudness* A_i

while *(t < T)* ***do***

Generate new solutions by adjusting the frequency and update the velocities and positions using equations (5.12) – (5.14);

if *(rand >* R_i*)* ***then***

Select a solution among the best solutions randomly;

Generate a local solution around the selected best solution using equation (5.15);

end if

if *(rand ,* A_i *& &f (*X_i*) < f (*X_{best}*))* ***then***

Accept the new solutions;

Increase R_i and reduce A_i using equations (5.16) and (5.17);

end if

Rank the bats and find the current X_{best};

$T = t + 1$;

end while

Output the best solution X_{best}

5.3.2 Quantum-Behaved BAT Algorithm

Quantum-behaved bat algorithm (QBA) evolved as an improvement of the basic BA whereby quantum theory is applied to the basic BA. However, the Doppler Effect as well as the idea of foraging of bats were not considered in the basic BA. Another shortcoming of the basic BA is prematuration when the best bat falls into local point other bats are misguided by the current optimal solution. Also, the basic BA regarded bats foraged only in one habitat; however, bats can adapt to different habitats by adjusting their echolocation behavior [205]. Therefore, in order to improve the efficiency of the basic BA, two additional approximate rules have been added as follows:

i. Bats are not limited to a single foraging habitat that relies on a stochastic selection but can forage in different habitats.
ii. Bats can make up for Doppler Effect in echoes as a result of their self-adaptive ability.

Hence, in QBA, the behavior of quantum of bats is included in the algorithm to expand the population mix and also to prevent prematuration [203]. The positions of bats that possess the following equation define quantum behavior cab:

$$X_{id}^{t} = g_d^t + \beta \left| mbest_d - X_{id}^{t-1} \right| \ln(\frac{1}{u}), u(0,1) < 0.5 \tag{5.18}$$

$$X_{id}^{t} = g_d^t - \beta \left| mbest_d - X_{id}^{t-1} \right| \ln(\frac{1}{u}), u(0,1) \geq 0.5 \tag{5.19}$$

Where X_{id}^{t} is the position of the i^{th} bat in dimension d for i^{th} iteration. B represents the contraction-expansion coefficient, it can be adjusted to control the speed of convergence of the algorithm as thus:

$$\beta = \beta_0 + (T - t)(\beta_1 - \beta_0) / T \tag{5.20}$$

Where β_0 and β_1 are respectively the initial and final values of β and T is the maximum number of iteration. In order to consider the compensation for Doppler Effect, equations (5.12) to (5.14) can be written assuming the velocity of sound through air is 340 m/s as follows:

$$f_{id} = \frac{(340 + V_i^{t-1})}{(340 + V_g^{t-1})} \times f_{id}^{t-1} \left[1 + C_i \times \frac{(g_d^t - X_{id}^t)}{\left| g_d^t - X_{id}^t \right| + \varepsilon} \right] \tag{5.21}$$

$$V_{id}^t = (w \times V_{id}^{t-1}) + (g_d^t - X_{id}^t) f_{id} \tag{5.22}$$

$$X_{id}^t = X_{id}^{t-1} + V_{id}^t \tag{5.23}$$

Where f_{id} is the frequency of the i^{th} bat at dimension d, V_g^{t-1} is the velocity of the global best position at $(t-1)^{th}$ iteration and C_i represents a positive number of the i^{th} bat in the range of [0,1]. For the purpose of clarity, the assumption of C = 0 means the bats are not able to compensate for the Doppler Effect and when C = 1 , it means the bats are fully capable to compensate for the Doppler Effect in the echoes[206]. The flowchart the further illustrate the QBA is shown in figure 5.1

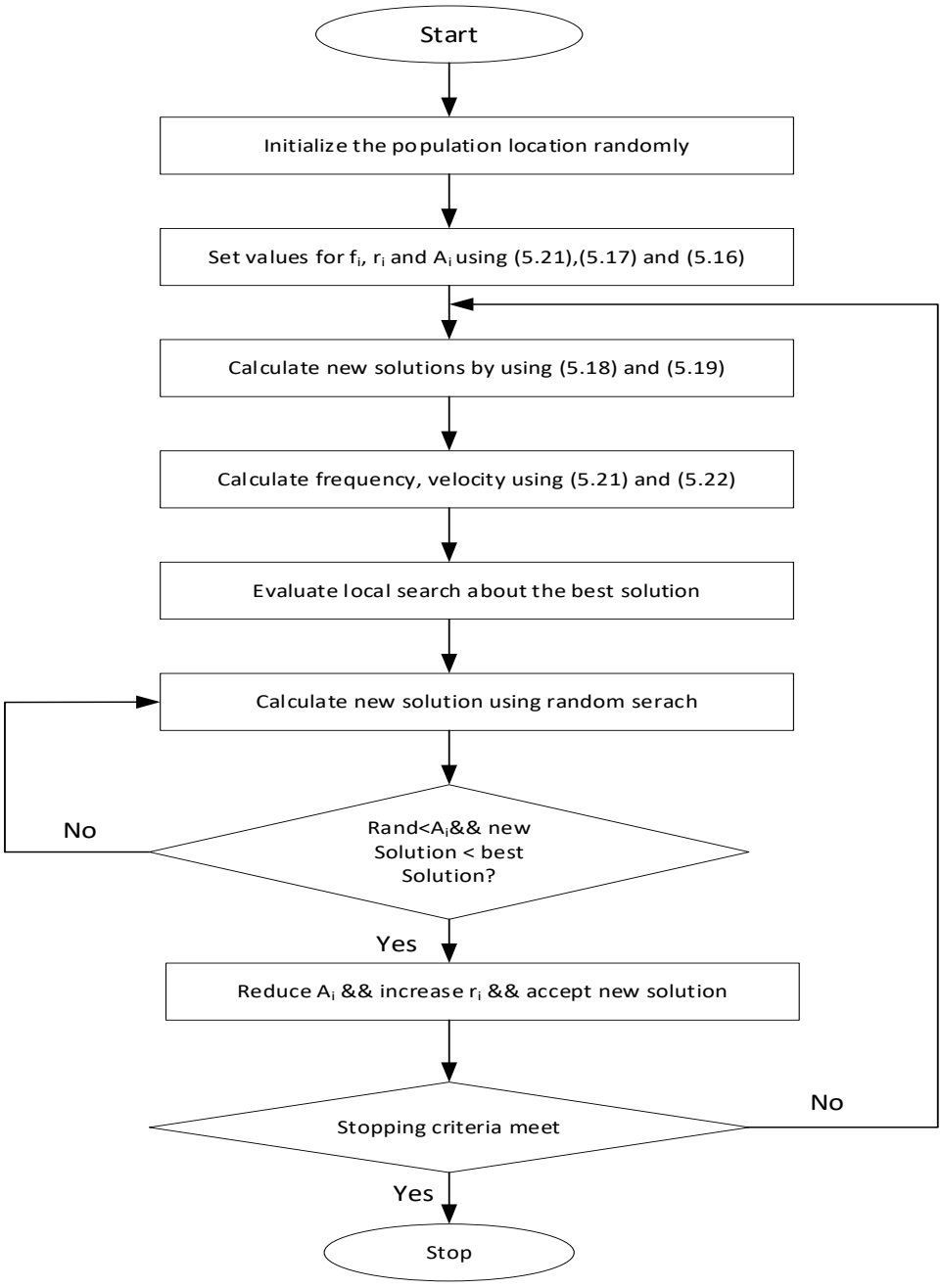

Figure 5. 1: Flowchart of QBA

5.4 Results and Discussion

This work considers a university campus as a case study with on-site (campus) generation comprising six conventional generators powered by natural gas or diesel, a wind turbine, and a solar PV array. All-weather and load data are the same with chapter four. The conventional IEEE 30-bus test system was modified to an 8-bus system (6 CGs and 2 RGs) and simulated as an off-grid microgrid for the analysis.

The study investigates the potential of QBAT to solve the CEED problem. The QBAT has been carried out in MATLAB 2019a and executed with i5-4590 CPU @3.30 GHz,~3.30GHz, and 4 GB RAM personal computer. The proposed QBAT is carried out to comprehensively investigate the CEED problem of the two campuses considering load demands for typical days in the summer and winter periods. The influence of the RGs on the fuel and emission costs is also investigated.

5.4.1 Howard Campus

This subsection presents the simulation results of the proposed methodology in the Howard campus for two different periods (summer and winter), considering two different systems (CGs only and RG-integrated systems). In this analysis, the results of the dispatch at midday in summer are given in Tables 5.3 and 5.4, and Figures 5.3 and 5.4 for the CGs only and RG-integrated systems, respectively, and the results of the dispatch at midday in winter are given in Tables 5.5 and 5.6 and Figures 5.5 and 5.6 for the CGs only and RG-integrated systems respectively. With the integration of RGs, it is shown that the total cost of fuel and emission is lower compared to the CGs only base case. The proposed QBA algorithm outperforms the ABC algorithm in the ED with a reduced fuel cost of 15.58% in the summer with CG only, 18.43% in the summer with RG-integrated, 17.46% in the winter with CGs only, and 21.27% in the winter with RG-integrated system respectively. The results also show the performance of the proposed QBA on the three dispatch problems; the CEED objective function gave a better performance with 34.45% improvement than the ED objective function, as seen in Figures 5.3 and 5.5 for the CG-only system and Figures 5.4 and 5.6 for the RG-integrated system. The proposed QBA algorithm dispatched the CGs to meet the load at the Howard campus without exceeding the constraints of the CGs and prioritizing the maximum power extraction from the RGs, thus mitigating the levels of emissions.

Table 5. 3: Simulation results for Howard College Campus @ 12h00 during summer (Only CGs dispatched)

Gen Unit	**Pg,min (MW)**	**Pg,max (MW)**	**ABC_ED (MW)**	**Economic dispatch (MW)**	**Emission dispatch (MW)**	**CEED (MW)**
1	0.300	0.900	0.6705	0.300	0.900	0.300
2	0.270	0.800	0.8000	0.270	0.750	0.270
3	0.210	0.700	0.7000	0.210	0.210	0.210
4	0.200	1.600	0.2000	0.200	1.600	1.430
5	0.170	1.800	0.1700	1.800	0.170	1.428
6	0.170	1.200	1.2000	1.070	0.170	0.170
PV				N/A	N/A	N/A
WT				N/A	N/A	N/A

Power loss				0.107	0.060	0.068
Fuel cost ($/h)			63.30	52.37	60.42	53.44
Emission Cost ($/h)			59.91	50.34	51.74	47.70
PV Cost ($/h)				0	0	0
WT Cost ($/h)				0	0	0
Total Cost ($/h)			123.21	102.71	112.16	**101.14**
Emission, (kg/h)			58.43	72.84	45.45	**58.08**

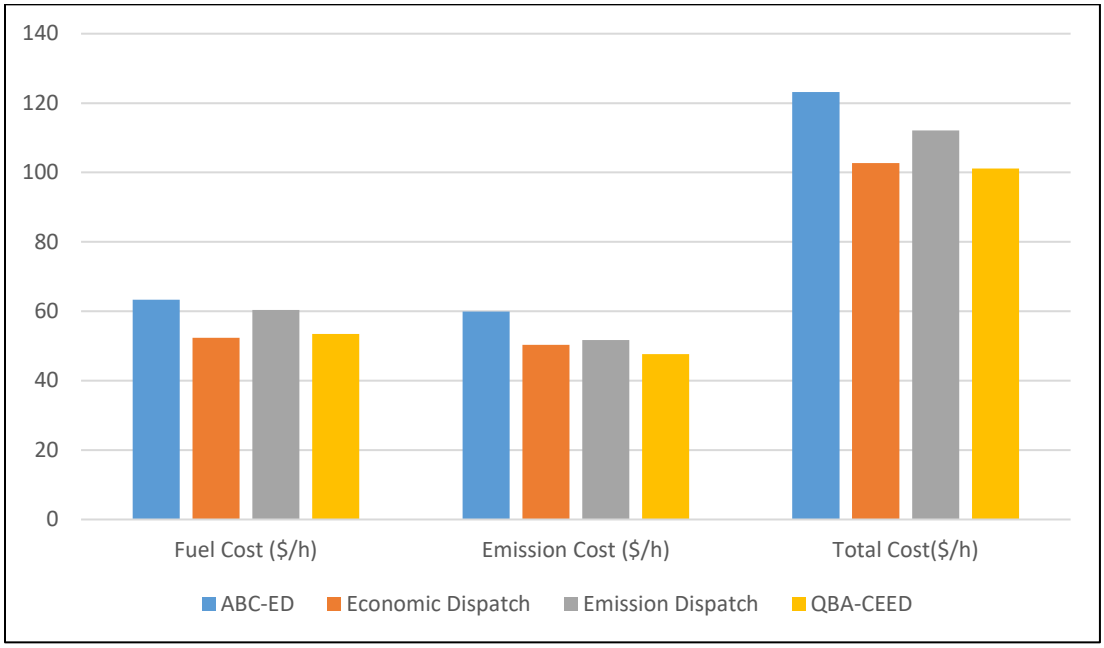

Figure 5. 2: Cost of Production for Howard Summer Period with CGs only

Table 5. 4: Simulation results for Howard College Campus @ 12h00 during summer (CGs & RGs dispatched)

Gen Unit	**Pg,min (MW)**	**Pg,max (MW)**	**ABC_ED (MW)**	**Economic dispatch (MW)**	**Emission dispatch (MW)**	**CEED (MW)**
1	0.300	0.900	0.3003	0.300	0.900	0.300

2	0.270	0.800	0.8000	0.270	0.270	0.270
3	0.210	0.700	0.7000	0.210	0.210	0.210
4	0.200	1.600	0.2000	0.200	1.216	0.995
5	0.170	1.800	0.1700	1.800	0.170	0.996
6	0.170	1.200	0.7252	0.188	0.170	0.170
PV				0.519	0.519	0.519
WT				0.326	0.326	0.326
Power loss				0.073	0.041	0.046
Fuel cost ($/h)			51.88	41.29	44.55	42.37
Emission Cost ($/h)			50.06	39.27	37.10	38.07
PV Cost ($/h)				1.83	1.83	1.83
WT Cost ($/h)				2.43	2.43	2.43
Total Cost ($/h)			101.94	84.82	85.91	**84.70**
Emission, (kg/h)			44.17	53.40	35.39	**44.38**

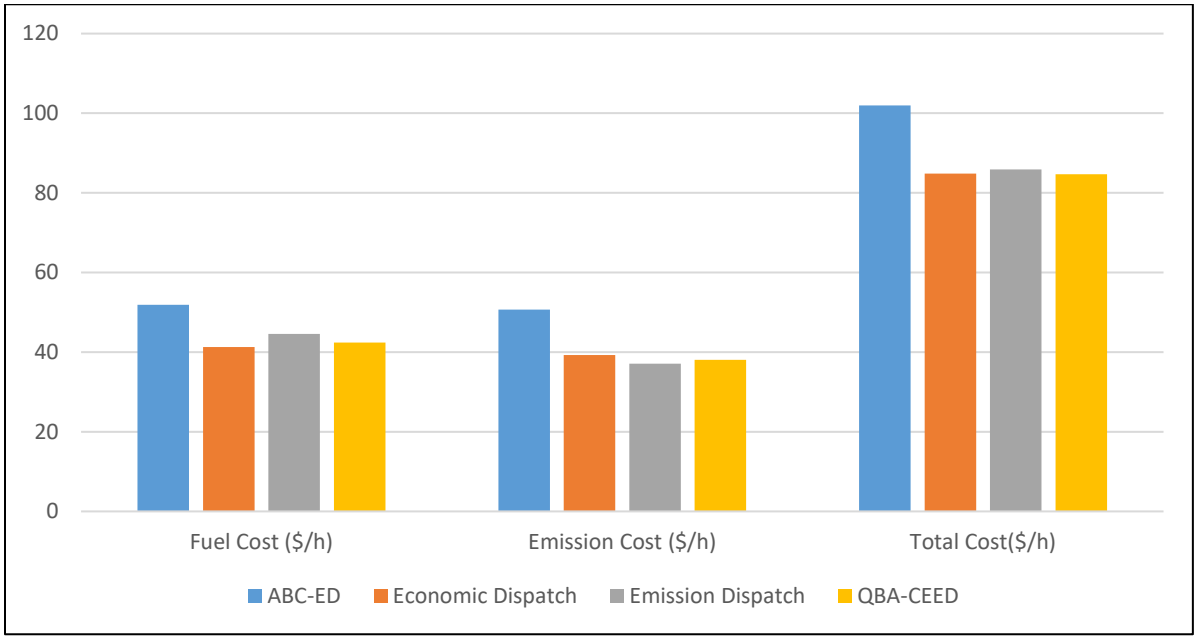

Figure 5. 3: Cost of Production for Howard Summer Period with RG integration

Table 5. 5: Simulation results for Howard College Campus @ 13h00 during winter (Only CGs dispatched)

Gen Unit	**Pg,min (MW)**	**Pg,max (MW)**	**ABC_ED (MW)**	**Economic dispatch**	**Emission dispatch**	**CEED (MW)**

				(MW)	(MW)	
1	0.300	0.900	0.3002	0.300	0.900	0.300
2	0.270	0.800	0.8000	0.270	0.270	0.270
3	0.210	0.700	0.7000	0.210	0.210	0.210
4	0.200	1.600	0.2000	0.200	1.395	1.090
5	0.170	1.800	0.1700	1.800	0.170	1.081
6	0.170	1.200	0.9021	0.369	0.170	0.170
PV				N/A	N/A	N/A
WT				N/A	N/A	N/A
Power loss				0.077	0.043	0.049
Fuel cost ($/h)			54.12	43.56	47.01	44.67
Emission Cost ($/h)			52.28	41.54	39.00	40.06
PV Cost ($/h)				0	0	0
WT Cost ($/h)				0	0	0
Total Cost ($/h)			106.4	85.10	86.01	**84.73**
Emission, (kg/h)			48.09	57.40	37.27	**47.17**

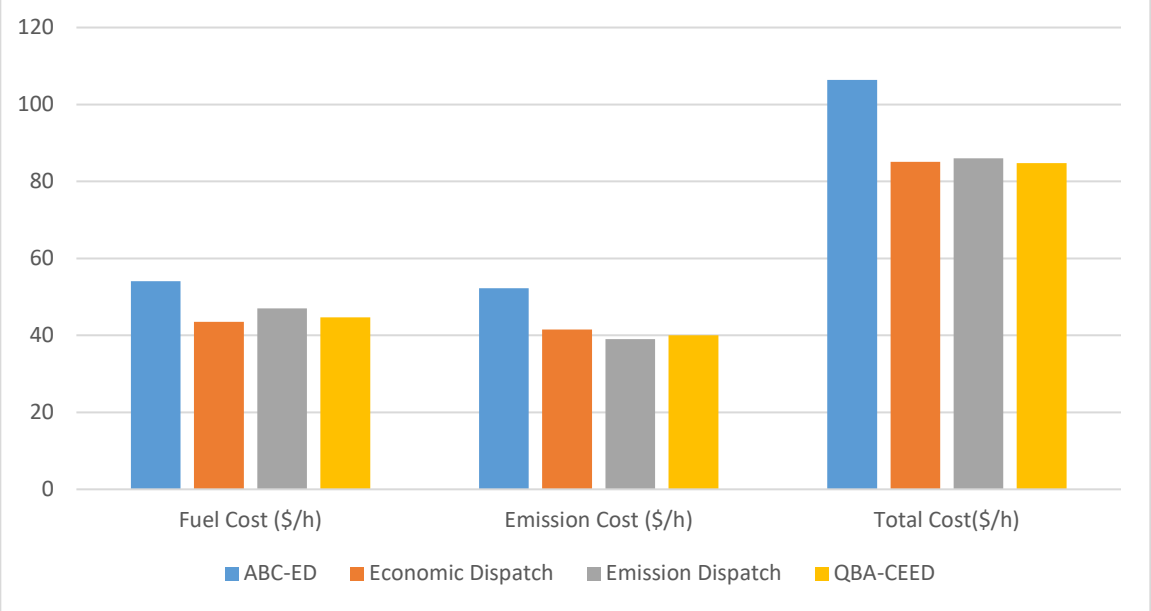

Figure 5. 4: Cost of Production for Howard Winter Period with CGs only

Table 5. 6: Simulation results for Howard College Campus @ 13h00 during winter (CGs & RGs dispatched)

Gen Unit	**Pg,min (MW)**	**Pg,max (MW)**	**ABC_ED (MW)**	**Economic dispatch**	**Emission dispatch**	**CEED (MW)**

				(MW)	(MW)	
1	0.300	0.900	0.3073	0.300	0.900	0.300
2	0.270	0.800	0.8000	0.270	0.270	0.270
3	0.210	0.700	0.7000	0.210	0.210	0.210
4	0.200	1.600	0.2000	0.200	0.691	0.730
5	0.170	1.800	0.1700	1.284	0.170	0.735
6	0.170	1.200	0.2049	1.070	0.170	0.170
PV				0.690	0.690	0.690
WT				0	0	0
Power loss				0.052	0.029	0.033
Fuel cost ($/h)				34.93	37.36	35.69
Emission Cost ($/h)				33.03	31.56	32.24
PV Cost ($/h)			45.45	1.70	1.70	1.70
WT Cost ($/h)			43.59	0.22	0.22	0.22
Total Cost ($/h)			89.04	69.88	70.84	**69.85**
Emission, (kg/h)			32.76	42.10	29.86	**36.09**

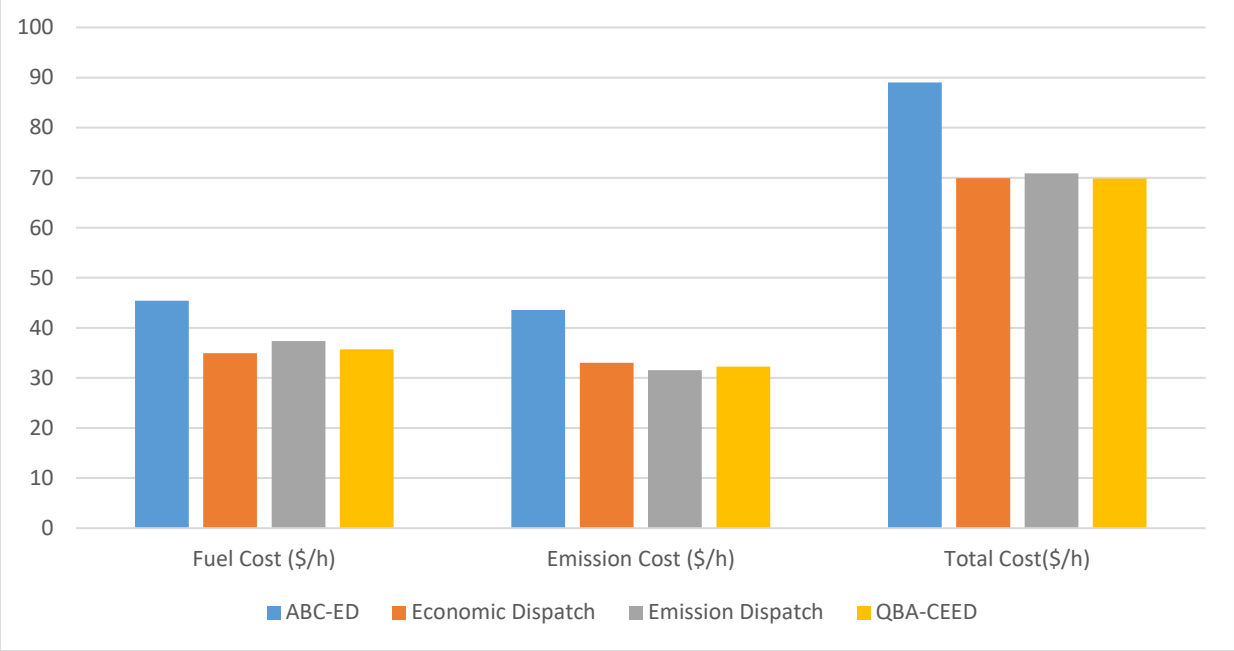

Figure 5. 5: Cost of Production for Howard Winter Period with RG Integration

5.4.2 PMB Campus

Similar to the Howard campus scenario, this subsection presents the results of the simulation of the proposed methodology in the PMB campus of UKZN for two different periods (summer and winter), considering two different systems (CGs only and RG-integrated systems). In this analysis, the results of the dispatch at midday in summer are given in Tables 5.7 and 5.8 and Figures 5.6 and 5.7 for the CGs only and RG-integrated systems, respectively and the results of the dispatch at midday in winter are given in Tables 5.9 and 5.10 and Figures 5.8 and 5.9 for the CGs only and RG-integrated systems respectively. With the integration of RGs, it is shown that the total cost of fuel and emission is lower compared to the CGs only base case. The proposed QBA algorithm outperforms the ABC algorithm in the ED with a reduced fuel cost of 18.55% in the summer with CG only, 15.51% in the summer with RG-integrated, and 16.87% in the winter with CG only systems, respectively, while the emission cost reduced by 23.711% in the summer with CG only, 19% in the summer with RG-integrated, and 20.59% in the winter with CG only systems respectively. The results also show the performance of the proposed QBA on the three objective functions or dispatch problems; the CEED objective function gives the best performance with improvement than the economic and emission dispatch objective functions, as seen in Table 5.9 for the summer RG-integrated system and Table 5.9 for the winter CG-only system. Due to the random initialization search process of the proposed QBA, results in Tables 5.7 to 5.10 showed that despite the variations in fuel cost and emission cost for the study cases, the total cost varies slightly. The proposed QBA algorithm dispatched the CGs to meet the load at the PMB campus without exceeding the constraints of the CGs and prioritizing the maximum power extraction from the RGs, thus mitigating the levels of emissions.

Table 5. 7: Simulation results for PMB Campus @ 16h00 during summer (Only CGs dispatched)

Gen Unit	**Pg,min (MW)**	**Pg,max (MW)**	**ABC_ED (MW)**	**Economic dispatch (MW)**	**Emission dispatch (MW)**	**CEED (MW)**
1	0.300	0.900	0.3000	0.300	0.327	0.300
2	0.270	0.800	0.8000	0.270	0.270	0.270
3	0.210	0.700	0.7000	0.210	0.210	0.210
4	0.200	1.600	0.2000	0.200	1.600	0.902
5	0.170	1.800	0.1700	1.626	0.170	0.900
6	0.170	1.200	0.5402	0.170	0.170	0.170
PV				N/A	N/A	N/A
WT				N/A	N/A	N/A
Power loss				0.065	0.036	0.041

Fuel cost ($/h)			49.55	38.99	41.47	40.36
Emission Cost ($/h)			47.53	37.02	35.16	36.26
PV Cost ($/h)				0	0	0
WT Cost ($/h)				0	0	0
Total Cost ($/h)			97.28	76.01	76.63	**76.62**
Emission, (kg/h)			40.08	49.33	33.64	**41.65**

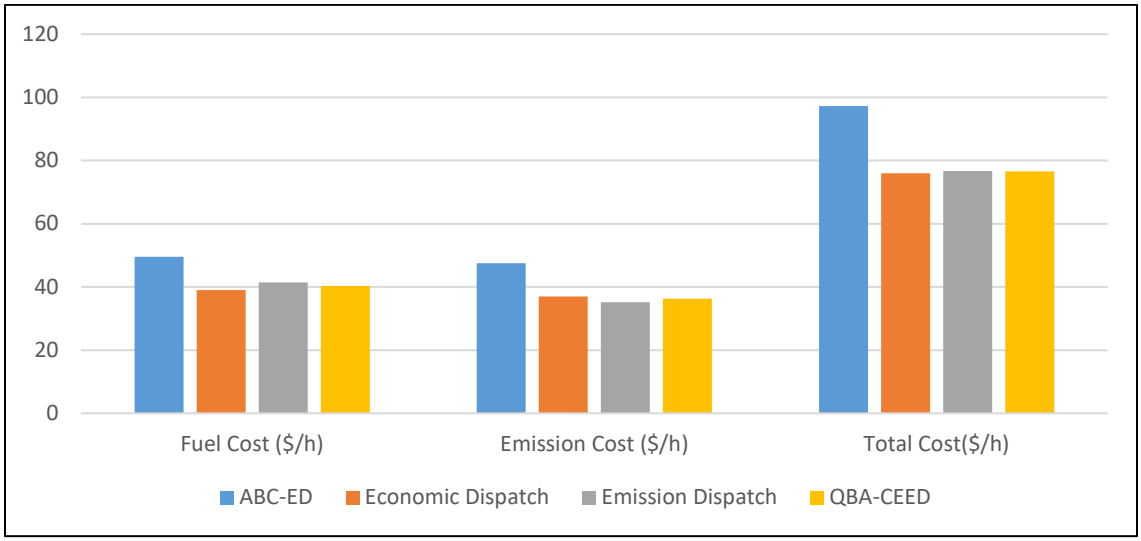

Figure 5. 6: Cost of Production for PMB Summer Period with CGs only

Table 5. 8: Simulation results for PMB Campus @ 16h00 during summer (CGs & RGs dispatched)

Gen Unit	**Pg,min (MW)**	**Pg,max (MW)**	**ABC_ED (MW)**	**Economic dispatch (MW)**	**Emission dispatch (MW)**	**CEED (MW)**
1	0.300	0.900	0.3068	0.300	0.300	0.300
2	0.270	0.800	0.7197	0.270	0.270	0.270
3	0.210	0.700	0.3526	0.210	0.210	0.210
4	0.200	1.600	0.2000	0.200	0.821	0.500
5	0.170	1.800	0.1700	0.808	0.170	0.494
6	0.170	1.200	0.1700	0.170	0.170	0.170
PV				0.791	0.791	0.791
WT				0	0	0
Power loss				0.038	0.021	0.024

Fuel cost ($/h)			35.21	29.34	30.37	29.75
Emission Cost ($/h)			33.36	27.50	26.65	27.02
PV Cost ($/h)				3.81	3.81	3.81
WT Cost ($/h)				0.16	0.16	0.16
Total Cost ($/h)			68.57	60.81	60.99	**60.74**
Emission, (kg/h)			26.27	32.06	25.16	**28.60**

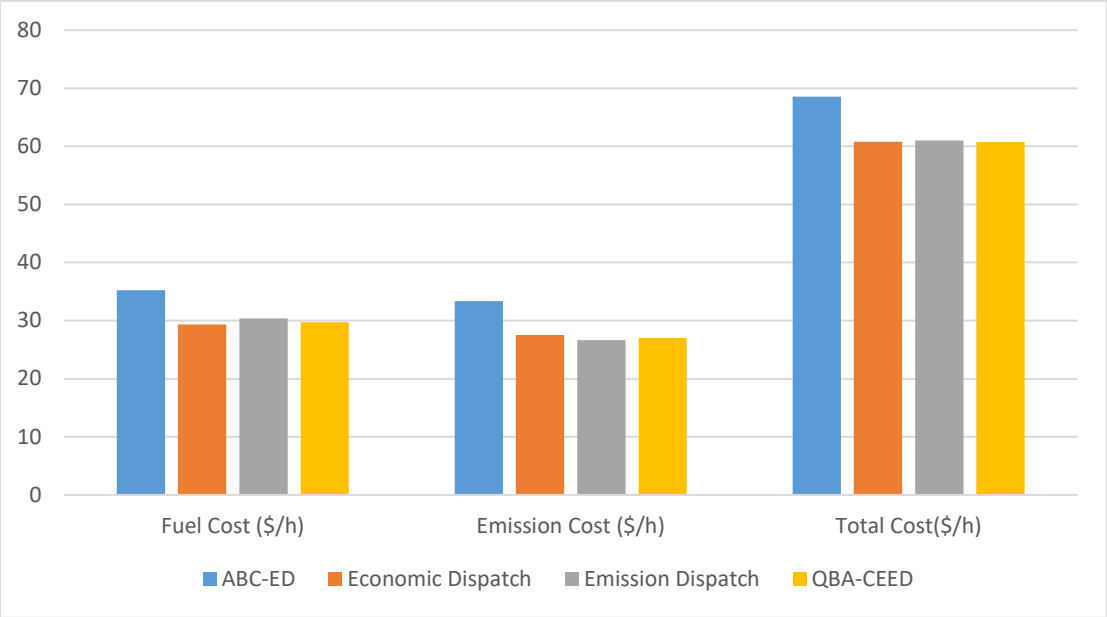

Figure 5. 7: Cost of Production for PMB Summer Period with RG Integration

Table 5. 9: Simulation results for PMB Campus @ 17h00 during winter (Only CGs dispatched)

Gen Unit	**Pg,min (MW)**	**Pg,max (MW)**	**ABC_ED (MW)**	**Economic dispatch (MW)**	**Emission dispatch (MW)**	**CEED (MW)**
1	0.300	0.900	0.3011	0.300	0.300	0.300
2	0.270	0.800	0.7216	0.270	0.270	0.270
3	0.210	0.700	0.4235	0.210	0.210	0.210
4	0.200	1.600	0.2000	0.200	0.889	0.530
5	0.170	1.800	0.1700	0.876	0.170	0.532
6	0.170	1.200	0.1700	0.17	0.170	0.170
PV				N/A	N/A	N/A
WT				N/A	N/A	N/A

Power loss				0.040	0.023	0.026
Fuel cost ($/h)			36.81	30.13	31.30	30.6
Emission Cost ($/h)			34.97	28.29	27.37	27.77
PV Cost ($/h)				0	0	0
WT Cost ($/h)				0	0	0
Total Cost ($/h)			71.78	58.42	58.67	**58.37**
Emission, (kg/h)			27.19	33.49	25.88	**29.72**

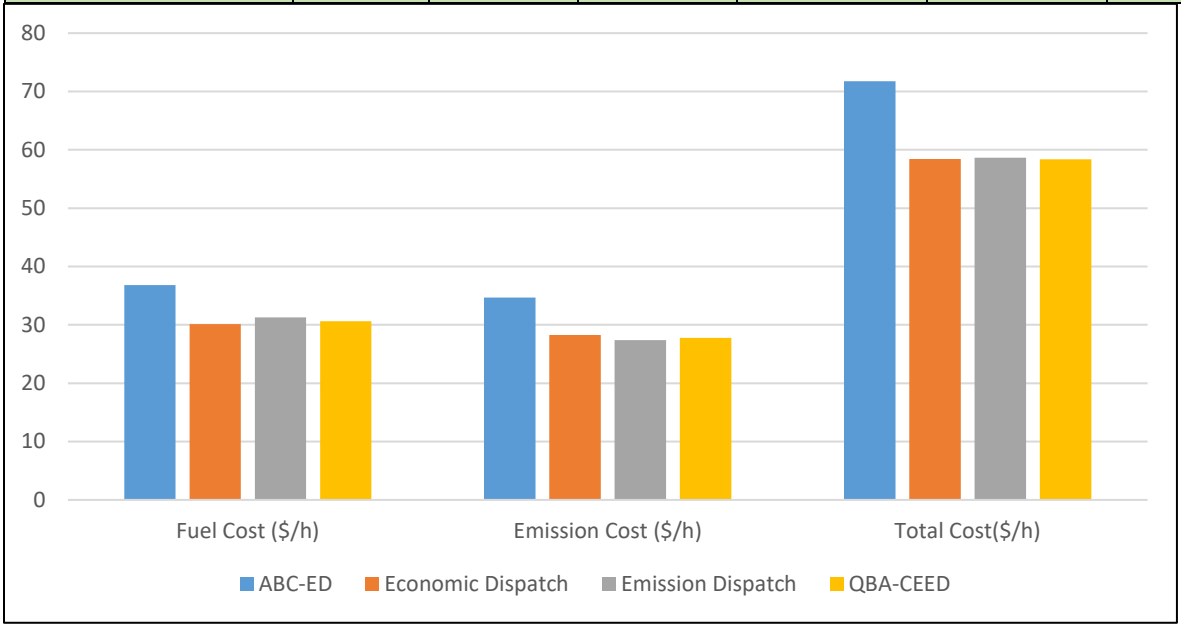

Figure 5. 8: Cost of Production for PMB Winter Period with CGs only

Table 5. 10: Simulation results for PMB Campus @ 17h00 during winter (CGs & RGs dispatched)

Gen Unit	**Pg,min (MW)**	**Pg,max (MW)**	**ABC_ED (MW)**	**Economic dispatch (MW)**	**Emission dispatch (MW)**	**CEED (MW)**
1	0.300	0.900	0.300	0.300	0.300	0.300
2	0.270	0.800	0.270	0.270	0.270	0.270
3	0.210	0.700	0.210	0.210	0.210	0.210
4	0.200	1.600	0.200	0.200	0.200	0.200
5	0.170	1.800	0.170	0.170	0.170	0.170
6	0.170	1.200	0.170	0.170	0.170	0.170
PV				0.416	0.416	0.416
WT				0.299	0.299	0.299

Power loss			0.076	0.076	0.076	0.076
Fuel cost ($/h)			21.92	21.92	21.92	21.92
Emission Cost ($/h)			20.09	20.09	20.09	20.09
PV Cost ($/h)			2.95	2.95	2.95	2.95
WT Cost ($/h)			3.81	3.81	3.81	3.81
Total Cost ($/h)			48.77	48.77	48.77	48.77
Emission, (kg/h)			18.64	18.64	18.64	18.64

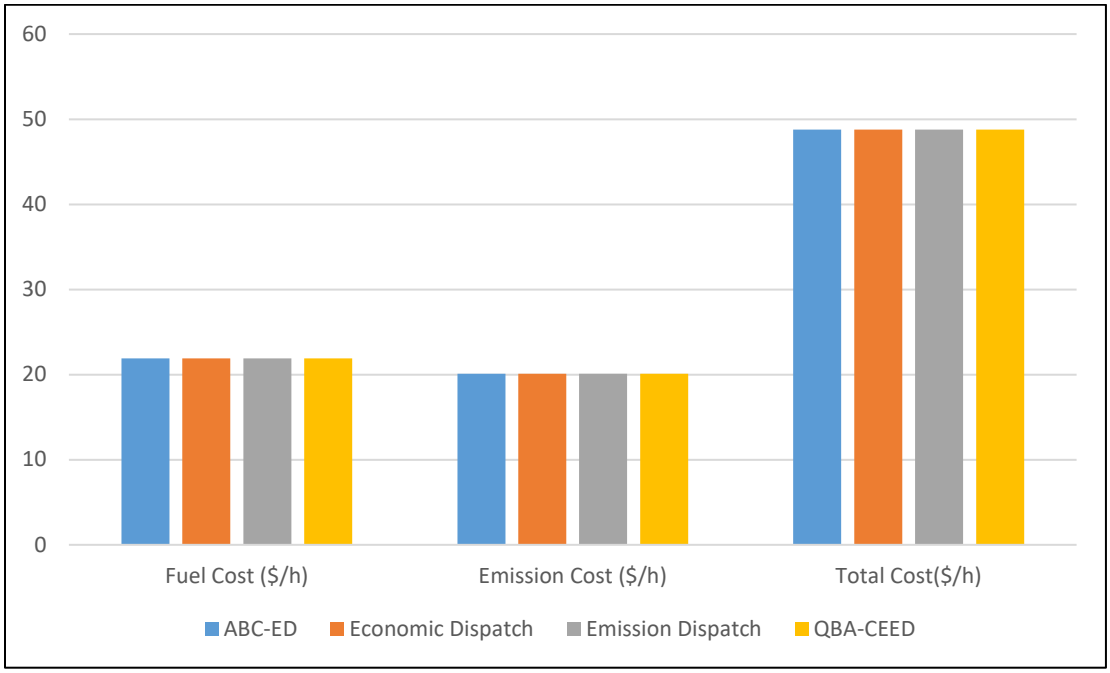

Figure 5. 9: Cost of Production for PMB Winter Period with RG Integration

5.4 Chapter Summary

In this chapter, a new metaheuristic-based power dispatch solution using the quantum-behaved BA optimization is proposed for solving the combined economic emission dispatch problem in a power system considering the integration of renewable energy sources. Without compromising the system's resilience or security, the proposed QBA solution for the CEED problem permits the maximum penetration of the available renewable energy sources at any given time while maintaining the outputs of the conventional generators within the specified constraints. The robustness of the proposed methodology is shown by simulating two study cases (Howard and PMB campuses) with renewable energy (wind and solar) penetrations. The results revealed that the QBA is capable of dispatching power at least fuel cost and emission levels with the CEED objection function when compared to the economic dispatch and emission

dispatch objective functions. Likewise, the comparative performance of the proposed QBA algorithm with the ABC algorithm showed superiority with optimal dispatch, reduced total cost, and emission levels. It can be concluded that this work can be adopted by the municipal electricity industry and other critical facilities.

CHAPTER SIX

CONCLUSION AND RECOMMENDATION

6.1 Conclusion

This section presents the conclusion of the thesis. This thesis presents a robust literature review on microgrids and three different analyses of a typical university campus microgrid. The first study in chapter 3 investigates the economic and environmental impacts of a grid-connected university campus microgrid and proposes a novel hybrid configuration for five campuses considering utility cost-saving and CO_2 emission reduction. The result shows that the COE varies from R1.04/kWh to R1.45/kWh ($0.072/kWh to $0.1/kWh), comparable to similar studies on university campus microgrids reported in the literature. The payback period is approximately 4 years for all campuses except Pietermaritzburg, which is 6 years because of low wind speed. The annual utility bill savings range from R3.97 million to R17.42 million and are directly proportional to the peak load. The average emission reduction for all campuses is 49.6% except Pietermaritzburg (33.7 %) for the same reason stated before. The result obtained from this study can be used as a benchmark for meeting the load demand of other university campuses within and outside South Africa with similar meteorological conditions. It is evident from the result that the proposed hybrid systems are both economically and environmentally viable, considering the values of key performance indexes mentioned above. In addition, the study establishes that a grid connected hybrid system can provide sustainable energy to the university campuses at a reduced operational cost.

The second study reported in chapter 4 proposes an optimization model along with the objective function, system constraints, and parameters to investigate the performance of an autonomous university campus microgrid in MATLAB. The proposed hybrid power system (HPS) is made up of solar PV, wind turbine, diesel generator, and battery storage. The daily load demand for summer and winter study and vacation are considered to assess the effectiveness and feasibility of the HPS for a period of 24-hour. The diesel generator is dispatched using a load-following strategy, the power flow and fuel costs are analyzed. In order to obtain the cost-benefit of the HPS, a comparison is made between the HPS model and diesel generator-only model for summer and winter days. Also, the Levelized cost of energy (LCOE) for each source type and the HPS are calculated. The results reflect how changes in season, erratic nature of RES, and academic activities affect the campus load, power generated by RES, and hence the operational cost of the HPS.

The last study in chapter 5 proposes a novel metaheuristic method, Quantum behaved bat algorithm, to solve a CEED problem in a power system with RES. To find out the effectiveness of the proposed algorithm, two university campuses (same as in chapter 4) have been used as case studies; in each case, economic dispatch, emission dispatch, and CEED are formulated and applied to determine the total system cost with

and without RGs. As seen from the results, for Howard campus, the total system cost ($/h) and the emission (kg/h) reduced by 17% and 23.5%, respectively, while for PMB campus, the reduction in total system cost ($/h) and emission ($/h) are 18.5% and 34.3% respectively with the integration of RES.

6.2 Recommendations

The following areas are recommended for future extension of this thesis:

- Biomass from organic wastes is another renewable energy source that could be considered in a university environment and new storage technologies as well.
- Energy management techniques, demand response programs, or demand-side management could be considered to reduce university campuses' utility bills and the integration of RES.
- Other pollutant gases from coal-fired power plants such as Nitrogen oxides (NOx) and Sulphur dioxide (SO2) could be considered.
- Hybridized optimization algorithm could be used to solve the CEED problem considering the impacts of different price penalty factor methods (Min-Max, Average, Weighted Sum) with or without transmission loss.
- Energy efficiency and energy conservation measures could be considered as a means of reducing electricity bills.

References

[1] IRENA, "Renewable Energy Statistics 2019," The International Renewable Energy Agency, Abu Dhabi, 2019. [Online]. Available: www.irena.org

[2] A. L. Salvia and L. L. Brandli, "Energy Sustainability at Universities and Its Contribution to SDG 7: A Systematic Literature Review," in *Universities as Living Labs for Sustainable Development: Supporting the Implementation of the Sustainable Development Goals*, W. Leal Filho *et al.* Eds. Cham: Springer International Publishing, 2020, pp. 29-45.

[3] IEA, "Africa Energy Outlook 2019," Paris, 2019. [Online]. Available: https://www.iea.org/reports/africa-energy-outlook-2019

[4] A. M. Sani, "Control strategies for the next generation microgrids," Doctor of Philosophy, Electrical and Computer Engineering, University of Toronto, Toronto, 2011.

[5] A. R. Metke and R. L. Ekl, "Security Technology for Smart Grid Networks," *IEEE Transactions on Smart Grid,* vol. 1, no. 1, pp. 99-107, 2010, doi: 10.1109/tsg.2010.2046347.

[6] F. Shahnia, A. Ghosh, S. Rajakaruna, and R. P. S. Chandrasena, "Primary control level of parallel distributed energy resources converters in system of multiple interconnected autonomous microgrids within self-healing networks," *IET Generation, Transmission & Distribution,* vol. 8, no. 2, pp. 203-222, 2014, doi: 10.1049/iet-gtd.2013.0126.

[7] S. Luthra, S. Kumar, R. Kharb, M. F. Ansari, and S. L. Shimmi, "Adoption of smart grid technologies: An analysis of interactions among barriers," *Renewable and Sustainable Energy Reviews,* vol. 33, pp. 554-565, 2014, doi: 10.1016/j.rser.2014.02.030.

[8] N. A. Luu, "Control and management strategies for a microgrid," Electric Power, University of Grenoble, Grenoble, 2014.

[9] K. T. Akindeji, "A review on protection and control of Microgrid with distributed energy resources integration," presented at the Protection Automation Control World Conference 2015, Glasgow, 29 June - 2 July 2015.

[10] N. I. Nwulu, "Optimal energy management of power systems and microgrids incorporating demand response programs," Doctor of Philosophy, Electrical, Electronic and Computer Engineering, University of Pretoria, Pretoria, 2015.

[11] H. Rui, "Integration of renewable distributed energy resources into microgrids," Doctor of Philosophy, Mechanical Engineering, University of California, Los Angeles, 2015.

[12] N. D. Hatziargyriou, *Microgrids : architectures and control*. West Sussex: Wiley-IEEE Press, 2014.

[13] D. R. Danley. *Defining a Microgrid Using IEEE 2030.7*. (2019). National Rural Electric Cooperative Association.

[14] *Microgrids - Part 1: Guidelines for microgrid projects planning and specification*, IEC, Geneva, Switzerland, 18 May 2017.

[15] K. T. Akindeji and I. E. Davidson, "Microgrid and Active Management of Distribution Networks with Renewable Energy Sources," in *South African Universities Power Engineering Conference (SAUPEC)*, Vanderbijlpark, South Africa, 26-28 January 2016, pp. 171 - 175.

[16] T. Chakravorti, R. K. Patnaik, and P. K. Dash, "Detection and classification of islanding and power quality disturbances in microgrid using hybrid signal processing and data mining techniques," *IET Signal Processing,* vol. 12, no. 1, pp. 82-94, 2018, doi: 10.1049/iet-spr.2016.0352.

[17] A. Cagnano, E. De Tuglie, and P. Mancarella, "Microgrids: Overview and guidelines for practical implementations and operation," *Applied Energy,* vol. 258, 2020, doi: 10.1016/j.apenergy.2019.114039.

[18] H. Damgacioglu, "Integrated Microgrid Design and Operation Optimization Using Dynamic-Data-Driven Approaches," Doctor of Philosophy Industrial Engineering, University of Miami, Coral Gables, Florida, 2019.

[19] B. Yan, P. B. Luh, G. Warner, and P. Zhang, "Operation and Design Optimization of Microgrids With Renewables," *IEEE Transactions on Automation Science and Engineering,* vol. 14, no. 2, pp. 573-585, 2017, doi: 10.1109/tase.2016.2645761.

[20] K. T. Akindeji, R. Tiako, and I. E. Davidson, "Use of Renewable Energy Sources in University Campus Microgrid - A Review," in *Domestic Use of Energy*, Wellington, 25-27 March 2019, pp. 76-83.

[21] A. Khamis, H. Shareef, E. Bizkevelci, and T. Khatib, "A review of islanding detection techniques for renewable distributed generation systems," *Renewable and Sustainable Energy Reviews,* vol. 28, pp. 483-493, 2013, doi: 10.1016/j.rser.2013.08.025.

[22] A. Khamis, H. Shareef, A. Mohamed, and E. Bizkevelci, "Islanding detection in a distributed generation integrated power system using phase space technique and probabilistic neural network," *Neurocomputing,* vol. 148, pp. 587-599, 2015, doi: 10.1016/j.neucom.2014.07.004.

[23] I. Serban, "A control strategy for microgrids: Seamless transfer based on a leading inverter with supercapacitor energy storage system," *Applied Energy,* vol. 221, pp. 490-507, 2018, doi: 10.1016/j.apenergy.2018.03.122.

[24] S. Chandak, P. Bhowmik, M. Mishra, and P. K. Rout, "Autonomous microgrid operation subsequent to an anti-islanding scheme," *Sustainable Cities and Society,* vol. 39, pp. 430-448, 2018, doi: 10.1016/j.scs.2018.03.009.

[25] S. K. Sahoo, A. K. Sinha, and N. K. Kishore, "Control Techniques in AC, DC, and Hybrid AC–DC Microgrid: A Review," *IEEE Journal of Emerging and Selected Topics in Power Electronics,* vol. 6, no. 2, pp. 738-759, 2018, doi: 10.1109/jestpe.2017.2786588.

[26] L. Meng, A. Luna, E. Diaz, B. Sun, T. Dragicevic, M. Savaghebi, . . . M. Graells, "Flexible System Integration and Advanced Hierarchical Control Architectures in the Microgrid Research Laboratory of Aalborg University," *IEEE Transactions on Industry Applications,* pp. 1-1, 2015, doi: 10.1109/tia.2015.2504472.

[27] L. Moretti, S. Polimeni, L. Meraldi, P. Raboni, S. Leva, and G. Manzolini, "Assessing the impact of a two-layer predictive dispatch algorithm on design and operation of off-grid hybrid microgrids," *Renewable Energy,* vol. 143, pp. 1439-1453, 2019, doi: 10.1016/j.renene.2019.05.060.

[28] A. H. Fathima and K. Palanisamy, "Optimization in microgrids with hybrid energy systems – A review," *Renewable and Sustainable Energy Reviews,* vol. 45, pp. 431-446, 2015, doi: 10.1016/j.rser.2015.01.059.

[29] M. Shahidehpour and M. Khodayar, "Cutting Campus Energy Costs with Hierarchical Control: The Economical and Reliable Operation of a Microgrid," *IEEE Electrification Magazine,* vol. 1, no. 1, pp. 40-56, 2013, doi: 10.1109/MELE.2013.2273994.

[30] L. ı. Igualada, C. Corchero, M. Cruz-Zambrano, and F.-J. Heredia, "Optimal Energy Management for a Residential Microgrid Including a Vehicle-to-Grid System," *IEEE TRANSACTIONS ON SMART GRID,* vol. 5, no. 4, pp. 2163-2172, July 2014, doi: 10.1109/TSG.2014.2318836.

[31] J. Zhao, C. Wang, B. Zhao, F. Lin, Q. Zhou, and Y. Wang, "A Review of Active Management for Distribution Networks: Current Status and Future Development Trends," *Electric Power Components and Systems,* vol. 42, no. 3-4, pp. 280-293, 2014, doi: 10.1080/15325008.2013.862325.

[32] W. Su and J. Wang, "Energy Management Systems in Microgrid Operations," *The Electricity Journal,* vol. 25, no. 8, pp. 45-60, 2012, doi: 10.1016/j.tej.2012.09.010.

[33] T. J. T. Hashim, A. Mahomed, and H. Shareef, "A review on voltage control methods for active distribution networks," *Przegm d Elektrotechniczny,* pp. 304-312, 2012.

[34] R. Majumder and G. Bag, "Parallel operation of converter interfaced multiple microgrids," *International Journal of Electrical Power & Energy Systems,* vol. 55, pp. 486-496, 2014, doi: 10.1016/j.ijepes.2013.09.008.

[35] S.Chowdhury, S.P.Chowdhury, and P. Crossley, *Microgrids and Active Distribution Networks*. London: Institution of Engineering and Technology, 2009.

[36] A. K. Basu, S. P. Chowdhury, S. Chowdhury, and S. Paul, "Microgrids - Energy management by strategic deployment of DERs—A comprehensive survey," *Renewable and Sustainable Energy Reviews,* vol. 15, pp. 4348-4356, 2011, doi: 10.1016/j.rser.2011.07.116.

[37] W. Shi, X. Xie, C.-C. Chu, and R. Gadh, "Distributed Optimal Energy Management in Microgrids," *IEEE TRANSACTIONS ON SMART GRID,* vol. 6, no. 3, pp. 1137-1146, May 2015, doi: 10.1109/TSG.2014.2373150.

[38] E. Bullich-Massagué, F. Díaz-González, M. Aragüés-Peñalba, F. Girbau-Llistuella, P. Olivella-Rosell, and A. Sumper, "Microgrid clustering architectures," *Applied Energy,* vol. 212, pp. 340-361, 2018, doi: 10.1016/j.apenergy.2017.12.048.

[39] T. S. Abdelgayed, W. G. Morsi, and T. S. Sidhu, "A New Approach for Fault Classification in Microgrids Using Optimal Wavelet Functions Matching Pursuit," *IEEE Transactions on Smart Grid,* vol. 9, no. 5, pp. 4838-4846, 2018, doi: 10.1109/tsg.2017.2672881.

[40] K. R. Khan, M. S. Siddiqui, Y. A. Saawy, N. Islam, and A. Rahman, "Condition Monitoring of a Campus Microgrid Elements using Smart Sensors," *Procedia Computer Science,* vol. 163, pp. 109-116, 2019.

[41] B. K. Panigrahi, P. K. Ray, P. K. Rout, A. Mohanty, and K. Pal, "Detection and classification of faults in a microgrid using wavelet neural network," *Journal of Information and Optimization Sciences,* vol. 39, no. 1, pp. 327-335, 2017, doi: 10.1080/02522667.2017.1374738.

[42] M. Mishra and P. K. Rout, "Detection and classification of micro-grid faults based on HHT and machine learning techniques," *IET Generation, Transmission & Distribution,* vol. 12, no. 2, pp. 388-397, 2018, doi: 10.1049/iet-gtd.2017.0502.

[43] S. C. Madathil, "Modeling and Analysis of Remote Off-grid Microgrids," PhD, Industrial Engineering, Clemson University, Clemson, South Carolina,USA, 2017.

[44] F. Nejabatkhah, "Optimal Design and Operation of a Remote Hybrid Microgrid," *CPSS Transactions on Power Electronics and Applications,* vol. 3, no. 1, pp. 3-13, 2018, doi: 10.24295/cpsstpea.2018.00001.

[45] M. Kaur, S. Dhundhara, Y. P. Verma, and S. Chauhan, "Techno-economic analysis of photovoltaic-biomass-based microgrid system for reliable rural electrification," *International Transactions on Electrical Energy Systems,* 2020, doi: 10.1002/2050-7038.12347.

[46] J. Ahmad, M. Imran, A. Khalid, W. Iqbal, S. R. Ashraf, M. Adnan, . . . K. S. Khokhar, "Techno economic analysis of a wind-photovoltaic-biomass hybrid renewable energy system for rural electrification: A case study of Kallar Kahar," *Energy,* vol. 148, pp. 208-234, 2018, doi: 10.1016/j.energy.2018.01.133.

[47] G. Veilleux, T. Potisat, D. Pezim, C. Ribback, J. Ling, A. Krysztofiński, . . . S. Chucherd, "Techno-economic analysis of microgrid projects for rural electrification: A systematic approach to the redesign of Koh Jik off-grid case study," *Energy for Sustainable Development,* vol. 54, pp. 1-13, 2020, doi: 10.1016/j.esd.2019.09.007.

[48] M. R. Fuad, D. Octavianthy, and W. W. Purwanto, "Techno-economic analysis of natural gas-fired microgrid for electricity, fresh water, and cold storage in rural area," 2019, doi: 10.1063/1.5095006

[49] S. You, H. Tong, J. Armin-Hoiland, Y. W. Tong, and C.-H. Wang, "Techno-economic and greenhouse gas savings assessment of decentralized biomass gasification for electrifying the rural areas of Indonesia," *Applied Energy,* vol. 208, pp. 495-510, 2017, doi: 10.1016/j.apenergy.2017.10.001.

[50] S. Mazzola, M. Astolfi, and E. Macchi, "The potential role of solid biomass for rural electrification: A techno economic analysis for a hybrid microgrid in India," *Applied Energy,* vol. 169, pp. 370-383, 2016, doi: 10.1016/j.apenergy.2016.02.051.

[51] M. Warneryd, M. Håkansson, and K. Karltorp, "Unpacking the complexity of community microgrids: A review of institutions' roles for development of microgrids," *Renewable and Sustainable Energy Reviews,* vol. 121, 2020, doi: 10.1016/j.rser.2019.109690.

[52] "Types of microgrids." http://microgridprojects.com/types-of-microgrids (accessed 7 August 2020).

[53] "Community Microgrids- A guide for mayors and city leaders."

[54] E. M. Gui, M. Diesendorf, and I. MacGill, "Distributed energy infrastructure paradigm: Community microgrids in a new institutional economics context," *Renewable and Sustainable Energy Reviews,* vol. 72, pp. 1355-1365, 2017, doi: 10.1016/j.rser.2016.10.047.

[55] Y.-Y. Hong, W.-C. Chang, Y.-R. Chang, Y.-D. Lee, and D.-C. Ouyang, "Optimal sizing of renewable energy generations in a community microgrid using Markov model," *Energy,* vol. 135, pp. 68-74, 2017, doi: 10.1016/j.energy.2017.06.098.

[56] H. Lotfi and A. Khodaei, "Hybrid AC/DC microgrid planning," *Energy,* vol. 118, pp. 37-46, 2017, doi: 10.1016/j.energy.2016.12.015.

[57] A. Gupta, S. Doolla, and K. Chatterjee, "Hybrid AC–DC Microgrid: Systematic Evaluation of Control Strategies," *IEEE Transactions on Smart Grid,* vol. 9, no. 4, pp. 3830-3843, 2018, doi: 10.1109/tsg.2017.2727344.

[58] Y. Xia, W. Wei, M. Yu, X. Wang, and Y. Peng, "Power Management for a Hybrid AC/DC Microgrid With Multiple Subgrids," *IEEE Transactions on Power Electronics,* vol. 33, no. 4, pp. 3520-3533, 2018, doi: 10.1109/tpel.2017.2705133.

[59] T. Ma, M. H. Cintuglu, and O. A. Mohammed, "Control of a Hybrid AC/DC Microgrid Involving Energy Storage and Pulsed Loads," *IEEE Transactions on Industry Applications,* vol. 53, no. 1, pp. 567-575, 2017, doi: 10.1109/tia.2016.2613981.

[60] L. Xiong, W. Peng, and L. Poh Chiang, "A Hybrid AC/DC Microgrid and Its Coordination Control," *IEEE Transactions on Smart Grid,* vol. 2, no. 2, pp. 278-286, 2011, doi: 10.1109/tsg.2011.2116162.

[61] X. Liu, P. Wang, and P. C. Loh, "A Hybrid AC-DC Microgrid," in *2010 Conference Proceedings IPEC*, Singapore, Singapore, 27-29 Oct 2010.

[62] Y. Wang, Y. Li, Y. Cao, Y. Tan, L. He, and J. Han, "Hybrid AC/DC microgrid architecture with comprehensive control strategy for energy management of smart building," *International Journal of Electrical Power & Energy Systems,* vol. 101, pp. 151-161, 2018, doi: 10.1016/j.ijepes.2018.02.048.

[63] E. Wood. "Military microgrids: four examples of innovation." https://microgridknowledge.com/military-microgrids-four-examples/ (accessed 31 August, 2020).

[64] G. Oriti, A. L. Julian, N. Anglani, and G. D. Hernandez, "Novel Economic Analysis to Design the Energy Storage Control System of a Remote Islanded Microgrid," *IEEE Transactions on Industry Applications,* vol. 54, no. 6, pp. 6332-6342, 2018, doi: 10.1109/tia.2018.2853041.

[65] K. E. Garcia, "Optimization of microgrids at military remote base camps," MSc, NAVAL POSTGRADUATE SCHOOL, Monterey,California USA, 2017.

[66] W. Leal Filho, A. L. Salvia, A. d. Paço, R. Anholon, O. L. Gonçalves Quelhas, I. S. Rampasso, . . . L. L. Brandli, "A comparative study of approaches towards energy efficiency and renewable energy use at higher education institutions," *Journal of Cleaner Production,* vol. 237, 2019, doi: 10.1016/j.jclepro.2019.117728.

[67] H. TALEI, B. ZIZI, M. R. ABID, M. ESSAAIDI, D. BENHADDOU, and N. KHALIL, "Smart Campus Microgrid- Advantages and the Main Architectural components," in *2015 3rd International Renewable and Sustainable Energy Conference (IRSEC)*, Marrakech, Morocco, 10-13 Dec 2015.

[68] N. Kalkan, K. Bercin, O. Cangul, M. G. Morales, M. M. K. M. Saleem, I. Marji, . . . E. Tsigkogianni, "A renewable energy solution for Highfield Campus of University of Southampton," *Renewable and Sustainable Energy Reviews,* vol. 15, no. 6, pp. 2940-2959, 2011, doi: 10.1016/j.rser.2011.02.040.

[69] O. A. Mafimidiwo, "Impact of Three-dimensional Photovoltaic Structure on Solar Power Generation," Doctor of Philosophy, Discipline of Electrical, Electronic and Computer Engineering, University of KwaZulu-Natal, Durban, 2016.

[70] S. Lalljith, A. G. Swanson, and A. Goudarzi, "An intelligent alternating current-optimal power flow for reduction of pollutant gases with incorporation of variable generation resources," *Journal of Energy in Southern Africa,* vol. 31, no. 1, pp. 40-61, 2020, doi: 10.17159/2413-3051/2020/v31i1a7008.

[71] CANADIANSOLAR. *MAXPOWER CS6U- 325| 330| 335P*. (2018). Ontario N1K 1E6, Canada.

[72] Indiamart. "UPT 220 W 24V Polycrystalline Solar PV Module." https://www.indiamart.com/proddetail/220-w-24v-polycrystalline-solar-pv-module-23227067733.html (accessed 19 January, 2022).

[73] S. Sumathi, L. A. Kumar, and P. Surekha, *Solar PV and Wind Energy Conversion Systems:An Introduction to Theory, Modeling with MATLAB/SIMULINK, and the Role of Soft Computing Techniques* (Green Energy and Technology). Switzerland: Springer, 2015.

[74] A. O. Aluko and K. T. Akindeji, "Mitigation of Low Voltage Contingency of Doubly FED Induction Generator Wind Farm Using Static Synchronous Compensator in South Africa," in *2018 IEEE PES/IAS PowerAfrica*, Cape Town,South Africa, 28-29 June 2018, pp. 13-18. doi: doi: 10.1109/PowerAfrica.2018.8521033

[75] O. A. Aluko and K. T. Akindeji, "Performance analysis of grid connected scig and dfig based windfarm," in *26th South African Universities Power Engineering Conference (SAUPEC)*, Johannesburg, South Africa, 24-26 January 2018, pp. 20-25.

[76] M. İnci and Ö. Türksoy, "Review of fuel cells to grid interface: Configurations, technical challenges and trends," *Journal of Cleaner Production,* vol. 213, pp. 1353-1370, 2019, doi: 10.1016/j.jclepro.2018.12.281.

[77] A. Khan and R. Khan, "Cost Optimization of Hybrid Microgrid using Solar PV, Fuel Cell and Diesel Generator in HOMER," in *2018 2nd International Conference on Energy Conservation and Efficiency (ICECE)*, Lahore, Pakistan, 16-17 Oct 2018.

[78] A. Ganeshan, D. G. Holmes, L. Meegahapola, and B. P. McGrath, "Improved Controller Design for a Microgrid Fuel-Cell Based Energy Storage System," in *2018 IEEE 27th International Symposium on Industrial Electronics (ISIE)*, Cairns, QLD, Australia, 13-15 June 2018.

[79] P. Kumar, S. K. Kannaiah, S. R. Choudhury, and N. Rajasekar, "Genetic Algorithm-based Modeling of PEM Fuel Cells Suitable for Integration in DC Microgrids," *Electric Power Components and Systems,* vol. 45, no. 10, pp. 1152-1160, 2017, doi: 10.1080/15325008.2017.1318980.

[80] Z. Li, Z. Zheng, L. Xu, and X. Lu, "A review of the applications of fuel cells in microgrids-opportunities and challenges," *BMC Energy,* vol. 1, no. 8, 2019, doi: 10.1186/s42500-019-0008-3.

[81] S. Gupta, R. Garg, and A. Singh, "Modeling, Simulation and Control of Fuel cell based microgrid," *Journal of Green Engineering,* vol. 7, pp. 129-158, 2017, doi: 10.13052/jge1904-4720.7127.

[82] G. Brunaccini, F. Sergi, D. Aloisio, N. Randazzo, M. Ferraro, and V. Antonucci, "Fuel cells hybrid systems for resilient microgrids," *International Journal of Hydrogen Energy,* vol. 44, no. 38, pp. 21162-21173, 2019, doi: 10.1016/j.ijhydene.2019.04.121.

[83] M. S. Islam, R. Akhter, M. A. Rahman, s. Skolan för elektro- och, and Kth, "A thorough investigation on hybrid application of biomass gasifier and PV resources to meet energy needs for a northern

rural off-grid region of Bangladesh: A potential solution to replicate in rural off-grid areas or not?," *Energy,* vol. 145, pp. 338-355, 2018, doi: 10.1016/j.energy.2017.12.125.

[84] J. M. Aberilla, A. Gallego-Schmid, and A. Azapagic, "Environmental sustainability of small-scale biomass power technologies for agricultural communities in developing countries," *Renewable Energy,* vol. 141, pp. 493-506, 2019, doi: 10.1016/j.renene.2019.04.036.

[85] S. W. Nene and K. T. Akindeji, "Energy efficiency evaluation of a bagasse gasification system for the south african sugar industry," in *26th South African Universities Power Engineering Conference (SAUPEC)*, Johannesburg, South Africa, 24-26 January 2018, pp. 610-615.

[86] HOMER. *HOMER GRID Local User Manual*. (2020).

[87] A. Tiwary, S. Spasova, and I. D. Williams, "A community-scale hybrid energy system integrating biomass for localised solid waste and renewable energy solution: Evaluations in UK and Bulgaria," *Renewable Energy,* vol. 139, pp. 960-967, 2019, doi: 10.1016/j.renene.2019.02.129.

[88] M. J. Deasy, S. M. O'Shaughnessy, L. Archer, and A. J. Robinson, "Electricity generation from a biomass cookstove with MPPT power management and passive liquid cooling," *Energy for Sustainable Development,* vol. 43, pp. 162-172, 2018, doi: 10.1016/j.esd.2018.01.004.

[89] C. Y. Li, Y. Shen, J. Y. Wu, Y. J. Dai, and C.-H. Wang, "Experimental and modeling investigation of an integrated biomass gasifier–engine–generator system for power generation and waste heat recovery," *Energy Conversion and Management,* vol. 199, p. 112023, 2019, doi: 10.1016/j.enconman.2019.112023.

[90] M. Jahangiri, R. A. Rizi, and A. A. Shamsabadi, "Feasibility study on simultaneous generation of electricity and heat using renewable energies in Zarrin Shahr, Iran," *Sustainable Cities and Society,* vol. 38, pp. 647-661, 2018, doi: 10.1016/j.scs.2018.01.043.

[91] R. Rajbongshi, D. Borgohain, and S. Mahapatra, "Optimization of PV-biomass-diesel and grid base hybrid energy systems for rural electrification by using HOMER," *Energy,* vol. 126, pp. 461-474, 2017, doi: 10.1016/j.energy.2017.03.056.

[92] A. A. Angeline, J. Jayakumar, L. G. Asirvatham, J. J. Marshal, and S. Wongwises, "Power generation enhancement with hybrid thermoelectric generator using biomass waste heat energy," *Experimental Thermal and Fluid Science,* vol. 85, pp. 1-12, 2017, doi: 10.1016/j.expthermflusci.2017.02.015.

[93] S. Khanmohammadi, M. Saadat-Targhi, A. A. A. A. Al-Rashed, and M. Afrand, "Thermodynamic and economic analyses and multi-objective optimization of harvesting waste heat from a biomass gasifier integrated system by thermoelectric generator," *Energy Conversion and Management,* vol. 195, pp. 1022-1034, 2019, doi: 10.1016/j.enconman.2019.05.075.

[94] N. Hussin, A. A. Razak, and F. Baharum, "A study of electricity consumption of library in UiTM Bertam," 2018, doi: 10.1063/1.5066685

[95] A. Gambarotta, M. Morini, M. Rossi, and M. Stonfer, "A Library for the Simulation of Smart Energy Systems: The Case of the Campus of the University of Parma," *Energy Procedia,* vol. 105, pp. 1776-1781, May 2017, doi: 10.1016/j.egypro.2017.03.514.

[96] M. Medrano, J. M. Martí, L. Rincón, G. Mor, J. Cipriano, and M. Farid, "Assessing the nearly zero-energy building gap in university campuses with a feature extraction methodology applied to a case study in Spain," *International Journal of Energy and Environmental Engineering,* vol. 9, no. 3, pp. 227-247, 2018, doi: 10.1007/s40095-018-0264-x.

[97] V. B. Hau, M. Husein, I.-Y. Chung, D.-J. Won, W. Torre, and T. Nguyen, "Analyzing the impact of renewable energy incentives and parameter uncertainties on financial feasibility of a campus microgrid," *Energies,* vol. 11, no. 9, p. 2446, 2018, doi: 10.3390/en11092446.

[98] W. Chen, Y. Zeng, and C. Xu, "Energy storage subsidy estimation for microgrid: A real option game-theoretic approach," *Applied Energy,* vol. 239, pp. 373-382, 2019, doi: 10.1016/j.apenergy.2019.01.232.

[99] M. Goransson, N. Larsson, L. A. Tuan, and D. Steen, "Cost-benefit analysis of battery storage investment for microgrid of Chalmers university campus using μ-OPF framework," 2017, pp. 1-6. doi: 10.1109/PTC.2017.7981160

[100] E. L. Karfopoulos, P. Papadopoulos, S. Skarvelis-Kazakos, I. Grau, and L. M. Cipciga, "Introducing electric vehicles in the microgrids concept," in *2011 16th International Conference on Intelligent System Applications to Power Systems*, Hersonissos, Greece, 25-28 Sept 2011.

[101] M. Bayati, M. Abedi, G. B. Gharehpetian, and M. Farahmandrad, "Short-term interaction between electric vehicles and microgrid in decentralized vehicle-to-grid control methods," *Protection and Control of Modern Power Systems,* vol. 4, no. 1, 2019, doi: 10.1186/s41601-019-0118-4.

[102] R. Villafafila-Robles, P. Lloret-Gallego, D. Heredero-Peris, A. Sumper, I. Cairo, M. Cruz-Zambrano, and N. Vidal, "Electric vehicles in power systems with distributed generation: Vehicle to Microgrid (V2M) project," presented at the 11th International Conference on Electrical Power Quality and Utilisation, 2011.

[103] D. Wang, X. Guan, J. Wu, P. Li, P. Zan, and H. Xu, "Integrated Energy Exchange Scheduling for Multimicrogrid System With Electric Vehicles," *IEEE Transactions on Smart Grid,* vol. 7, no. 4, pp. 1762-1774, 2016, doi: 10.1109/tsg.2015.2438852.

[104] M. Pyne. "Large Scale Vehicle Charging Problem." Energy Storage Systems Lab. https://labs.utdallas.edu/essl/projects/large-scale-vehicle-charging-problem/ (accessed 29 August 2020).

[105] M. Goody. "The role of electric vehicles in a microgrid before V2G." https://www.fleetcarma.com/microgrids-and-v2g/ (accessed 29 August, 2020).

[106] S. Abdool. "Used electric-vehicle batteries for microgrid." https://www.ee.co.za/article/used-electric-vehicle-batteries-for-microgrid.html (accessed 29 August 2020).

[107] A. Khamis, M. S. M. Aras, H. N. M. Shah, M. Z. A. Rashid, M. K. M. Zambri, A. Ahmad, and M. A. H. N. Rahim, "Design and Analysis of Diesel Generator with Battery Storage for Microgrid System," *International Journal of Advanced Engineering Research and Technology,* vol. 5, no. 3, pp. 26-32, 2017, doi: 10.4314/jfas.v10i6s.69.

[108] Q. Tang, N. Liu, and J. Zhang, "Optimal Operation Method for Microgrid with Wind/PV/Diesel Generator/Battery and Desalination," *Journal of Applied Mathematics,* vol. 2014, pp. 1-12, 2014, doi: 10.1155/2014/857541.

[109] M. Alramlawi, A. F. Timothy, A. Gabash, E. Mohagheghi, and P. Li, "Optimal Operation of PV-Diesel MicroGrid with Multiple Diesel Generators under Grid Blackouts," presented at the 18th IEEE International Conference on Environment and Electrical Engineering, Palermo, Italy, 12-15 June, 2018.

[110] R. Ghanizadeh and G. B. Gharehpetian, "Distributed hierarchical control structure for voltage harmonic compensation and harmonic current sharing in isolated MicroGrids," *Sustainable Energy, Grids and Networks,* vol. 16, pp. 55-69, 2018, doi: 10.1016/j.segan.2018.05.005.

[111] W. Kou, K. Bisson, and S.-Y. Park, "A Distributed Demand Response Algorithm and its Application to Campus Microgrid," in *IEEE Electronic Power Grid (eGrid)*, Charleston, SC, USA, 12-14 Nov 2018, doi: 10.1109/eGRID.2018.8598668

[112] K. S. Saritha, S. Sreedharan, and U. Nair, "A generalized setup of a campus microgrid - A case study," in *International Conference on Energy, Communication, Data Analytics and Soft Computing (ICECDS)*, Chennai, India, 1-2 Aug 2017, pp. 2182-2188. doi: 10.1109/ICECDS.2017.8389838

[113] M. Soshinskaya, W. H. J. Crijns-Graus, J. M. Guerrero, and J. C. Vasquez, "Microgrids: Experiences, barriers and success factors," *Renewable and Sustainable Energy Reviews,* vol. 40, pp. 659-672, 2014.

[114] M. H. Bellido, L. P. Rosa, A. O. Pereira, D. M. Falcão, and S. K. Ribeiro, "Barriers, challenges and opportunities for microgrid implementation: The case of Federal University of Rio de Janeiro," *Journal of Cleaner Production,* vol. 188, pp. 203-216, 2018/07/01/ 2018, doi: doi.org/10.1016/j.jclepro.2018.03.012.

[115] "<Smart Campus Microgrid- Advantages and the Main Architectural components.pdf>."

[116] Y. Parag and M. Ainspan, "Sustainable microgrids: Economic, environmental and social costs and benefits of microgrid deployment," *Energy for Sustainable Development,* vol. 52, pp. 72-81, 2019.

[117] W. L. Filho, M. Mifsud, P. Molthan-Hill, G. J. Nagy, L. V. ávila, and A. L. Salvia, "Climate change scepticism at universities: A global study," *Sustainability (Switzerland),* vol. 11, no. 10, p. 2981, 2019, doi: 10.3390/su11102981.

[118] S. Bracco, F. Delfino, F. Pampararo, M. Robba, and M. Rossi, "A mathematical model for the optimal operation of the University of Genoa Smart Polygeneration Microgrid: Evaluation of technical, economic and environmental performance indicators," *Energy,* vol. 64, pp. 912-922, 2014, doi: 10.1016/j.energy.2013.10.039.

[119] Q. Tu, C. Zhu, and D. C. McAvoy, "Converting campus waste into renewable energy - a case study for the University of Cincinnati," *Waste Manag,* vol. 39, pp. 258-65, May 2015, doi: 10.1016/j.wasman.2015.01.016.

[120] M. Z. Elenkova, T. A. Papadopoulos, A. I. Psarra, and A. A. Chatzimichail, "A simulation platform for smart microgrids in university campuses," in *52nd International Universities Power Engineering Conference (UPEC)*, Heraklion, Greece, 28-31 Aug 2017, doi: 10.1109/UPEC.2017.8231998

[121] J. Vourdoubas, "Energy Consumption and Carbon Emissions in an Academic Institution in Greece: Can It Become Carbon Neutral?," *Studies in Engineering and Technology,* vol. 6, no. 1, 2019, doi: 10.11114/set.v6i1.4013.

[122] B. G. Rebelatto, A. Lange Salvia, G. Reginatto, R. C. Daneli, and L. L. Brandli, "Energy efficiency actions at a Brazilian university and their contribution to sustainable development Goal 7," *International Journal of Sustainability in Higher Education,* vol. 20, no. 5, pp. 842-855, 2019, doi: 10.1108/ijshe-01-2019-0023.

[123] A. Dehghanmongabadi and Ş. Hoşkara, "Challenges of Promoting Sustainable Mobility on University Campuses: The Case of Eastern Mediterranean University," *Sustainability,* vol. 10, no. 12, 2018, doi: 10.3390/su10124842.

[124] D. Hasapis, N. Savvakis, T. Tsoutsos, K. Kalaitzakis, S. Psychis, and N. P. Nikolaidis, "Design of large scale prosuming in Universities: The solar energy vision of the TUC campus," *Energy and Buildings,* vol. 141, pp. 39-55, 2017, doi: 10.1016/j.enbuild.2017.01.074.

[125] H. Makkonen, J. Partanen, V. Tikka, P. Silventoinen, and J. Lassila, "Green campus – energy management system," in *22nd International Conference and Exhibition on Electricity Distribution (CIRED 2013)*, Stockholm, Sweden, 10-13 June 2013, doi: 10.1049/cp.2013.1088

[126] Hadiyanto, A. Ambariyanto, Y. J. Utama, Purwanto, Sudarno, and Maryono, "Managing Campus Energy: Compromising between Rapid Needs and Environmental Requirement," *E3S Web of Conferences,* vol. 31, 2018, doi: 10.1051/e3sconf/20183101003.

[127] L. Hadjidemetriou, L. Zacharia, E. Kyriakides, B. Azzopardi, S. Azzopardi, R. Mikalauskiene, . . . D. Tzovaras, "Design factors for developing a university campus microgrid," in *IEEE International Energy Conference (ENERGYCON)*, Limassol, Cyprus, 3-7 June 2018, doi: 10.1109/ENERGYCON.2018.8398791

[128] M. Shahidehpour, M. Khodayar, and M. Barati, "Campus microgrid: High reliability for active distribution systems," in *IEEE Power and Energy Society General Meeting*, San Diego, CA, USA, 22-26 July 2012, doi: 10.1109/PESGM.2012.6345754

[129] B. H. Vu, M. A. Husein, and I.-Y. Chung, "Design of a grid-connected campus microgrid considering energy efficiency and financial feasibility," presented at the CIRED Workshop, Ljubljana, 7-8 June 2018.

[130] J. S. Crisis and R. H. Van Els, *Design of a smart microgrid laboratory platform for university campus*: IOS Press, 2016, pp. 206-215.

[131] B. Dursun, "Determination of the optimum hybrid renewable power generating systems for Kavakli campus of Kirklareli University, Turkey," *Renewable and Sustainable Energy Reviews,* vol. 16, no. 8, pp. 6183-6190, 2012, doi: 10.1016/j.rser.2012.07.017.

[132] F. Bisegna, L. Cirrincione, B. M. Lo Casto, G. Peri, G. Rizzo, G. Scaccianoce, and G. Sorrentino, "Fostering the energy efficiency through the energy savings: the case of the University of Palermo," in *2019 IEEE International Conference on Environment and Electrical Engineering and 2019 IEEE Industrial and Commercial Power Systems Europe (EEEIC / I&CPS Europe)*, Genova, Italy, 11-14 June 2019, doi: 10.1109/EEEIC.2019.8783774

[133] B. Washom, J. Dilliot, D. Weil, J. Kleissl, N. Balac, W. Torre, and C. Richter, "Ivory Tower of Power: Microgrid Implementation at the University of California, San Diego," *IEEE Power and Energy Magazine,* vol. 11, no. 4, pp. 28-32, 2013, doi: 10.1109/MPE.2013.2258278.

[134] P. Sreedharan, J. Farbes, E. Cutter, C. K. Woo, and J. Wang, "Microgrid and renewable generation integration: University of California, San Diego," *Applied Energy,* vol. 169, pp. 709-720, 2016, doi: 10.1016/j.apenergy.2016.02.053.

[135] S. Budea, L. Mândrea, and R. E. Huluba, "Micro smart grid to increase the efficiency of electrical power supply for university campus," *International Multidisciplinary Scientific GeoConference : SGEM,* vol. 18, no. 4.1, pp. 449-456, 2018, doi: 10.5593/sgem2018/4.1/S17.059.

[136] R. Morales Gonzalez, T. A. J. van Goch, M. F. Aslam, A. Blanch, and P. F. Ribeiro, "Microgrid design considerations for a smart-energy university campus," in *IEEE PES Innovative Smart Grid Technologies, Europe*, Istanbul, Turkey, 12-15 Oct 2014, doi: 10.1109/ISGTEurope.2014.7028743

[137] H. Dagdougui, L. Dessaint, G. Gagnon, and K. Al-Haddad, "Modeling and optimal operation of a university campus microgrid," in *2016 IEEE Power and Energy Society General Meeting (PESGM)*, Boston, MA, USA, 17-21 July 2016, doi: 10.1109/PESGM.2016.7741207

[138] T. Adefarati, T. Adefarati, and G. D. Obikoya, "Techno-economic evaluation of a grid-connected microgrid system," *International Journal of Green Energy,* vol. 16, no. 15, pp. 1497-1517, 2019, doi: 10.1080/15435075.2019.1671421.

[139] R. K. Rajkumar, V. K. Ramachandaramurthy, B. L. Yong, and D. B. Chia, "Techno-economical optimization of hybrid pv/wind/battery system using Neuro-Fuzzy," *Energy,* vol. 36, no. 8, pp. 5148-5153, 2011, doi: 10.1016/j.energy.2011.06.017.

[140] P. Nagapurkar and J. D. Smith, "Techno-economic optimization and social costs assessment of microgrid-conventional grid integration using genetic algorithm and Artificial Neural Networks: A case study for two US cities," *Journal of Cleaner Production,* vol. 229, pp. 552-569, 2019, doi: 10.1016/j.jclepro.2019.05.005.

[141] A. Singh and P. Baredar, "Techno-economic assessment of a solar PV, fuel cell, and biomass gasifier hybrid energy system," *Energy Reports,* vol. 2, pp. 254-260, 2016, doi: 10.1016/j.egyr.2016.10.001.

[142] A. A. Masud, "The Application of Homer Optimization Software to Investigate the Prospects of Hybrid Renewable Energy System in Rural Communities of Sokoto in Nigeria," *International Journal of Electrical and Computer Engineering (IJECE),* vol. 7, no. 2, 2017, doi: 10.11591/ijece.v7i2.pp596-603.

[143] M. Izdin.Hlal, V. K. Ramachandaramurthy, F. Hafiz Nagi, and T. A. R. bin Tuan Abdullah, "Optimal Techno-Economic Design of Standalone Hybrid Renewable Energy System Using Genetic

Algorithm," *IOP Conference Series: Earth and Environmental Science,* vol. 268, p. 012012, 2019/07/02 2019, doi: 10.1088/1755-1315/268/1/012012.

[144] S. A. Amirkhalili and A. R. Zahedi, "Techno-economic Analysis of a Stand-alone Hybrid Wind/Fuel Cell Microgrid System: A Case Study in Kouhin Region in Qazvin," *Fuel Cells,* vol. 18, no. 4, pp. 551-560, 2018, doi: 10.1002/fuce.201700149.

[145] L. Tribioli and R. Cozzolino, "Techno-economic analysis of a stand-alone microgrid for a commercial building in eight different climate zones," *Energy Conversion and Management,* vol. 179, pp. 58-71, 2019, doi: 10.1016/j.enconman.2018.10.061.

[146] M. Ramesh and R. P. Saini, "Dispatch strategies based performance analysis of a hybrid renewable energy system for a remote rural area in India," *Journal of Cleaner Production,* vol. 259, 2020, doi: 10.1016/j.jclepro.2020.120697.

[147] A. Samadhiya and K. Namrata, "A multi objective control technique for interfacing hybrid renewable energy sources in an islanded microgrid subsequent to unbalanced and non linear load conditions," in *2017 Innovations in Power and Advanced Computing Technologies (i-PACT)*, Vellore, India, 21-22 April, doi: 10.1109/IPACT.2017.8245152

[148] B. C. Phan and Y. C. Lai, "Control Strategy of a Hybrid Renewable Energy System Based on Reinforcement Learning Approach for an Isolated Microgrid," *Appl. Sci.,* vol. 9, no. 19, 2019, doi: 10.3390/app9194001.

[149] M. Ghiasi, "Detailed study, multi-objective optimization, and design of an AC-DC smart microgrid with hybrid renewable energy resources," *Energy,* vol. 169, pp. 496-507, 2019, doi: 10.1016/j.energy.2018.12.083.

[150] K. Sundaramoorthy, "Development of the hard and soft constraints based optimisation model for unit sizing of the hybrid renewable energy system designed for microgrid applications," *International Journal of Sustainable Energy,* vol. 36, no. 2, pp. 192-208, 2017, doi: 10.1080/14786451.2015.1005087.

[151] Y. Sawle, S. Gupta, and A. K. Bohre, "Socio-techno-economic design of hybrid renewable energy system using optimization techniques," *Renewable Energy,* vol. 119, pp. 459-472, 2018, doi: 10.1016/j.renene.2017.11.058.

[152] S. Goel and R. Sharma, "Feasibility study of hybrid energy system for off-grid rural water supply and sanitation system in Odisha, India," *International Journal of Ambient Energy,* vol. 37, no. 3, pp. 314-320, 2016/05/03 2016, doi: 10.1080/01430750.2014.962089.

[153] L. M. Halabi and S. Mekhilef, "Flexible hybrid renewable energy system design for a typical remote village located in tropical climate," *Journal of Cleaner Production,* vol. 177, pp. 908-924, 2018, doi: 10.1016/j.jclepro.2017.12.248.

[154] M. O. Ajewole, P. A. Owolawi, J. S. Ojo, and O. M. Oyedele, "Hybrid renewable energy system for 5G mobile telecommunication applications in Akure, Southwestern Nigeria," *Nigeria Journal of Pure and Applied Physics,* vol. 8, no. 1, 2019, doi: 10.4314/njpap.v8i1.4.

[155] L. Bartolucci, S. Cordiner, V. Mulone, V. Rocco, and J. L. Rossi, "Hybrid renewable energy systems for renewable integration in microgrids: Influence of sizing on performance," *Energy,* vol. 152, pp. 744-758, 2018, doi: 10.1016/j.energy.2018.03.165.

[156] J. Senthil kumar, S. Charles Raja, D. Srinivasan, and P. Venkatesh, "Hybrid renewable energy-based distribution system for seasonal load variations," *International Journal of Energy Research,* vol. 42, no. 3, pp. 1066-1087, 2018, doi: 10.1002/er.3902.

[157] M. R. Akhtari and M. Baneshi, "Techno-economic assessment and optimization of a hybrid renewable co- supply of electricity, heat and hydrogen system to enhance performance by recovering excess electricity for a large energy consumer," *Energy Conversion and Management,* vol. 188, pp. 131-141, 2019, doi: 10.1016/j.enconman.2019.03.067.

[158] D. Feroldi and D. Zumoffen, "Sizing methodology for hybrid systems based on multiple renewable power sources integrated to the energy management strategy," *International Journal of Hydrogen Energy,* vol. 39, pp. 8609-8620, 2014, doi: 10.1016/j.ijhydene.2014.01.003.

[159] S. M. Dawoud, X. Lin, and M. I. Okba, "Hybrid renewable microgrid optimization techniques: A review," *Renewable and Sustainable Energy Reviews,* vol. 82, pp. 2039-2052, 2018, doi: 10.1016/j.rser.2017.08.007.

[160] S. Mishra, C. K. Panigrahi, and D. P. Kothari, "Design and simulation of a solar–wind–biogas hybrid system architecture using HOMER in India," *International Journal of Ambient Energy,* vol. 37, no. 2, pp. 184-191, 2016/03/03 2016, doi: 10.1080/01430750.2014.915886.

[161] J. Calitz and J. Wright, "Statistics of utility-scale power generation in South Africa in 2020," CSIR Energy Centre, March, 2021.

[162] Y. Gu, X. Zhang, J. Are Myhren, M. Han, X. Chen, and Y. Yuan, "Techno-economic analysis of a solar photovoltaic/thermal (PV/T) concentrator for building application in Sweden using Monte Carlo method," *Energy Conversion and Management,* vol. 165, pp. 8-24, 2018, doi: 10.1016/j.enconman.2018.03.043.

[163] J. Jung and M. Villaran, "Optimal planning and design of hybrid renewable energy systems for microgrids," *Renewable and Sustainable Energy Reviews,* vol. 75, pp. 180-191, 2017, doi: 10.1016/j.rser.2016.10.061.

[164] N. S. Savic, V. A. Katic, N. A. Katic, B. Dumnic, D. Milicevic, and Z. Corba, "Techno-economic and environmental analysis of a microgrid concept in the university campus," in *2018 International Symposium on Industrial Electronics (INDEL)*, Banja Luka, Bosnia and Herzegovina, 1-3 Nov 2018, doi: 10.1109/INDEL.2018.8637613

[165] P. Jimenez Zabalaga, E. Cardozo, L. A. Choque Campero, and J. A. Araoz Ramos, "Performance Analysis of a Stirling Engine Hybrid Power System," *Energies,* vol. 13, no. 4, 2020, doi: 10.3390/en13040980.

[166] P. O. Oviroh and T.-C. Jen, "The Energy Cost Analysis of Hybrid Systems and Diesel Generators in Powering Selected Base Transceiver Station Locations in Nigeria," *Energies,* vol. 11, no. 3, 2018, doi: 10.3390/en11030687.

[167] T. Adefarati and R. C. Bansal, "Economic and environmental analysis of a co-generation power system with the incorporation of renewable energy resources," *Energy Procedia,* vol. 158, pp. 803-808, 2019, doi: 10.1016/j.egypro.2019.01.212.

[168] M. R. Basir Khan, J. Pasupuleti, J. Al-Fattah, and M. Tahmasebi, "Optimal Grid-Connected PV System for a Campus Microgrid," *Indonesian Journal of Electrical Engineering and Computer Science,* vol. 12, no. 3, 2018, doi: 10.11591/ijeecs.v12.i3.pp899-906.

[169] E. Hamatwi, C. N. Nyirenda, and I. E. Davidson, "Cost Optimization and Design of a Hybrid Distributed Generation System for a DC Microgrid," presented at the 2018 IEEE PES/IAS PowerAfrica, 2018.

[170] N. Chowdhury, C. Hossain, M. Longo, and W. Yaïci, "Optimization of Solar Energy System for the Electric Vehicle at University Campus in Dhaka, Bangladesh," *Energies,* vol. 11, no. 9, 2018, doi: 10.3390/en11092433.

[171] F. Iqbal and A. S. Siddiqui, "Optimal configuration analysis for a campus microgrid—a case study," *Protection and Control of Modern Power Systems,* vol. 2, no. 1, 2017, doi: 10.1186/s41601-017-0055-z.

[172] O. M. Longe, N. D. Rao, F. Omowole, A. S. Oluwalami, and O. T. Oni, "A Case Study on Off-grid Microgrid for Universal Electricity Access in the Eastern Cape of South Africa," *International Journal of Energy Engineering,* vol. 7, no. 2, pp. 55-63, 2017, doi: 10.5923/j.ijee.20170702.03.

[173] H. Sharma and G. Kaur, "Optimization and simulation of smart grid distributed generation: A case study of university campus," 2016, pp. 153-157. doi: 10.1109/SEGE.2016.7589517

[174] E. Park and S. J. Kwon, "Solutions for optimizing renewable power generation systems at Kyung-Hee University's Global Campus, South Korea," *Renewable and Sustainable Energy Reviews,* vol. 58, pp. 439-449, 2016, doi: 10.1016/j.rser.2015.12.245.
[175] NREL, "HOMER:The Micropower Optimization Model," NREL, Ed., ed. Colorado: National Renewable Energy Laboratory, 2004.
[176] L. Olatomiwa, S. Mekhilef, A. S. N. Huda, and K. Sanusi, "Techno-economic analysis of hybrid PV-diesel-battery and PV-wind-diesel-battery power systems for mobile BTS: the way forward for rural development," *Energy Science & Engineering,* vol. 3, no. 4, pp. 271-285, 2015, doi: 10.1002/ese3.71.
[177] SARS. "Carbon Tax." https://www.sars.gov.za/ClientSegments/Customs-Excise/Excise/Environmental-Levy-Products/Pages/Carbon-Tax.aspx (accessed 31 October, 2020).
[178] M. Solution, "GERMAN AUTOMOTIVE SUPPLIER SAYS "GOODBYE MUNICIPAL ELECTRICITY GRID, HELLO MICROGRID"," ed, 2020.
[179] J. S. Ojo, P. A. Owolawi, and A. M. Atoye, "Designing a Green Power Delivery System for Base Transceiver Stations in Southwestern Nigeria," *SAIEE Africa Research Journal,* vol. 110, no. 1, pp. 19-25, 2019, doi: 10.23919/SAIEE.2019.8643147.
[180] S. T. Leholo, P. A. Owolawi, and K. T. Akindeji, "Modelling and Optimization of Hybrid RE for Powering Remote GSM Base Station," in *2018 IEEE PES/IAS PowerAfrica*, 28-29 June 2018 2018, pp. 869-874. doi: 10.1109/PowerAfrica.2018.8520994
[181] M. H. Chung, "Estimating Solar Insolation and Power Generation of Photovoltaic Systems Using Previous Day Weather Data," *Advances in Civil Engineering,* vol. 2020, pp. 1-13, 2020, doi: 10.1155/2020/8701368.
[182] H. Tazvinga, X. Xia, and J. Zhang, "Minimum cost solution of photovoltaic–diesel–battery hybrid power systems for remote consumers," *Solar Energy,* vol. 96, pp. 292-299, 2013, doi: 10.1016/j.solener.2013.07.030.
[183] H. Tazvinga, "Energy optimisation and management of off-grid hybrid power supply systems," Doctor of Philosophy, Department of Electrical, Electronic and computer engineering, University of Pretoria, Pretoria, 2015.
[184] L. Arturo Soriano, W. Yu, and J. d. J. Rubio, "Modeling and Control of Wind Turbine," *Mathematical Problems in Engineering,* vol. 2013, pp. 1-13, 2013, doi: 10.1155/2013/982597.
[185] M. H. H. Albadi, "On Techno-Economic Evaluation of Wind-Based DG," Doctor of Philosophy, Electrical and Computer Engineering, University of Waterloo, Waterloo, Ontario, Canada, 2010.
[186] S. Raikar and S. Adamson, "13 - Renewable energy finance in the international context," in *Renewable Energy Finance*, S. Raikar and S. Adamson Eds.: Academic Press, 2020, pp. 185-220.
[187] I. Dincer and A. Abu-Rayash, "Chapter 6 - Sustainability modeling," in *Energy Sustainability*, I. Dincer and A. Abu-Rayash Eds.: Academic Press, 2020, pp. 119-164.
[188] S. Ghose and M. J. Franchetti, "Chapter 11 - Economic Aspects of Food Waste-to-Energy System Deployment," in *Sustainable Food Waste-To-energy Systems*, T. A. Trabold and C. W. Babbitt Eds.: Academic Press, 2018, pp. 203-229.
[189] E. Wood, "Northeastern University Aims to Set New Standard for Higher Ed with Advanced Microgrid," *Microgrid Knowledge*, 7 May 2019. [Online]. Available: https://microgridknowledge.com/northeastern-university-microgrid/
[190] A. Burger, "Nigerian Universities Graduate to Off-Grid," *Microgrid Knowledge*, 19 July 2019. [Online]. Available: https://microgridknowledge.com/off-grid-microgrids-nigerian-universities/
[191] J. O. Okeniyi, A. A. Atayero, S. I. Popoola, E. T. Okeniyi, and G. M. Alalade, "Smart campus: Data on energy generation costs from distributed generation systems of electrical energy in a Nigerian University," *Data Brief,* vol. 17, pp. 1082-1090, Apr 2018, doi: 10.1016/j.dib.2018.02.022.

[192] "Sustainable Energy." https://facilities.princeton.edu/sustainable-campus/sustainable-energy (accessed 21 July 2021.
[193] "Tracking Princeton's Energy Impact." https://tiger-energy.appspot.com/home (accessed 21 July 2021.
[194] F. P. Mahdi, P. Vasant, M. Abdullah-Al-Wadud, V. Kallimani, and J. Watada, "Quantum-behaved bat algorithm for many-objective combined economic emission dispatch problem using cubic criterion function," *Neural Computing and Applications,* vol. 31, no. 10, pp. 5857-5869, 2018, doi: 10.1007/s00521-018-3399-z.
[195] D. C. Secui, "A new modified artificial bee colony algorithm for the economic dispatch problem," *Energy Conversion and Management,* vol. 89, pp. 43-62, 2015, doi: 10.1016/j.enconman.2014.09.034.
[196] U. Güvenç, Y. Sönmez, S. Duman, and N. Yörükeren, "Combined economic and emission dispatch solution using gravitational search algorithm," *Scientia Iranica,* vol. 19, no. 6, pp. 1754-1762, 2012, doi: 10.1016/j.scient.2012.02.030.
[197] A. Chatterjee, S. P. Ghoshal, and V. Mukherjee, "Solution of combined economic and emission dispatch problems of power systems by an opposition-based harmony search algorithm," *International Journal of Electrical Power & Energy Systems,* vol. 39, no. 1, pp. 9-20, 2012, doi: 10.1016/j.ijepes.2011.12.004.
[198] S. Jiang, C. Zhang, W. Wu, and S. Chen, "Combined Economic and Emission Dispatch Problem of Wind-Thermal Power System Using Gravitational Particle Swarm Optimization Algorithm," *Mathematical Problems in Engineering,* vol. 2019, pp. 1-19, 2019, doi: 10.1155/2019/5679361.
[199] A. K. Wadhwani, K. K. Swarnkar, and A. Gupta, "Combined Economic Emission Dispatch Problem using Particle Swarm Optimization," *International Journal of Computer Applications,* vol. 49, no. 6, pp. 1-6, 2012, doi: 10.5120/7628-0695.
[200] Z. Xin-gang, L. Ji, M. Jin, and Z. Ying, "An improved quantum particle swarm optimization algorithm for environmental economic dispatch," *Expert Systems with Applications,* vol. 152, 2020, doi: 10.1016/j.eswa.2020.113370.
[201] F. X. Rugema, G. Yan, S. Mugemanyi, Q. Jia, S. Zhang, and C. Bananeza, "A Cauchy-Gaussian Quantum-Behaved Bat Algorithm Applied to Solve the Economic Load Dispatch Problem," *IEEE Access,* vol. 9, pp. 3207-3228, 2021, doi: 10.1109/access.2020.3034730.
[202] P. Vasant, F. P. Mahdi, J. A. Marmolejo-Saucedo, I. Litvinchev, R. R. Aguilar, and J. Watada, "Quantum-Behaved Bat Algorithm for Solving the Economic Load Dispatch Problem Considering a Valve-Point Effect," *International Journal of Applied Metaheuristic Computing,* vol. 11, no. 3, pp. 41-57, July-September 2020, doi: 10.4018/IJAMC.2020070102.
[203] B. Zhu, W. Zhu, Z. Liu, Q. Duan, and L. Cao, "A Novel Quantum-Behaved Bat Algorithm with Mean Best Position Directed for Numerical Optimization," *Comput Intell Neurosci,* vol. 2016, p. 6097484, 2016, doi: 10.1155/2016/6097484.
[204] X. S. Yang and X. He, "Bat algorithm: literature review and applications," *International Journal of Bio-Inspired Computation,* vol. 5, no. 3, 2013, doi: 10.1504/ijbic.2013.055093.
[205] S. Gautham and J. Rajamohan, "Economic Load Dispatch using Novel Bat Algorithm," presented at the 2016 IEEE 1st International Conference on Power Electronics, Intelligent Control and Energy Systems (ICPEICES), 2016.
[206] J. Islam, B. Mamo Negash, P. Vasant, N. Ishtiaque Hossain, and J. Watada, "Quantum-Based Analytical Techniques on the Tackling of Well Placement Optimization," *Applied Sciences,* vol. 10, no. 19, 2020, doi: 10.3390/app10197000.